



Full Development Pharmacometrics (FD PMX)

lutetium (¹⁷⁷Lu) vipivotide tetraxetan

AAA617 ([¹⁷⁷Lu]Lu-PSMA-617)

**Population PK Modeling and Exposure-Response Analyses
on Organ Dosimetry and Acute Toxicity Based on
[¹⁷⁷Lu]Lu-PSMA-617 Sub-study Data
Modeling Report**

Document type: Modeling Report
Document status: Final
Version: 01
Release date: 02-Jun-2021

Property of Advanced Accelerator Applications, a Novartis Company
Confidential

May not be used, divulged, published or otherwise disclosed
without the consent of Advanced Accelerator Applications
Template version 2.0 16-Dec-2019

1 Synopsis

Report title:

Population PK Modeling and Exposure-Response Analyses on Organ Dosimetry and Acute Toxicity
Based on [¹⁷⁷Lu]Lu-PSMA-617 Sub-study Data

Objectives: A population PK (popPK) modeling and exposure-response (E-R) analyses on organ dosimetry and acute toxicity were performed to support the [¹⁷⁷Lu]Lu-PSMA-617 submission in metastatic castration-resistant prostate cancer (mCRPC).

1. The objectives of the popPK modeling were:
 - To characterize the overall radioactivity-blood PK of [¹⁷⁷Lu]Lu-PSMA-617 and PK parameters (e.g. clearance, volume) with their variability in mCRPC patients.
 - To explore covariates (i.e. weight, BMI, age, baseline creatinine clearance) that may explain the inter-individual variability on PK parameters in this population.
 - To predict individual PK (Bayes Estimates) and derive exposure metrics (i.e. AUCinf and Cmax) for E-R analyses.
2. The objective of the E-R analysis on organ dosimetry (Exposure-Dosimetry) was to explore the relationships between exposure and dosimetry in critical organs (i.e. kidney, bone marrow, salivary glands and lacrimal glands) during the first cycle of treatment with [¹⁷⁷Lu]Lu-PSMA-617 in mCRPC patients.
3. The objective of the E-R analysis on acute toxicity (Exposure/Dosimetry-Toxicity) was to explore relationships between exposure/dosimetry and acute toxicity related to kidney, bone marrow, salivary glands and lacrimal glands during the first cycle of treatment with [¹⁷⁷Lu]Lu-PSMA-617 in mCRPC patients.

Data: The analyses summarized in this report are based on radioactivity-blood PK, organ dosimetry and acute toxicity data during Cycle 1 from the PSMA-617-01 sub-study. PSMA-617-01 VISION study is a Phase 3 open-label, randomized study to evaluate the efficacy and safety of [¹⁷⁷Lu]Lu-PSMA-617 in adult patients with PSMA-positive mCRPC, when administered in addition to best supportive/best standard of care as compared to best supportive/best standard of care alone. A sub-study was conducted in a non-randomized cohort of 30 patients to provide a more complete assessment of the PK, dosimetry and some safety aspects of [¹⁷⁷Lu]Lu-PSMA-617.

The popPK dataset included 265 blood PK observations from 30 individuals after the first dose administration. Dosimetry assessments for each organ of interest (i.e. bone marrow, kidney, lacrimal glands and salivary glands) were available from 29 patients. Longitudinal laboratory data during Cycle 1 as well as any adverse events related to the organs at risk were collected for the 30 subjects.

Methods: First, a base popPK model was developed including components of the structural model, random effect and residual error models that adequately characterized the radioactivity-blood PK of decay-corrected [¹⁷⁷Lu]Lu-PSMA-617. Next, a full model was constructed by incorporating covariate-parameter relationships with Pearson correlation coefficient ≥ 0.3 between post-hoc random effect and covariate. Potential correlations between candidate covariates were investigated and correlated covariates were tested separately to identify the most appropriate ones to include in the model. Then, a final model was established from reduction of the full model by removing covariates per predefined criteria (e.g. p-value ≥ 0.05 from Wald test, no BICc reduction). The applications of the popPK model included evaluation of covariate effects, and prediction of individual PK metrics (i.e. AUCinf and Cmax) that were further used in E-R analyses.

Exposure-Dosimetry analyses were based on descriptive plots and linear regressions to explore the relationships between the exposure metrics and organ dosimetry. Exposure/Dosimetry-Toxicity analyses explored the relationships between exposure metrics/organ dosimetry, and the related organ acute toxicity. Due to the limited number of patients and adverse events, only descriptive plots were generated.

Results: A three-compartment model with a delayed 0-order absorption and linear elimination adequately described the radioactivity-blood PK data. Baseline creatinine clearance (CrCl_{BL}) had a statistically significant impact on clearance (Cl), with a decrease of CrCl_{BL} by 40%, such as a decrease from 101.5 mL/min to 60.9 mL/min, leading to an average decrease of Cl by 21%. Baseline weight (WT_{BL}) had a statistically significant impact on the central volume of distribution (V_1), with a decrease of WT_{BL} by 23%, such as a decrease from 88.5 kg to 68.1 kg, leading to an average decrease of V_1 by 18%. All parameters were estimated with reasonable precision, and the diagnostic plots suggested a good description and prediction of the data. For a typical subject with $\text{CrCl}_{\text{BL}}=101.5 \text{ mL/min}$ and $\text{WT}_{\text{BL}}=88.5 \text{ kg}$, Cl was estimated to be 2.50 L.h^{-1} . Volume of distribution from the three compartments, V_1 , V_2 and V_3 were estimated at 11.53 L, 29.34 L and 11.51 L, respectively. The inter-compartmental clearance, Q_2 and Q_3 , were estimated at 0.52 L.h^{-1} and 12.00 L.h^{-1} , respectively. Variabilities on Cl and V_1 were moderate (CV% = 22% and 42% respectively), while variabilities on Q_2 and V_2 were estimated at relatively high values (CV% = 80% and 93% respectively). Tlag and Tk0, reproducing an artificial delayed absorption after the start of administration, were estimated at 0.01 h and 0.06 h with high variability (CV% = 291% and 264% respectively).

Simulations showed a 42% and 20% increase in median of simulated AUCinf for moderate and mild renal impairment (based on CrCl_{BL}) respectively vs. for normal renal function. There was no significant effect of renal function on Cmax and of WT_{BL} on Cmax. Individual patients' data, including dosing information, WT_{BL} and CrCl_{BL} values, were used to predict longitudinal concentrations during the first cycle and to derive Cmax and AUCinf for the 30 sub-study patients.

Exposure-dosimetry analyses suggested that only radioactivity-blood AUCinf was a statistically significant predictor of kidney dosimetry ($p=0.005$). However, the relationship between AUCinf and kidney dosimetry may not be a causal relationship as it is confounded by the inclusion of CrCl_{BL} as a covariate on Cl. Exploratory correlations between dosimetry and covariates showed that higher CrCl_{BL} was associated with lower values of absorbed radiation dose in kidney, bone marrow and lacrimal gland. Older subjects were associated with higher values of kidney and bone marrow dosimetry, which is consistent with lower CrCl_{BL} . A trend toward higher bone marrow dosimetry values in patients with a large number of bone lesions (>20) was also noted. In addition, a trend was detected toward higher kidney dosimetry values in patients with mild or moderate renal impairment compared to those with normal renal function.

Descriptive longitudinal laboratory profiles showed a decrease in leukocytes, neutrophils and platelets starting from 8 days after treatment administration. Among the sub-study patients, 59% presented a decrease in CrCl and 86% a decrease in platelet count. Worsening from baseline of at least one hematological adverse events (CTCAE Grade ≥ 2) during Cycle 1 was observed in 20% of the sub-study patients. None of them had any renal adverse event (CTCAE Grade ≥ 2) or lacrimal gland toxicity during Cycle 1. A total of 2 patients had a salivary gland adverse event at Cycle 1, limited to Grade 1. Descriptive plots showed a trend toward higher injected activity and higher kidney dosimetry associated with larger decrease from baseline in CrCl. No consistent trend was detected in the relationships between platelet count decrease, hematological adverse events and salivary gland toxicities with exposure metrics.

Discussion: The findings from this report need to be interpreted with caution as the analyses were limited by the small sample size (N=30) and the number of adverse events. In addition, the current work could only explore Cycle 1 data, and additional assessments are needed at the end of all cycles to account for the risk of cumulative doses. Finally, clinical implication of covariate effect is difficult to interpret as no clear relationship has been established between blood exposure and clinical efficacy and safety.

Conclusions:

1. Key results from the popPK modeling of radioactivity-blood PK of [¹⁷⁷Lu]Lu-PSMA-617 were:
 - The final structural model was a three-compartment model with a delayed 0-order absorption and linear elimination.

- PopPK parameter estimates were $\text{Cl}=2.50 \text{ L.h}^{-1}$, $V_1=11.53 \text{ L}$, $Q_2=0.52 \text{ L.h}^{-1}$, $V_2=29.34 \text{ L}$, $Q_3=12.00 \text{ L.h}^{-1}$ and $V_3=11.51 \text{ L}$ for a typical subject (with $\text{CrCl}_{\text{BL}}=101.5 \text{ mL/min}$ and $\text{WT}_{\text{BL}}=88.5 \text{ kg}$).
- The inter-individual variabilities on Cl and V_1 were moderate ($\text{CV}\% = 22\%$ and 42% respectively), while variabilities on Q_2 and V_2 were estimated at relatively high values ($\text{CV}\% = 80\%$ and 93% respectively).
- T_{lag} and T_{k0} , reproducing an artificial delayed absorption after the start of administration, were estimated at 0.01 h and 0.06 h with high variability ($\text{CV}\% = 291\%$ and 264% respectively).
- The residual proportional error of the model was estimated at a low value (13.96%).
- CrCl_{BL} had a statistically significant impact on Cl, with a decrease of CrCl_{BL} by 40% , such as a decrease from 101.5 mL/min to 60.9 mL/min , leading to an average decrease of Cl by 21% . An increase in CrCl_{BL} was subsequently associated with a lower AUC_{inf} . Simulations showed a 42% and 20% increase in median of simulated AUC_{inf} for moderate and mild renal impairment respectively vs. for normal renal function. There was no significant effect on C_{max} .
- WT_{BL} had a statistically significant impact on V_1 , with a decrease of WT_{BL} by 23% , such as a decrease from 88.5 kg to 68.1 kg , leading to an average decrease of V_1 by 18% . There was no significant effect of WT_{BL} on exposure.

2. Key results from the Exposure-Dosimetry analyses at Cycle 1 were:

- There was no consistent association between exposure metrics (i.e. injected activity, AUC_{inf} , C_{max}) and dosimetry in the organs at risk, namely kidney, bone marrow, salivary glands and lacrimal glands.
- Only AUC_{inf} in blood was a statistically significant predictor of kidney dosimetry ($p=0.005$), but confounded by CrCl_{BL} .
- Renal impairment (mild/moderate vs. normal) showed a trend toward higher kidney dosimetry values.

3. Key results from the descriptive Exposure/Dosimetry-Toxicity analyses at Cycle 1 were:

- Longitudinal laboratory profiles showed a decrease in leukocytes, neutrophils and platelets starting from 8 days after treatment administration.
- Higher injected activity and higher kidney dosimetry tend to be associated with larger decrease from baseline in CrCl .
- No consistent trend was detected in the relationships between platelet count decrease, hematological adverse events and salivary gland toxicities with exposure metrics.

Date of the report: 02-Jun-2021

2 Table of contents

1	Synopsis	2
2	Table of contents.....	5
	List of tables.....	6
	List of figures.....	7
	List of abbreviations	10
3	Introduction.....	12
4	Objectives	13
5	Data	13
5.1	Study selection, study design(s) and assessment schedule	13
5.2	Description of assessment of interest.....	14
5.2.1	Assessment of radioactivity-blood [¹⁷⁷ Lu]Lu-PSMA-617 PK	14
5.2.2	Calculation of organ dosimetry	14
5.2.3	Reported adverse events	15
5.3	Dataset specification	15
5.3.1	Population PK dataset.....	16
5.3.2	E-R analyses datasets	16
6	Methods	19
6.1	Population PK modeling methods.....	19
6.1.1	Background.....	19
6.1.2	Missing data and imputations	19
6.1.3	Outliers and data exclusions	19
6.1.4	Modeling strategy	19
6.1.5	Structural model	20
6.1.6	General NLME expression	20
6.1.7	Covariate model.....	22
6.1.8	Decision criteria.....	23
6.1.9	Sensitivity analysis	23
6.1.10	Simulations	23
6.1.11	Derivation of patients' model-based PK exposure metrics	24
6.1.12	Analysis software	24
6.2	E-R analyses methods	24
6.2.1	Missing data and imputations	24
6.2.2	E-R analyses strategy	24
6.2.3	Analysis software	25
7	Results.....	25
7.1	Population PK modeling results.....	25

7.1.1	Description of observed data	26
7.1.2	Deviations from the analysis plan	34
7.1.3	Base model	34
7.1.4	Covariate selection	37
7.1.5	Final model: description	40
7.1.6	Final model: parameter estimates	40
7.1.7	Final model: evaluation	42
7.1.8	Simulations	44
7.1.9	Derivation of patients' model-based PK exposure metrics	47
7.2	E-R analyses results	48
7.2.1	Exposure-dosimetry analyses	48
7.2.2	Exposure/Dosimetry-toxicity analyses	58
8	Discussion	66
8.1	Population PK modeling	66
8.2	Exposure-response analyses	67
8.2.1	Exposure-Dosimetry	67
8.2.2	Exposure/Dosimetry-Toxicity	68
9	Conclusions	69
10	References	71
11	Appendices	72
11.1	Appendix 1: Goodness-of-fit plots	72
11.1.1	Appendix 1.1: Goodness-of-fit plots from the base popPK model	72
11.1.2	Appendix 1.2: Additional goodness-of-fit plots from the final popPK model	78
11.2	Appendix 2: Model control streams from the final popPK model (Run16 mlxtran)	85
11.3	Appendix 3: Analysis plan	87
11.4	Appendix 4: Data specifications of columns used in Monolix for the final popPK model	87
11.5	Appendix 5: Additional documentation	89
11.5.1	Appendix 5.1: Additional descriptive plots and information on PK data	89
11.5.2	Appendix 5.2: Additional descriptive plots on organ dosimetry	92
11.5.3	Appendix 5.3: Additional documentation on toxicity	93
Table 5-1	Study assessments during the first cycle	14

List of tables

Table 5-2	Datasets used for popPK modeling and E-R analyses.....	15
Table 5-3	Description of the PK-Dosimetry dataset.....	17
Table 5-4	Description of the PK/Dosimetry-Toxicity-Lab dataset.....	17
Table 5-5	Description of the PK/Dosimetry-Toxicity-AE dataset	18
Table 6-1	Covariate-PK parameter candidates	22
Table 7-1	List of key programs and popPK models	25
Table 7-2	Summary of demographic variables and baseline characteristics	32
Table 7-3	Base model building steps	34
Table 7-4	Parameter estimates from the base popPK model	36
Table 7-5	Models for covariate selection.....	39
Table 7-6	Parameter estimates from the final popPK model	41
Table 7-7	Summary of observed data by renal impairment and weight categories.....	45
Table 7-8	Summary of simulated AUCinf and Cmax by baseline renal impairment and baseline weight categories.....	47
Table 7-9	Summary of predicted individual PK exposure metrics.....	47
Table 7-10	Programs used to generate E-R analyses	48
Table 7-11	Summary of dosimetry values (Gy) per organs on Cycle 1	49
Table 7-12	Summary of individual baseline characteristics	51
Table 7-13	p-values from linear regression between exposure metrics and dosimetry	54
Table 7-14	Results from the linear regressions between AUCinf and kidney dosimetry	54
Table 7-15	Summary of kidney dosimetry by renal impairment category	56
Table 7-16	Summary of adverse events from the organs at risk during Cycle 1 (N=30)	61
Table 11-1	Description of the columns used in Monolix for the final popPK model	87
Table 11-2	List of individual durations of infusion and individual actual times of first post-dose sample.....	90
Table 11-3	Number of individuals with a decrease from baseline in CrCl and platelet count during Cycle 1.....	93

List of figures

Figure 7-1

Spaghetti plots of observed individual radioactivity-blood PK of [¹⁷⁷Lu]Lu-PSMA-617 (Linear scale).....
27

Figure 7-2	Spaghetti plots of observed individual radioactivity-blood PK of [¹⁷⁷ Lu]Lu-PSMA-617 (Log-linear scale)	28
Figure 7-3	Distribution of actual PK sampling times	29
Figure 7-4	Distribution of [¹⁷⁷ Lu]Lu-PSMA-617 doses administered at the first cycle	30
Figure 7-5	Distribution of infusion durations for the first dose	31
Figure 7-6	Example of 4 individual PK profiles during the first 2 hours together with the duration of infusion	32
Figure 7-7	Correlations between baseline covariates.....	33
Figure 7-8	Structural PK model	35
Figure 7-9	Observed concentrations vs. population prediction or individual prediction on log scale from the base popPK model	37
Figure 7-10	Post-hoc random effects from the base popPK model vs. covariates of interest.....	38
Figure 7-11	Observed concentrations vs. population prediction (PRED) or individual prediction (IPRED) on log scale for the final popPK model	42
Figure 7-12	Residual diagnostics from the final popPK model	43
Figure 7-13	pcVPC from the final popPK model	44
Figure 7-14	Box plot of simulated AUCinf and Cmax by renal impairment category	46
Figure 7-15	Box plot of simulated AUCinf and Cmax by WT _{BL}	46
Figure 7-16	Predicted AUCinf and Cmax vs. injected dose	48
Figure 7-17	Boxplot of dosimetry values per organ on Cycle 1 (N=29)	50
Figure 7-18	Distribution of the exposure metrics at Cycle 1 (N=29)	51
Figure 7-19	Correlations between exposure and organ dosimetry at Cycle 1 (N=29)	53
Figure 7-20	Correlations between organ dosimetry and continuous baseline characteristics (N=29)	55
Figure 7-21	Correlations between organ dosimetry and baseline number of bone lesions (N=26)	56
Figure 7-22	Correlation between kidney dosimetry and renal impairment category (N=29).....	57
Figure 7-23	Spaghetti plots of laboratory values at Cycle 1 (N=30)	59
Figure 7-24	Mean (\pm 95% CI) longitudinal laboratory profiles throughout Cycle 1 (N=30)	60
Figure 7-25	Worst individual CrCl decrease from baseline vs. exposure metrics (N=17)	62
Figure 7-26	Worst individual platelet count decrease vs. exposure metrics (N=25)	63

Figure 7-27	Worst hematological toxicity grades after first injection and during Cycle 1 vs. exposure metrics	64
Figure 7-28	Distribution of exposure metrics in relation to patients experiencing a worsening from baseline of at least one hematological adverse event of Grade ≥ 2	65
Figure 7-29	Distribution of exposure metrics in relation to patients experiencing any salivary gland toxicity	66
Figure 11-1	IWRES/NPDE vs. time/population predictions from the base popPK model	72
Figure 11-2	IWRES/NPDE distributions from the base popPK model	73
Figure 11-3	Parameter distribution from the base popPK model.....	74
Figure 11-4	pcVPC from the base popPK model.....	75
Figure 11-5	SAEM convergence from the base popPK model	76
Figure 11-6	Post-hoc random effects for Q ₂ and V ₂ against covariates from the base popPK model.....	77
Figure 11-7	IWRES/NPDE distribution from the final popPK model.....	78
Figure 11-8	Random effect distribution and shrinkage from the final popPK model	79
Figure 11-9	Distribution and correlation of random effects from the final popPK model	80
Figure 11-10	Post-hoc random effects from the final popPK model vs. covariates of interest.....	81
Figure 11-11	Individual fits from the final popPK model	82
Figure 11-12	SAEM convergence from the final popPK model.....	84
Figure 11-13	Convergence assessment plot from the sensitivity analysis on the final popPK model.....	85
Figure 11-14	Spaghetti plots of observed individual radioactivity-blood PK of [¹⁷⁷ Lu]Lu-PSMA-617 limited to the first 7 hours (Linear scale)	89
Figure 11-15	Spaghetti plots of observed individual radioactivity-blood PK of [¹⁷⁷ Lu]Lu-PSMA-617 limited to the first 7 hours (Log-linear scale)....	90
Figure 11-16	Density histograms of dosimetry values per organ at Cycle 1 (N=29)	92
Figure 11-17	Individual dosimetry values per organ at Cycle 1	93

List of abbreviations

AAA	Advanced Accelerator Applications
AUC	area under the concentration time curve
AUCinf	area under the concentration time curve from 1 st administration start to 2 nd administration
BICc	corrected Bayesian information criteria
BLOQ	below the limit of quantification
BMI	body mass index
Bq	Becquerel
BSA	body surface area
CI	confidence interval
Cl	clearance
Cmax	maximum concentration
CrCl	creatinine clearance
CrCl _{BL}	baseline creatinine clearance
CRL	Charles River laboratories
CTCAE	common terminology criteria for adverse events
CV	coefficient of variation
EBEs	empirical Bayes estimates
ECG	electrocardiogram
E-R	exposure-response
GBq	giga Becquerel
Gy	Gray
GOF	goodness of fit
HPCE	high performance computing environment
HPLC	high-performance liquid chromatography
IIV	inter-individual variability
IPRED	individual predicted value
IV	intravenous
IWRES	individual weighted residual
kBq	kilo Becquerel
LOQ	limit of quantitation
mCRPC	metastatic castration-resistant prostate cancer
NLME	non-linear mixed effects
NPDE	normalized prediction distribution errors
OLINDA	organ level internal dose assessment
pcVPC	prediction-corrected visual-predictive check
PK	pharmacokinetics
popPK	population pharmacokinetics
PRED	population prediction
PSMA	prostate specific membrane antigen
RDS	radiation dosimetry systems, Inc.
RLT	radioligand therapy
ROI	region-of-interest

RSE	relative standard error
SAEM	stochastic approximation expectation-maximization
SD	standard deviation
SE	standard error
SPECT/CT	single-photon emission computed tomography/computerized tomography
VPC	visual predictive check
WT _{BL}	baseline weight

Divulgué par Santé Canada à des fins non commerciales et sous réserve des conditions d'utilisation
renseignements-cliniques.canada.ca/ci-rc/conditions

Disclosed by Health Canada for non-commercial purposes and subject to the Terms of Use
clinicalinformation.canada.ca/ci-rc/terms

3 Introduction

[¹⁷⁷Lu]Lu-PSMA-617 (lutetium (177Lu) vipivotide tetraxetan) is a radioligand therapy (RLT) targeting cells over-expressing prostate specific membrane antigen (PSMA) and enabling tumor targeted delivery of β-radiation (via Lutetium-177). It is being developed by Advanced Accelerator Applications (AAA) and Endocyte for the treatment of adult patients with PSMA-positive metastatic castration-resistant prostate cancer (mCRPC) who have been treated with androgen receptor-directed therapy and taxane-based chemotherapy.

Targeted RLT offers the possibility to treat the cancer lesions in a specific and tumor-selective manner by exploiting cell surface receptors mainly expressed on malignant cells. Literature data have demonstrated that [¹⁷⁷Lu]Lu-PSMA-617 exhibits high and prolonged PSMA-specific tumor uptake, rapid background clearance, and fast kidney excretion. Since [¹⁷⁷Lu]Lu-PSMA-617 accumulates mainly in the tumor tissue and the unused radioactive materials are excreted from the body, this treatment strategy is generally well-tolerated.

However, normal tissues can be at risk for potential toxicity via exposure to radiation from [¹⁷⁷Lu]Lu-PSMA-617. The organ dosimetry, corresponding to the absorbed radiation dose to the normal tissues, is usually calculated for such therapy, and cumulative values compared with recommended dose limits from external beam radiation. Dosimetry data from literature have identified the lacrimal glands, salivary glands and kidneys as the normal organs considered at risk from radiation due to their exposure levels (Yadav et al 2017, Kratochwil et al 2016, Kabasakal et al 2017, Delker et al 2016, Scarpa et al 2017, Maffey-Steffan et al 2020, Kamaldeep et al 2020). The bone marrow is also of interest due to the presence of extensive prostate cancer bone metastases and prior therapies in the mCRPC population that can reduce the normal capacity of bone marrow function.

[¹⁷⁷Lu]Lu-PSMA-617 has been evaluated in the PSMA-617-01 study (VISION study), an international, prospective, open label, multicenter and randomized Phase 3 study in patients with progressive PSMA-positive mCRPC [Study PSMA-617-01 Appendix 16.1.1 Study protocol].

The PSMA-617-01 study also includes a sub-study conducted in a non-randomized cohort of 30 patients to collect Pharmacokinetics (PK), urine high-performance liquid chromatography (HPLC), organ dosimetry and electrocardiogram (ECG) data in order to provide a more complete assessment of the safety aspects of [¹⁷⁷Lu]Lu-PSMA-617.

Data from the patients in the sub-study are not considered in the primary and secondary analysis of the main study. The results of this sub-study are included in separate reports addendum that accompanies the main study report. Most of these analyses were outsourced. Radiation Dosimetry Systems, Inc. (RDS) calculated the organ dosimetry values. Charles River Laboratories (CRL) performed non-compartmental and compartmental blood PK and urine sampling analyses. ERT performed ECG and concentration-QTc analyses.

The objective of the analyses from this report was to provide additional investigations on radioactivity-blood PK of [¹⁷⁷Lu]Lu-PSMA-617, organ dosimetry and acute toxicity data to support the initial global submission of [¹⁷⁷Lu]Lu-PSMA-617 in adult patients with PSMA-positive mCRPC who have been treated with androgen receptor-directed therapy and taxane-based chemotherapy.

This document outlines the strategy, methodology and results from the population PK (popPK) modeling and exposure-response (E-R) analyses on organ dosimetry (Exposure-Dosimetry) and acute toxicity (Exposure/Dosimetry-Toxicity) based on Cycle 1 data from the PSMA-617-01 sub-study.

4 Objectives

A population PK (popPK) modeling and exposure-response (E-R) analyses on organ dosimetry and acute toxicity were performed to support the [¹⁷⁷Lu]Lu-PSMA-617 submission in metastatic castration-resistant prostate cancer (mCRPC).

1. The objectives of the popPK modeling were:
 - To characterize the overall radioactivity-blood PK of [¹⁷⁷Lu]Lu-PSMA-617 and PK parameters (e.g. clearance, volume) with their variability in mCRPC patients.
 - To explore covariates (i.e. weight, BMI, age, baseline creatinine clearance) that may explain the inter-individual variability on PK parameters in this population.
 - To predict individual PK (Bayes Estimates) and derive exposure metrics (i.e. AUCinf and Cmax) for E-R analyses.
2. The objective of the E-R analysis on organ dosimetry (Exposure-Dosimetry) was to explore the relationships between exposure and [¹⁷⁷Lu]Lu-PSMA-617 dosimetry in critical organs (i.e. kidney, bone marrow, salivary glands and lacrimal glands) during the first cycle of treatment with [¹⁷⁷Lu]Lu-PSMA-617 in mCRPC patients.
3. The objective of the E-R analysis on acute toxicity (Exposure/Dosimetry-Toxicity) was to explore relationships between exposure/dosimetry and acute toxicity related to kidney, bone marrow, salivary glands and lacrimal glands during the first cycle of treatment with [¹⁷⁷Lu]Lu-PSMA-617 in mCRPC patients.

5 Data

5.1 Study selection, study design(s) and assessment schedule

PSMA-617-01 study (VISION study) is a Phase 3, open-label, international, randomized study to evaluate the efficacy and safety of [¹⁷⁷Lu]Lu-PSMA-617 in adult patients with PSMA-positive mCRPC, when administered in addition to best supportive/best standard of care as compared to best supportive/best standard of care alone.

These patients received best supportive/best standard of care and 7.4 GBq ($\pm 10\%$) [¹⁷⁷Lu]Lu-PSMA-617 through IV infusion once every 6 weeks (± 1 week) for a maximum of 6 cycles (1 cycle=6 weeks).

A dosimetry, PK, and ECG sub-study was also conducted in a non-randomized cohort in which all patients received the same treatment ([¹⁷⁷Lu]Lu-PSMA-617 plus best supportive/best standard of care). The sub-study enrolled 30 patients at four sites in Germany to provide a more complete assessment of the PK and some safety aspects of [¹⁷⁷Lu]Lu-PSMA-617. The treatment regimen and patient care management was identical to that implemented in the main PSMA-617-01 study.

The reported analyses were based on radioactivity-blood PK, organ dosimetry and acute toxicity data from the sub-study. Data available up to the cut-off date of 27-Jan-2021, corresponding to the cut-off date of the database lock for the main PSMA-617-01 study, were used. For each patient, only data from the Cycle 1 (after the first [¹⁷⁷Lu]Lu-PSMA-617 IV infusion) were analyzed.

Study assessments with their respective sampling visit and time during the first cycle are reported in [Table 5-1](#).

Table 5-1 Study assessments during the first cycle

Assessment type	Scheduled time points
Radioactivity-blood [¹⁷⁷ Lu]Lu-PSMA-617 PK ^a	Pre-dose, end of infusion, 20 ± 5min, 60 ± 5min, 120 ± 30min, 4h ± 30min, 24h ± 2h, 48h ± 2h, 72h ± 2h, day 6
Organ dosimetry	See description in Section 5.2.2 for organ dosimetry calculation
Hematology and chemistry laboratory assessments	Within 3 days prior to days 1, 8, 15, 22, 29, and 36
Reported adverse events	Continuous monitoring

^a More details are provided in [Section 5.2.1](#) on the assessment of the radioactivity-blood PK.

5.2 Description of assessment of interest

5.2.1 Assessment of radioactivity-blood [¹⁷⁷Lu]Lu-PSMA-617 PK

Radioactivity in blood was measured at the investigational sites with a gamma-counter detector properly calibrated with a Lu-177 reference source of known activity counted in the same geometry as that of the biological samples (e.g. 1 mL in a vial).

The limit of quantification (LOQ) values were not available. In the clinical dataset, values below the limit of quantification (BLOQ) were set equal to 0. For the popPK analysis, the LOQ were assumed to be equal to the minimal (except 0) radioactivity-blood decay-corrected concentration observed among patients.

The decay-correction was applied by the SxR programming team on the sample values, as described in [Section 5.3.1](#).

5.2.2 Calculation of organ dosimetry

The organ dosimetry corresponds to the energy absorbed in one organ per unit mass of tissue, and is expressed in Gray (Gy).

Besides the therapeutically relevant β-particles, Lu-177 also emits λ-particles with low energy, enabling imaging of the biodistribution of Lu-177-labeled compounds in vivo by gamma camera. The radiation dose to a target organ is the sum of the self-dose from that organ and the cross doses from all other source organs. In order to calculate the radiation dose to the various target organs, the amount of radioactivity present in the source organs was measured.

Whole body conjugate planar image data, and abdominal SPECT/CT (Single Photon Emission Computed Tomography/Computed Tomography) images for the patients who received

[¹⁷⁷Lu]Lu-PSMA-617 were obtained at approximately 1-2 h, 18-26 h, 36-48 h, and 156-168 h post injection. Region-Of-Interests (ROIs) were constructed on the SPECT images for kidneys, liver, and spleen. ROIs were also constructed on the whole-body conjugate planar images for brain, gastrointestinal tract, heart, kidneys, lacrimal glands, liver, lungs, salivary glands, image reference standard, thyroid, and whole body. Patient specific organ volumes for kidneys, liver, and spleen were measured from the CT image. ROI count statistics were quantified to determine bio-kinetic (time-activity) data in the organs and tissues. Red marrow activity was estimated based on assay of blood samples. Kinetic data were modeled to determine normalized number of disintegrations. Normalized number of disintegrations were used with the RADAR/MIRD method for internal dosimetry as implemented in the FDA cleared OLINDA (Organ Level INternal Dose Assessment) software to produce radiation exposure estimates. The human alimentary model, and urinary voiding bladder model as implemented in OLINDA were utilized.

The actual dosimetry (in Gy) at Cycle 1 in each organ was provided by RDS.

5.2.3 Reported adverse events

All the grades were reported according to the Common Terminology Criteria for Adverse Events (CTCAE) Version 5.0 (CTCAE v5.0).

5.3 Dataset specification

Data were transferred from the AAA storage system to the Novartis storage system GPSII via IntraLinks IWC by the AAA Statistical Programming team.

The SxR programming group generated the popPK dataset and three datasets for E-R analyses: (i) one PK-dosimetry dataset for E-R analyses on organ dosimetry, and (ii) two PK-toxicity datasets for E-R analyses on acute toxicity.

Data available up to the cut-off date of 27-Jan-2021 were used. For each patient, only data from Cycle 1 were retained. The E-R datasets were limited to data up to the day before the second drug administration.

The datasets were created using SAS® Version 9.4 in the Novartis GPS programming environment. The programs were validated at the most critical level (independently reproduced by a second programmer).

The datasets derived from the SxR programming team, as listed in [Table 5-2](#), have been used for the popPK modeling and E-R analyses. None of them has been post-processed by the modeler.

Table 5-2 Datasets used for popPK modeling and E-R analyses

Description	Study data and version	GPSII location
PopPK dataset	mt78062.csv@@/main/14	CAAA000A1/CAAA000A12301/mas_1/data/output_001/
PK-Dosimetry dataset	aderpkdo.sas7bdat@@/main/41	CAAA000A1/pk/pk_1/analysis_data/
PK/Dosimetry-Toxicity-Lab dataset	adpkf2.sas7bdat@@/main/53	CAAA000A1/pk/pk_1/analysis_data/
PK/Dosimetry-Toxicity-AE dataset	adpkf1.sas7bdat@@/main/35	CAAA000A1/pk/pk_1/analysis_data/

5.3.1 Population PK dataset

The popPK dataset was constructed from dosing information, radioactivity-blood [¹⁷⁷Lu]Lu-PSMA-617 PK, demographic information (at baseline) and laboratory information (at baseline).

Details on the popPK dataset specification and programming requirements are stored in the Novartis tracker for pharmacometrics' activities, ModTracker, under the activity MT-78062.

All pre-dose samples were not included in the popPK dataset.

The SxR programming team applied a decay-correction on the radioactivity-blood PK sample values by considering the measurement time and dosing time, in order to accurately assess [¹⁷⁷Lu]Lu-PSMA-617 concentration at the time of sample collection. The following equation was used on all radioactivity-blood PK samples:

$$\text{Decay corrected PK}(kBq/mL) = \frac{\text{Activity}}{\text{Vol}} \cdot \exp\left(\frac{\ln 2}{t_{1/2Lu177}} \cdot \text{measret}\right)$$

With:

- Activity: aliquot activity, in kBq;
- Vol: volume of the sample aliquot counted, in mL;
- $t_{1/2Lu177}$: Lu-177 half-life = 6.647 days = 159.528 hours, in hours;
- measret: elapsed time between the start of the first [¹⁷⁷Lu]Lu-PSMA-617 IV infusion and the time of activity measurement; in hours.

In the following sections of this document, the radioactivity-blood PK refers to the decay-corrected PK.

In addition, individual baseline creatinine clearance (CrCl_{BL}) was evaluated as a covariate and derived from the serum creatinine laboratory values using the Cockcroft-Gault formula as follow:

$$\text{CrCl}_{BL}(mL/min) = \frac{(140 - AGE) \cdot \text{WEIGHT (kg)}}{\text{Serum creatinine(mg/dL)} \cdot 72} (\cdot 0.85 \text{ if female})$$

Serum creatinine, available in $\mu\text{mol/L}$ was converted to mg/dL: 1 mg/dL = 88.4 $\mu\text{mol/L}$.

5.3.2 E-R analyses datasets

E-R analyses used the PK-Dosimetry and PK/Dosimetry-Toxicity datasets defined below.

5.3.2.1 PK-Dosimetry dataset

The PK-Dosimetry dataset was constructed from organ dosimetry data at Cycle 1, predicted radioactivity-blood exposure metrics from the popPK model (AUCinf and Cmax), demographic information (at baseline) and other baseline characteristics (CrCl_{BL} and number of bone lesions).

For the PK-Dosimetry dataset, the response metrics, or analysis variables, are the dosimetry in the organs at risk. The exposure metrics, or exposure analysis variables, are the administered activity and the model-based predicted radioactivity-blood exposure metrics.

The [Table 5-3](#) contains a description of the data included in the PK-Dosimetry dataset.

Table 5-3 Description of the PK-Dosimetry dataset

Analysis variables	Exposure metrics	Demographics	Other baseline characteristics
Dosimetry (in Gy) in the organs at risk on Cycle 1: - Kidneys - Bone marrow - Salivary glands - Lacrimal glands	- Administered activity on Cycle 1 (GBq) - Model-based predicted radioactivity-blood exposure metrics on Cycle 1: AUCinf and Cmax	- Weight - Age - BMI	- CrCl _{BL} - Number of bone lesions

BMI: body mass index; CrCl_{BL}: baseline creatinine clearance.

5.3.2.2 PK/Dosimetry-Toxicity datasets

The PK/Dosimetry-Toxicity datasets were constructed from adverse events and laboratory information (up to the day before the 2nd injection), predicted radioactivity-blood exposure metrics derived from the popPK model (AUCinf and Cmax) and organ dosimetry at Cycle 1.

The response metrics, or analysis variables, are the acute short-term toxicity events and laboratory values related to the organs at risks. The exposure metrics, or exposure analysis variables, are the administered activity, the model-based predicted radioactivity-blood exposure metrics and the organ dosimetry.

Two PK/Dosimetry-Toxicity datasets were created: (i) a PK/Dosimetry-Toxicity-Lab dataset, including laboratory values with their associated grades, and (ii) a PK/Dosimetry-Toxicity-AE dataset, including the adverse events.

The [Table 5-4](#) contains a description of the data included in the PK/Dosimetry-Toxicity-Lab dataset.

Table 5-4 Description of the PK/Dosimetry-Toxicity-Lab dataset

Organs at risk	Analysis variables	Exposure metrics	Baseline characteristics
Kidneys	Worst CrCl decrease (%change from baseline) during Cycle 1	- Administered activity on Cycle 1 (GBq) - Model-based predicted radioactivity-blood exposure metrics on Cycle 1: AUCinf and Cmax - Kidney dosimetry on Cycle 1	CrCl _{BL}
	Worst platelet decrease (%change from baseline) during Cycle 1	- Administered activity on Cycle 1 (GBq) - Model-based predicted radioactivity-blood exposure metrics on Cycle 1: AUCinf and Cmax	Baseline platelet count
Bone marrow	Occurrence of thrombocytopenia, anemia, leukopenia and neutropenia with Grade ≥ 2 during Cycle 1	Baseline grades for each toxicity	

Organs at risk	Analysis variables	Exposure metrics	Baseline characteristics
	Occurrence of at least one hematological toxicity with Grade≥2 during Cycle 1	- Red marrow dosimetry on Cycle 1	Baseline hematological toxicity

CrCl: creatinine clearance; CrCl_{BL}: baseline creatinine clearance.

The [Table 5-5](#) contains a description of the data included in the PK/Dosimetry-Toxicity-AE dataset.

Table 5-5 Description of the PK/Dosimetry-Toxicity-AE dataset

Organs at risk	Analysis variables	Exposure metrics	Baseline characteristics
Kidneys	Worst grade of renal toxicity (AEBODSYS="Renal and urinary disorders" from ADRISK)	- Administered activity on Cycle 1 (GBq) - Model-based predicted radioactivity-blood exposure metrics on Cycle 1: AUCinf and Cmax - Kidney dosimetry on Cycle 1	CrCl _{BL}
Salivary glands	Worst grade of salivary gland toxicity (RKNAM="Dry mouth" from ADRISK)	- Administered activity on Cycle 1 (GBq) - Model-based predicted radioactivity-blood exposure metrics on Cycle 1: AUCinf and Cmax - Salivary gland dosimetry on Cycle 1	
Lacrimal glands	Worst grade of lacrimal gland toxicity (AEBODSYS=="Eye disorders" from ADAE)	- Administered activity on Cycle 1 (GBq) - Model-based predicted radioactivity-blood exposure metrics on Cycle 1: AUCinf and Cmax - Lacrimal gland dosimetry on Cycle 1	NA

CrCl_{BL}: baseline creatinine clearance; NA: not applicable

In the PK/Dosimetry-Toxicity-AE dataset, patients with no kidney, salivary gland or lacrimal gland event were censored (CNSR column set to 1 if no event observed in Cycle 1) and the grade set to missing.

These analyses focused only on the most common safety events related to the organs at risks in patients under [¹⁷⁷Lu]Lu-PSMA-617 treatment, based on literature data.

6 Methods

6.1 Population PK modeling methods

6.1.1 Background

No existing popPK model of [¹⁷⁷Lu]Lu-PSMA-617 has been found in the literature.

6.1.2 Missing data and imputations

Concentrations below or equal to the LOQ were set to the LOQ value and flagged as censored in the popPK dataset in the CENS column. As the LOQ value was not available, it was set to the minimal (except 0) radioactivity-blood decay-corrected activity observed among all patients in the dataset. A LIMIT variable was created with these censored samples, and set to 0, to identify that the censored samples were non-detectable, but somewhere between 0 and LOQ.

Missing continuous covariates were to be imputed either at population mean or median depending on the empirical distribution of the covariate; missing categorical covariates were to be imputed with the majority value.

Continuous covariates with a large fraction of subjects with a missing value (> 20%) were not investigated. Furthermore, categorical variables was only tested if sufficient number of subjects belong to each category, alternatively, grouping of categories was to be considered.

6.1.3 Outliers and data exclusions

The popPK dataset has been inspected by the modeler using R version 3.6.1 in the Novartis DaVinci-Statistical Workbench and MonolixSuite2020R1. Outliers were identified by visual inspection of data and outputs from initial model building runs.

Concentrations below or equal to the LOQ reported between two non-BLOQ values were flagged in the popPK dataset in the IGNORE column, by the SxR programmer, and were not used for the popPK modeling.

6.1.4 Modeling strategy

A popPK model was first developed to characterize the radioactivity-blood PK of [¹⁷⁷Lu]Lu-PSMA-617 in mCRPC patients. Covariate effects on key PK parameters were explored and the final model was used to derive exposure metrics (i.e. AUCinf and Cmax) that were further used in E-R analyses.

The programs related to the popPK modeling were validated at the critical level (programs checked by an independent modeler)

The non-linear mixed effects (NLME) modeling approach, also called population approach, was applied.

Base model

Two components of a population model are: the structural model, which accounts for the systematic trends in the data and, to the extent possible, the mechanisms generating those trends; and the random effects model, which accounts for variability about those trends. Together these

two components form the base model, which is thought to describe the data's systematic trends and variability except for refinements that might be made through the addition of covariates.

Final model

Once a base model is finalized, the covariate model is developed, building upon the final base model. The full model adds to the base model all covariates that were initially screened as explained in [Section 6.1.7](#). Limitations of data and modeling software sometimes prevent the successful fitting of the full model. The final model lies between the base model and the full model in complexity; it provides a parsimonious version of the model that best describes the data given the objective of the modeling exercise. Note that while the development of the base model typically precedes the inclusion of covariates, it is possible that inclusion of important covariates may alter properties of the base model. In other words development of the final model may involve recursive steps.

In this analysis, the model components were selected and assembled based on a combination of prior knowledge and data-driven decision-making guided by statistical and heuristic rules. Details about the model components and the model development criteria are described in the following subsections.

6.1.5 Structural model

Different PK model structures were tested including one, two or three compartments, with infusion and linear elimination. All the PK models were parameterized in terms of clearance and volume.

6.1.6 General NLME expression

For continuous data, the NLME model equation consisting of a single dependent variable (y) can be expressed by:

$$y_{ij} = f(t_{ij}, \psi_i) + g(t_{ij}, \psi_i, \xi) \varepsilon_{ij}$$

Where t_{ij} represents the time of measurement j for subject i , with $i = 1, \dots, N$ (= total number of subjects) and $j = 1, \dots, n_i$ (=number of observations for subject i). ψ_i is the parameter vector of the structural model f for the individual i . The residual error model is defined by the function g which depends on some additional vector of parameters ξ . The residual errors ε_{ij} are standardized Gaussian random variables (mean 0 and standard deviation 1).

To summarize, the main components of the NLME equation are:

- A model for the observations from a single individual: this is given by the function f (structural model);
- A model to capture variability in ψ_i among individuals (inter-individual variability), which can be described by observed data (covariates) or unobserved variations (random effects);
- A model for residual errors: this is given by the function g and the distribution of ε_{ij} .

6.1.6.1 Inter-individual variability

A model for observations depends on a vector of individual parameters ψ_i , for example, individual clearance or volume in a PK model. In the population approach, it is assumed that ψ_i comes from some probability distribution p_{ψ_i} . This distribution p_{ψ_i} plays a fundamental role since it describes the inter-individual variability (IIV) of the individual parameter ψ_i .

In Monolix, it is considered that some transformation of the individual parameters is normally distributed and is a linear function of the covariates:

$$h(\psi_i) = h(\psi_{pop}) + \beta \cdot (c_i - c_{pop}) + \eta_i, \text{ where } \eta_i \sim \mathcal{N}(0, \Omega)$$

Where ψ_{pop} denotes the typical value of ψ_i . The component $\beta \cdot (c_i - c_{pop})$ describes part of the variability by way of covariates c_i that fluctuate around a typical value c_{pop} . The random component η_i describes the remaining variability, i.e., variability between subjects that have the same covariate values. By definition, a mixed effects model combines these two components: fixed and random effects.

One way to extend the use of Gaussian distributions is to consider that some transformation of the parameters in which we are interested is Gaussian, i.e., assume the existence of a monotonic function h such that $h(\psi_i)$ is normally distributed. Then, there exists some ω such that, for each individual i :

$$h(\psi_i) \sim \mathcal{N}(h(\psi_{pop}), \omega^2)$$

The transformation h defines the distribution of ψ_i . IIV distributions are commonly modeled with a log-normal distribution. In that case, $h(\psi_i) = \log(\psi_i)$. A log-normally random variable takes positive values only. A log-normal distribution looks like a normal distribution for a small variance ω^2 . On the other hand, the asymmetry of the distribution increases when ω^2 increases.

$$\psi_i = \psi_{pop} \cdot \exp(\eta_i), \text{ where } \eta_i \sim \mathcal{N}(0, \omega^2)$$

Note that other distributions could be used such as normal or logit-normal distributions.

In the initial steps of searching for the most adequate structural model, a diagonal matrix for inter-individual random effects was used. First, random effects were included on all parameters and simplified afterwards if needed.

6.1.6.2 Between-occasion variability

Between-occasion variability was not considered, as only one PK profile was available per individual.

6.1.6.3 Correlation of random effects (covariance matrix)

Once the main components of IIV were identified, their covariance were explored. Scatter plots for each pair of random effects were displayed to identify potential correlations between random effects to be introduced in the model.

6.1.6.4 Residual variability

The residual variability was first modeled using a combined error model (with both a proportional component and an additive component). It supposed that the magnitude of errors is expected to increase with y values and a fixed measurement noise is also expected at lower y values.

In Monolix, the combined2 error model was tested first as described in the following equation:

$$y = f + \sqrt{a^2 + b^2 \cdot f^2} \cdot \varepsilon$$

The function is a combination of the constant term a , and the term b proportional to the structural model f . The additional parameters are $\xi = (a, b)$.

If one of the residual error components (additive or proportional) was estimated to be low and/or poorly estimated with high uncertainty, a residual error model removing that part was tested.

6.1.7 Covariate model

Once the base structural model was identified, the post-hoc random effects of the model parameters was plotted against all covariates of interest. The Pearson correlation coefficient was generated for post-hoc random effects against each covariate to evaluate any potential linear correlation. The post-hoc random effects-covariate relationships with a correlation coefficient ≥ 0.3 were included into the base model to form a full model.

Potential correlations between candidate covariates were investigated prior to the screening process (described above), and correlated covariates were tested separately to identify the most appropriate ones to include in the model.

Monolix performs a Wald test and reports the corresponding p-value for each covariate effects included in the model. Covariate-parameter relationships with a p-value ≥ 0.05 were excluded from the full model. Additional criteria was also considered for the remaining covariates: SAEM convergence assessment, reduction of BICc, reduction of IIV, uncertainty on parameter, plausibility of the relationship.

In addition, the use of automatic covariate model building algorithm, COSSAC (COnditional Sampling use for Stepwise Approach based on Correlation tests) implemented in Monolix was explored.

The list of potential covariates effect on PK parameters that were evaluated is provided in [Table 6-1](#).

Table 6-1 Covariate-PK parameter candidates

Covariates	Target PK parameters
Weight (kg)	Clearance and Volume
BMI (kg/m ²)	Clearance and Volume
Age (years)	Clearance and Volume
CrCl _{BL} (mL/min)	Clearance and Volume

BMI: body mass index; CrCl_{BL}: baseline creatinine clearance.

Continuous covariate effects in Monolix were modeled using the following equation:

$$\log(\psi_i) = \log(\psi_{pop}) + \beta_i \cdot \log\left(\frac{c_i}{c}\right) + \eta_i \text{ or } \psi_i = \psi_{pop} \cdot \left(\frac{c_i}{c}\right)^{\beta_i} \cdot \exp(\eta_i),$$

Where: β_i is the covariate effect, c is the weighted mean value (i.e. the average from the individual covariate values of the dataset weighted by the number of observed PK samples per individual) for normalization of the covariate, and c_i the individual covariate value.

Categorical binary (c_i coded 0 - 1) covariate effects were specified as follow:

$$\log(\psi_i) = \log(\psi_{pop}) + \beta_i \cdot c_i + \eta_i \text{ or } \psi_i = \psi_{pop} \cdot \exp(\beta_i \cdot c_i) \cdot \exp(\eta_i)$$

6.1.8 Decision criteria

Model selection and evaluation were assessed using the following criteria: SAEM convergence assessment, change in the objective function and BICc, visual inspection of different diagnostic plots (see below), precision of the parameter estimates (relative standard error or RSE) and degree of correlation between them, decreases in both inter-individual variability and residual variability.

At all stages of model development, diagnostic plots were examined to assess model adequacy, possible lack of fit or violation of assumptions. Plots of observations vs. predicted values (PRED) and observations vs. individual predicted value (IPRED) were evaluated for randomness around the line of unity. Plots of individual weighted residual (IWRES) and normalized prediction distribution errors (NPDE) vs. time and vs. IPRED were evaluated for randomness around the zero line. Assumption of Gaussian distributions of IWRES and NPDE were also assessed with histograms and quantile-quantile plots. Individual parameter distributions with their corresponding eta-shrinkage value were reported.

The predictive performance of the final model was evaluated by simulating data using parameter estimates (fixed and random effects) and conducting a visual predictive check (VPC). This plot compares the observations with their theoretical distribution under the estimated model. Selected percentiles (median, 10th and 90th percentiles) describing the central tendency and spread in the data are compared for the observations and simulated datasets, i.e. data that would arise using the observed data structure if the hypothesized model was true. If high variability is observed, prediction-corrected VPC (pcVPC) was provided. In a pcVPC, the variability coming from binning across independent variables is removed by normalizing the observed and simulated dependent variable based on the typical population prediction for the median independent variable in the bin.

6.1.9 Sensitivity analysis

Sensitivity analyses were performed on the final model to assess the robustness of the algorithm convergence. For that, the stability on each model parameter was evaluated with different initial values using the Convergence Assessment task in MonolixSuite2020R1.

6.1.10 Simulations

All significant covariate-parameter relationships were further explored by simulations to evaluate their effects on PK exposure, specifically on AUCinf and Cmax. The plasma AUCinf was derived from the popPK model by integrating the concentrations over time: from the time

of the first dose to the time of the second administration. The term AUCinf was used as the second administration occurs 6 weeks after the first injection and no accumulation was expected.

6.1.11 Derivation of patients' model-based PK exposure metrics

Individual patients' data, including dosing information, demographic data, and any other non-PK data required as a covariate in the final model, were used to predict longitudinal concentrations during the first cycle (up to the second administration). From these predictions, plasma Cmax and AUCinf on Cycle 1 were computed, and used for E-R analyses. The plasma AUCinf was derived from the popPK model by integrating the concentrations over time: from the time of the first dose to the time of the second administration.

6.1.12 Analysis software

The analysis was performed using MonolixSuite2020R1 (Lixoft, Paris, France) utilizing the DaVinci high performance computing environment (HPCE) accessed from GPSII. Population parameters were estimated using Stochastic Approximation Expectation Maximization (SAEM) method. Individual parameters were estimated by the empirical Bayes estimates (EBEs), corresponding to the modes of the conditional distributions for the parameters of each individual (conditional on the estimated population parameters and on the individual data).

R.3.6.1 was used for data analyses, outputs processing and for simulations. The R package ggPMX_1.0 was used to generate some goodness-of-fit plots for the final model. Simulations were performed with the Simulx2020R1 graphical user interface, and the R packages RsSimulx_1.0.0 and lixoftConnets_2020.1.

6.2 E-R analyses methods

6.2.1 Missing data and imputations

The PK-Dosimetry dataset included all subjects from the sub-study who received at least one dose of [¹⁷⁷Lu]Lu-PSMA-617 and who have one dosimetry value at Cycle 1.

The PK/Dosimetry-Toxicity datasets included all subjects from the sub-study who received at least one dose of [¹⁷⁷Lu]Lu-PSMA-617 in Cycle 1.

None of the missing data was imputed.

Categorical variables were only tested if sufficient number of subjects belong to each category, alternatively, grouping of categories was to be considered.

6.2.2 E-R analyses strategy

E-R analyses strategy on dosimetry and acute toxicity during Cycle 1 is described in the following sections. The programs were validated at the critical level (programs checked by an independent modeler).

6.2.2.1 Exposure-Dosimetry analyses

Exposure-Dosimetry analyses were based on the PK-Dosimetry dataset, to explore the potential correlations between exposure metrics and [¹⁷⁷Lu]Lu-PSMA-617 dosimetry in critical organs (i.e. kidney, bone marrow, salivary glands and lacrimal glands) in mCRPC patients.

Distribution of organ dosimetry data were first plotted, and correlations between exposure and organ dosimetry were displayed using scatterplots. Correlations between organ dosimetry and baseline covariates were graphically explored. Then, a linear regression was applied to analyze the relationship between the response variable Y (i.e. organ dosimetry), each exposure metric X and any potential baseline covariate Z. The mathematical equation can be generalized as follows:

$$Y = \alpha_0 + \beta_X \cdot X + \beta_Z \cdot Z + \varepsilon$$

Where α_0 is the intercept, β_X the regression coefficient corresponding to the exposure metric X, and β_Z the regression coefficient corresponding to the baseline covariate Z. ε corresponds to the error between the prediction of the model and the actual results.

Each exposure metric, listed in [Table 5-3](#) was evaluated independently as a predictor of dosimetry in the organs at risk. P-values were reported to indicate whether the hypothesis (i.e. $\beta=0$) can be rejected or accepted.

6.2.2.2 Exposure-Toxicity analyses

Exposure-toxicity analyses were based on the PK/Dosimetry-Toxicity datasets, to explore relationships between exposure metrics and organ dosimetry with acute toxicity at Cycle 1 related to the critical organs (i.e. kidney, bone marrow, salivary glands and lacrimal glands) in mCRPC patients.

Relationships between exposure metrics and the related organ toxicity listed in [Table 5-4](#) and [Table 5-5](#) were explored one by one. For continuous response metrics, scatter plots were generated with a linear regression to identify any trend. For categorical response metrics, summary statistics by category were reported, and distributions of exposure metrics in relation to toxicity events were displayed.

6.2.3 Analysis software

Data analyses, plots and linear regressions were performed in R.3.6.1 in the DaVinci HPCE.

7 Results

7.1 Population PK modeling results

The key programs and popPK models with their corresponding GPSII locations are listed in [Table 7-1](#).

Table 7-1 List of key programs and popPK models

Description	File name	GPSII location
Rscript with data summary and exploratory plots	Task01-Data.exploration.R	CAAA000A1/CAAA000A12301/mas_1/model/pgm_001/01-Data/
Rscript to run the key Monolix models	Task02-Run.Monolix.R	CAAA000A1/CAAA000A12301/mas_1/model/pgm_001/02-PopPK/Scripts/

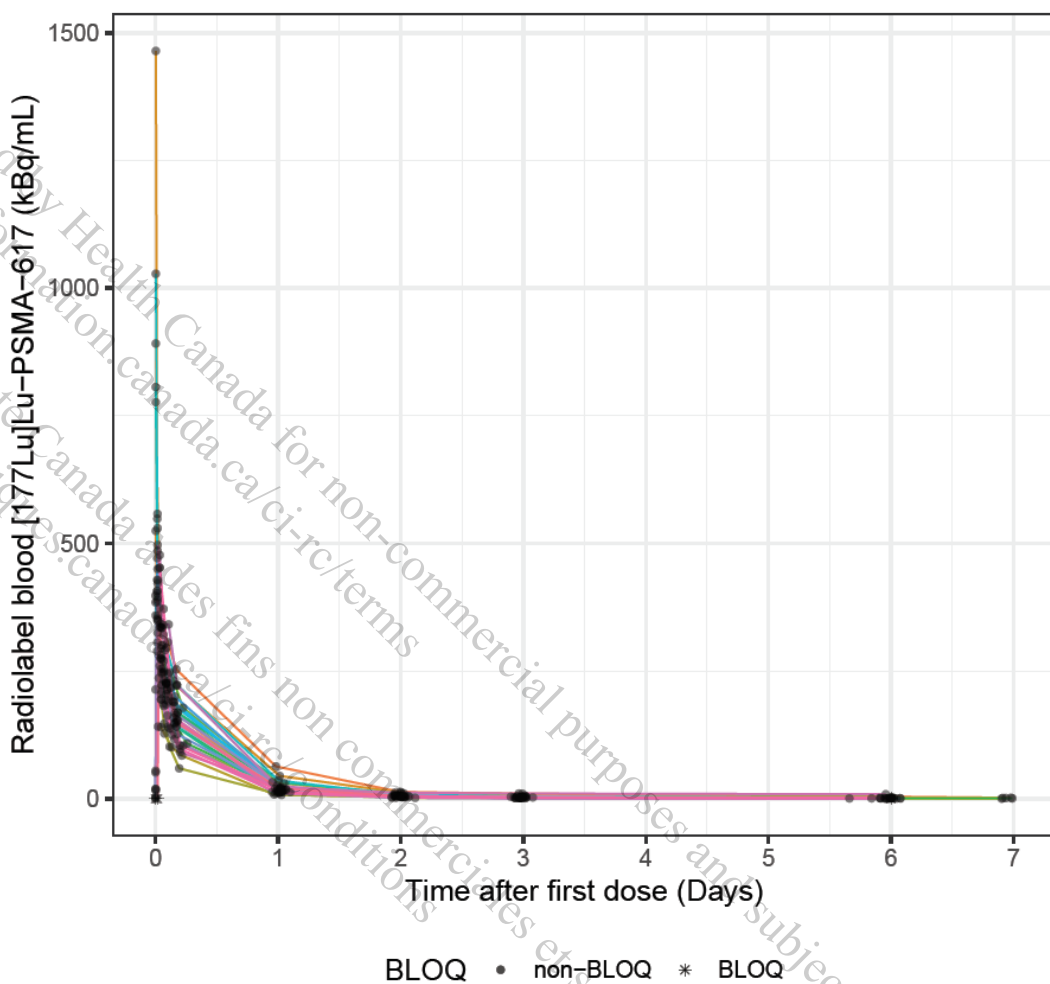
Description	File name	GPSII location
Base popPK model	Run8 mlxtran	CAAA000A1/CAAA000A12301/m as_1/model/pgm_001/02-PopPK/Runs.Submission/
Final popPK model	Run16 mlxtran	CAAA000A1/CAAA000A12301/m as_1/model/pgm_001/02-PopPK/Runs.Submission/
Model code including AUC calculation	Model.txt	CAAA000A1/CAAA000A12301/m as_1/model/pgm_001/02-PopPK/Runs.Submission/
Sycomore project for comparison of Monolix runs	Runs.Summary.syc	CAAA000A1/CAAA000A12301/m as_1/model/pgm_001/02-PopPK/Runs.Submission/
Rscript to generate diagnostic plots for the final popPK model	Task03-Diagnostic.plots.R	CAAA000A1/CAAA000A12301/m as_1/model/pgm_001/02-PopPK/Scripts/
Associated .Rmd file for diagnostic plots	GOFs.Run.Rmd	CAAA000A1/CAAA000A12301/m as_1/model/output_001/02-PopPK/
Rscript to predict individual PK exposure metrics	Task04-PK.Metrics.R	CAAA000A1/CAAA000A12301/m as_1/simulation/pgm_001/
Rscript to create covariate tables for simulations	Task05-Create.Simul.Cov.R	CAAA000A1/CAAA000A12301/m as_1/simulation/pgm_001/
Simulx project for covariate effect simulations	Covariate.Simulations.Run16.smlx	CAAA000A1/CAAA000A12301/m as_1/simulation/pgm_001/
Rscript to run the covariate effect simulations	Task05-Simul.Cov.R	CAAA000A1/CAAA000A12301/m as_1/simulation/pgm_001/

In the following sections, the radioactivity-blood PK refers to the decay-corrected PK.

7.1.1 Description of observed data

The analysis of [¹⁷⁷Lu]Lu-PSMA-617 PK used 265 observations available from 30 individuals after the first dose administration of 7.4 GBq ($\pm 10\%$). The BLOQ value was set at 0.015 kBq/mL, the minimal (except 0) radioactivity-blood concentration observed among patients. Two samples were ignored as they were BLOQ values reported between two non-BLOQ values. Only 3 (1%) observations were equal or below the LOQ. The median number of observations per subject was 9 (minimum 7 and maximum 9).

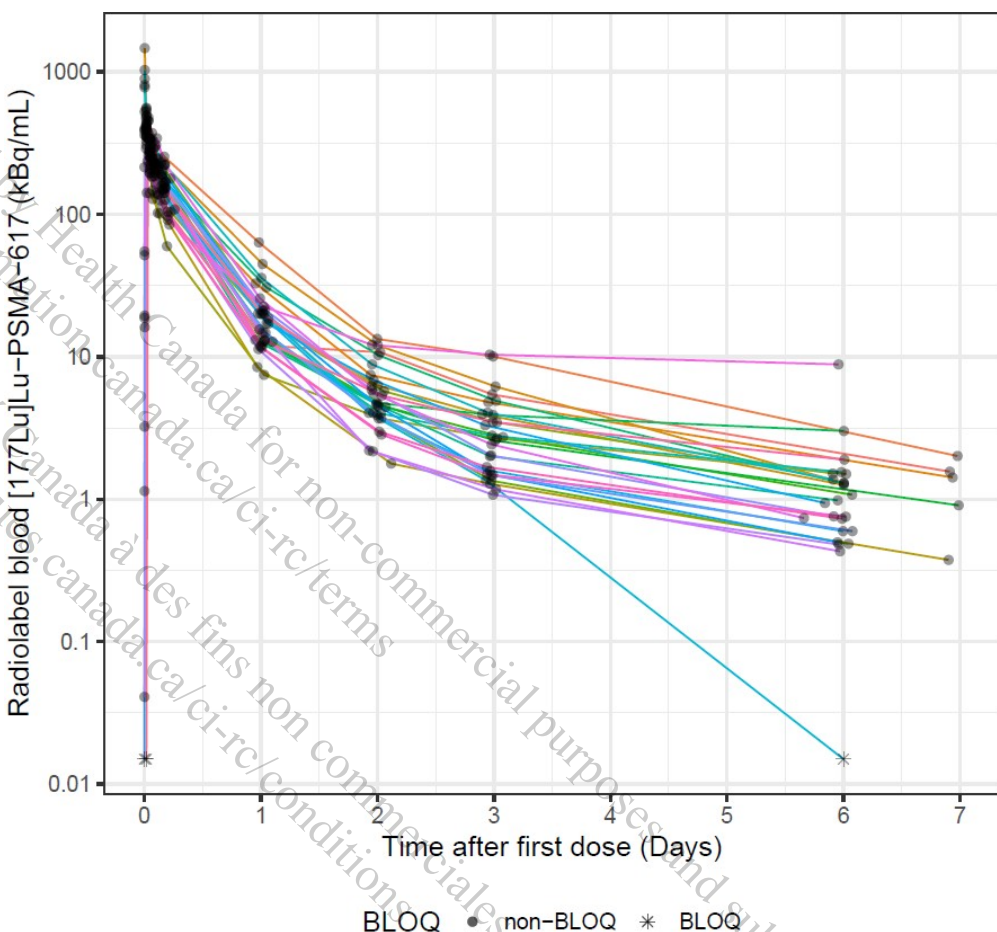
The observed individual data for the radioactivity-blood PK of [¹⁷⁷Lu]Lu-PSMA-617 on both linear and log-linear scales are shown in [Figure 7-1](#) and [Figure 7-2](#). Spaghetti plots limited to the first 7 hours are available in [Appendix 5.1](#) ([Figure 11-14](#) and [Figure 11-15](#)).

Figure 7-1 Spaghetti plots of observed individual radioactivity-blood PK of [^{177}Lu]Lu-PSMA-617 (Linear scale)

CAAA000A1/CAAA000A12301/mas_1/model/pgm_001/01-Data/Task01-Data.exploration.R
-> CAAA000A1/CAAA000A12301/mas_1/model/output_001/01-Data/Task01-Spaghetti.Lin.pdf

The black dots correspond to the observations above the LOQ, and black crosses to the observations below the LOQ. The lines are colored by subjects.

BLOQ: below the limit of quantification.

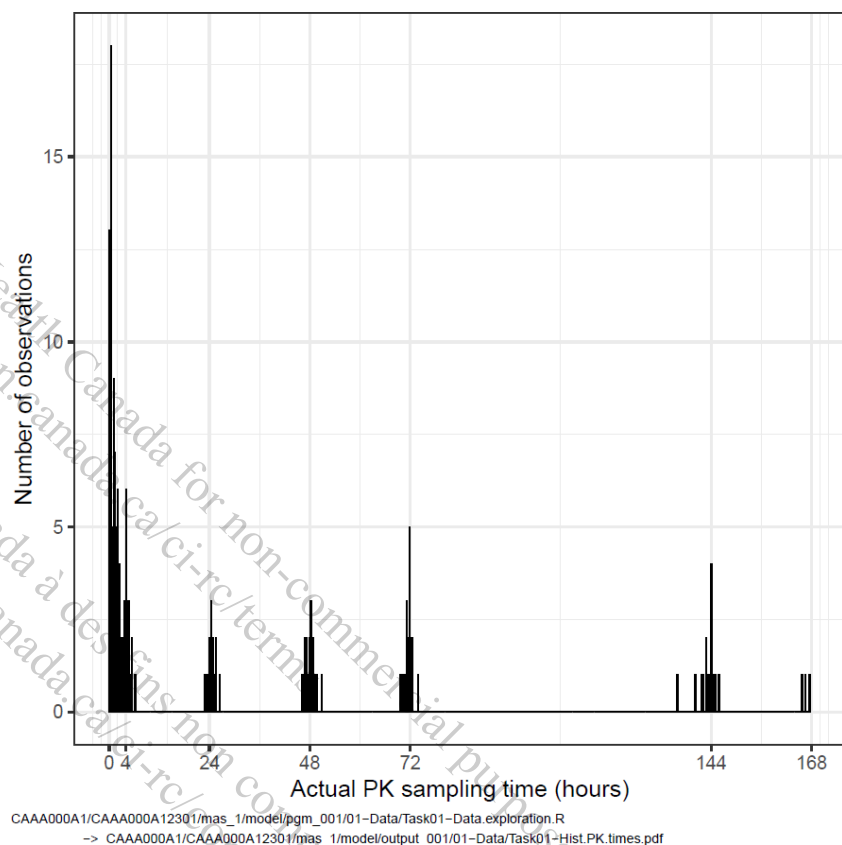
Figure 7-2 Spaghetti plots of observed individual radioactivity-blood PK of [^{177}Lu]Lu-PSMA-617 (Log-linear scale)

CAAA000A1/CAA000A12301/mas_1/model/pgm_001/01-Data/Task01-Data.exploration.R
-> CAAA000A1/CAA000A12301/mas_1/model/output_001/01-Data/Task01-Spaghetti.Log.pdf

The black dots correspond to the observations above the LOQ, and black crosses to the observations below the LOQ. The lines are colored by subjects.

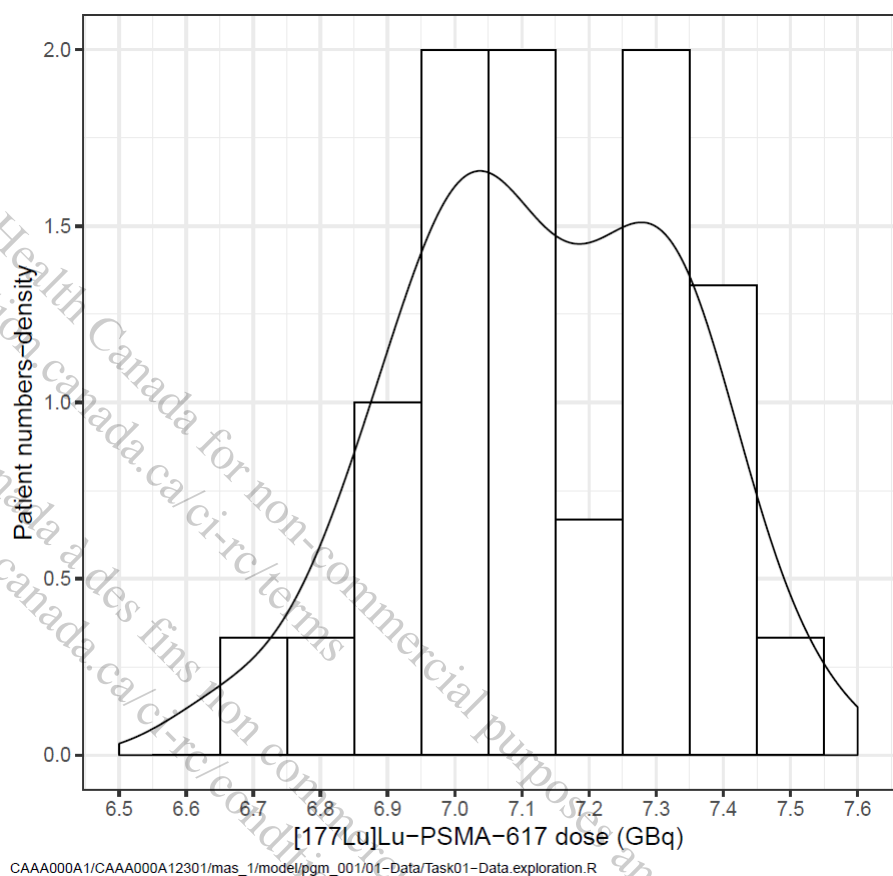
BLOQ: below the limit of quantification.

PK samples were collected at the following nominal times: at the end of infusion, and 20 min, 60 min, 2 h, 4 h, 24 h, 48 h, 72 h, Day 6 after the end of infusion. The distribution of actual sampling times used for the collection of the PK information is shown in Figure 7-3. The actual sampling times ranged from 0.017 h to 167.750 h.

Figure 7-3 Distribution of actual PK sampling times

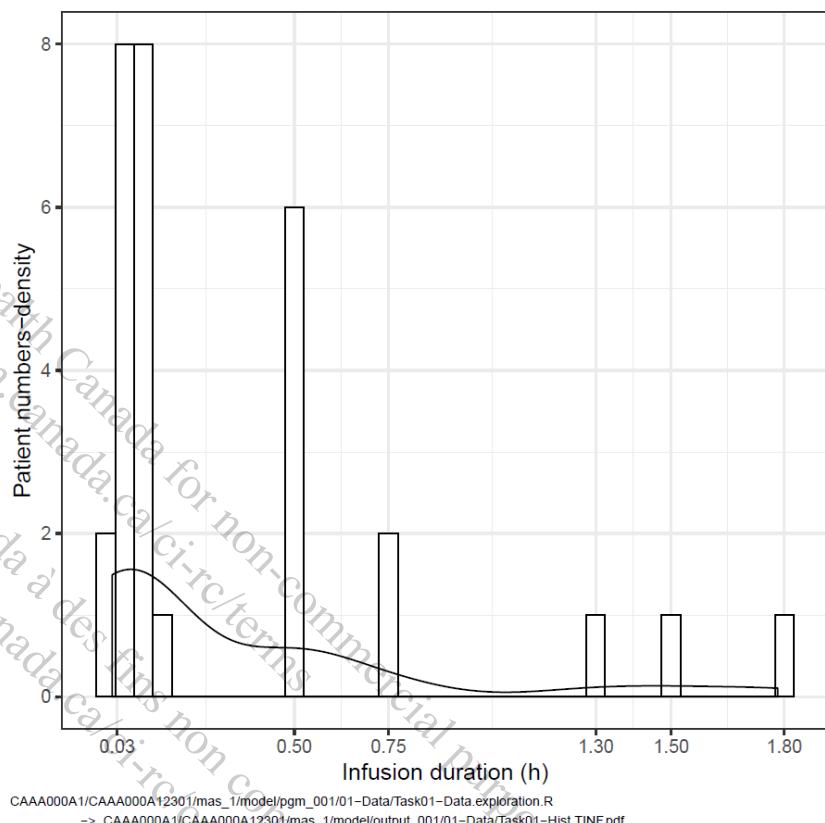
CAAA000A1/CAAA000A12301/mas_1/model/pgm_001/01-Data/Task01-Data.exploration.R
-> CAAA000A1/CAAA000A12301/mas_1/model/output_001/01-Data/Task01-Hist.PK.times.pdf

The first dose administered ranged from 6.66 GBq to 7.52 GBq, with a median dose of 7.12 GBq. The distribution of the doses, along with the density curve is shown in [Figure 7-4](#).

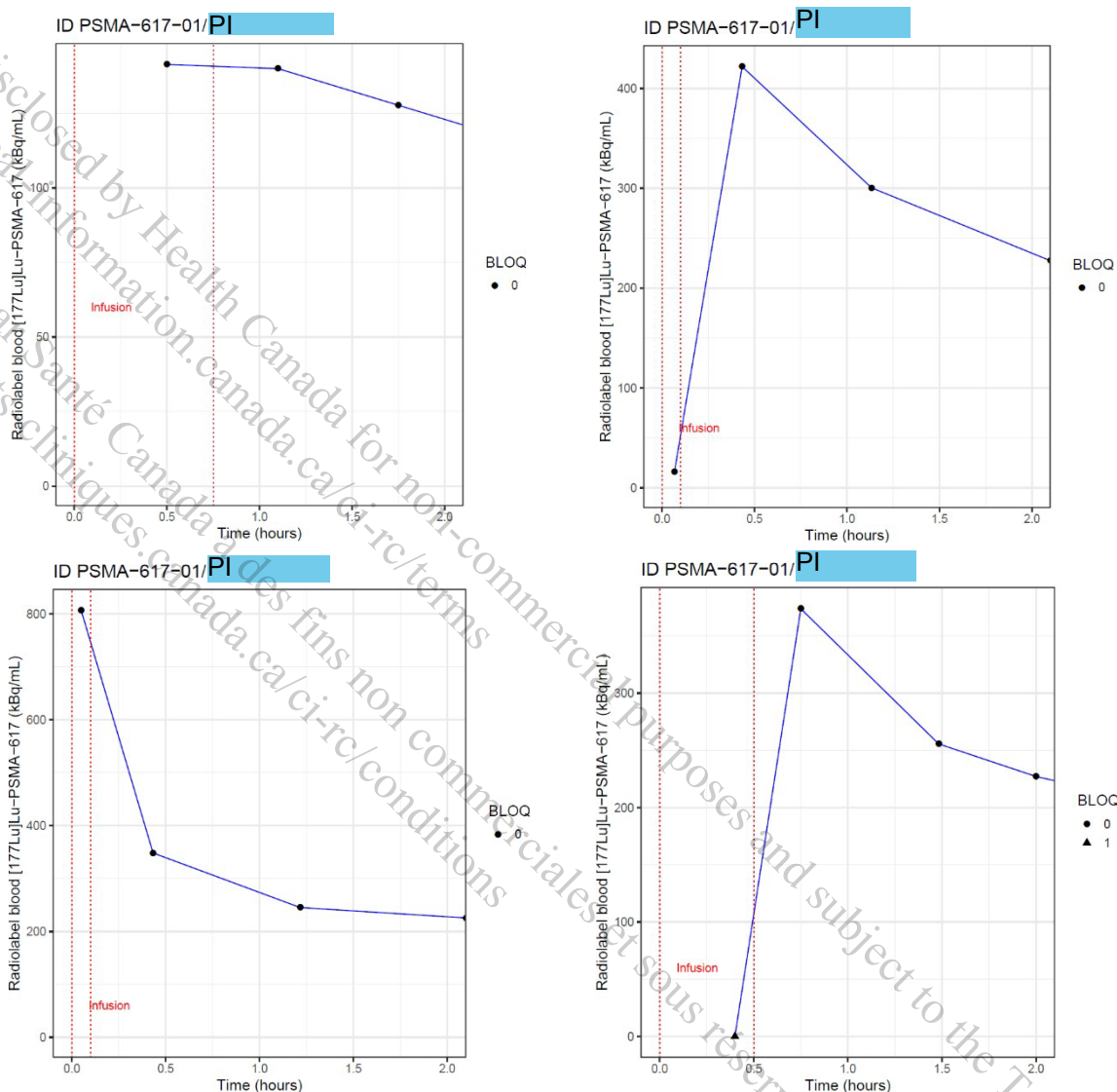
Figure 7-4 Distribution of $[^{177}\text{Lu}]\text{Lu-PSMA-617}$ doses administered at the first cycle

CAAA000A1/CAAA000A12301/mas_1/model/pgm_001/01-Data/Task01-Data.exploration.R
-> CAAA000A1/CAAA000A12301/mas_1/model/output_001/01-Data/Task01-Hist.Doses.pdf

The duration of the infusion is highly variable between individuals, it ranged from 0.017 h to 1.783 h, as illustrated in [Figure 7-5](#).

Figure 7-5 Distribution of infusion durations for the first dose

For all the individuals, the first post-dose sample (planned at the end of infusion per protocol) was observed during the infusion period, suggesting possible error in sampling time or infusion stop time reporting. The individual durations of infusion along with the individual actual times of first post-dose samples are listed in [Appendix 5.1 \(Table 11-2\)](#). In addition, [Figure 7-6](#) illustrated the PK, limited to the first 2 hours, together with the duration of infusion for 4 selected individuals: for 2 of them (015912-2035 and 684486-8330), the first post-dose sample was their maximum observed concentration, and for the other 2 patients (557518-3717 and 174234-7292), the first post-dose samples was their lowest observed concentration and equal or close to the LOQ.

Figure 7-6 Example of 4 individual PK profiles during the first 2 hours together with the duration of infusion

Black dots are the observed concentrations above the LOQ, and black triangles the observed concentrations below the LOQ. Vertical red dashed lines correspond to the start and end of infusion.
 Source: CAAA000A1/CAAA000A12301/mas_1/model/pgm_001/01-Data/Task01-Data.exploration.R
 Output: CAAA000A1/CAAA000A12301/mas_1/model/output_001/01-Data/Task01-Indiv.PK.TINF.pdf

A descriptive summary of demographic variables and baseline characteristics is given in [Table 7-2](#).

Table 7-2 Summary of demographic variables and baseline characteristics

	Continuous variables					
	Min	1 st quartile	Median	Mean	3 rd quartile	Max
Age (years)	52.0	61.5	67.0	66.7	72.8	80.0
Weight (kg)	63.8	78.5	88.8	89.9	97.8	143.0
BMI (kg/m ²)	18.3	24.8	28.4	28.6	31.8	38.8

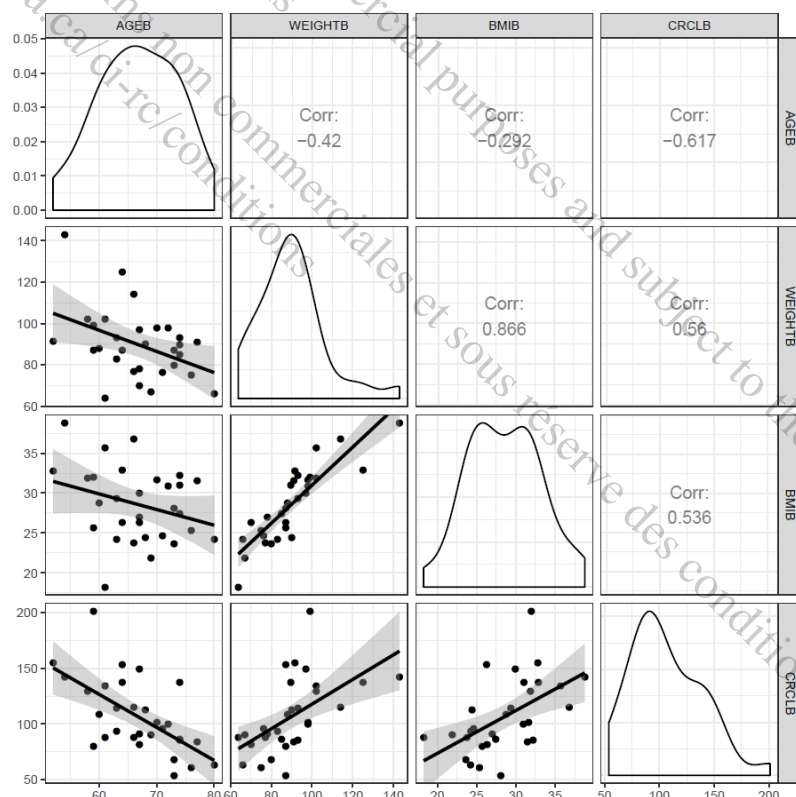
	Continuous variables					
	Min	1 st quartile	Median	Mean	3 rd quartile	Max
CrCl _{BL} (mL/min)	54.0	85.6	98.0	106.6	132.6	201.0
Categorical variables – number of patients (%)						
Race: White	30 (100%)					
Ethnicity:						
Not Hispanic or Latino	25 (83.3%)					
Hispanic or Latino	1 (3.3%)					
Not reported	4 (1.3%)					

CrCl_{BL}: baseline creatinine clearance; BMI: body mass index.

Source: CAAA000A1/CAAA000A12301/mas_1/model/pgm_001/01-Data/Task01-Data.exploration.R
Output: CAAA000A1/CAAA000A12301/mas_1/model/pgm_001/01-Data/Task01-Data.exploration.Rout (Lines 1242-1260)

Graphical exploration of correlations between baseline covariates is depicted in [Figure 7-7](#). The strongest correlation was observed between weight and BMI. CrCl_{BL} was also correlated with age, weight and BMI. Thus, these potential covariates were tested separately in the popPK model.

Figure 7-7 Correlations between baseline covariates



Corr: Correlation coefficient.

Source: CAAA000A1/CAAA000A12301/mas_1/model/pgm_001/01-Data/Task01-Data.exploration.R
Output: CAAA000A1/CAAA000A12301/mas_1/model/output_001/01-Data/Task01-Cov.pdf

7.1.2 Deviations from the analysis plan

To take into account concentrations observed during the infusion period, structural models including a 0-order absorption with and without delay were evaluated.

Covariates were normalized by the weighted mean value (i.e. the average from the individual covariate values of the dataset weighted by the number of observed PK samples per individual).

7.1.3 Base model

A few initial structural PK models were considered and explored, including one, two and three compartmental models with linear elimination. To reproduce concentrations observed during the infusion and their variability, including the low concentrations in some patients, structural models including a 0-order absorption, with and without delay, were evaluated.

An overview of the key model building steps, with statistical criteria BICc, results as well as the comparison made is summarized in [Table 7-3](#).

Table 7-3 Base model building steps

Model name	Description	BICc	Result / Comparison
Run 1	IV infusion 1 compartment Random effects: all	2678	PK elimination and distribution not well captured. High residual error.
Run 2	IV infusion 2 compartments Random effects: all	2449	PK after 4 days under-predicted.
Run 3	IV infusion 3 compartments Random effects: all	2276	PK elimination and distribution well captured. Over-prediction of the first collected samples. Small variability on Q ₃ and V ₃ , with high RSE.
Run 4	0-order absorption 3 compartments Random effects: all except Q ₃ and V ₃	2285	Remaining over-prediction of few initial samples.
Run 5	Delayed 0-order absorption 3 compartments Random effects: all except Q ₃ and V ₃	2150	Good prediction of all PK samples. Trend of correlations between random effects on CI/V ₁ and Q ₂ /V ₂ .
Run 6	Delayed 0-order absorption 3 compartments Correlation CI/V ₁ Random effects: all except Q ₃ and V ₃	2133	Correlation CI/V ₁ estimated at 0.8. Remaining trend of correlation between random effects on Q ₂ /V ₂ .
Run 7	Delayed 0-order absorption 3 compartments Correlation CI/V ₁ & Q ₂ /V ₂ Combined error model Random effects: all except Q ₃ and V ₃	2091	Correlation CI/V ₁ estimated at 0.9. No outlier in pcVPC. High RSE for the additive part of the error model.

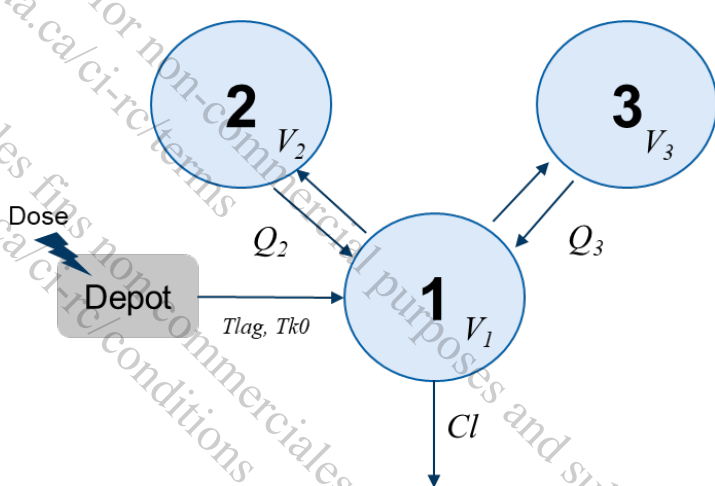
Model name	Description	BICc	Result / Comparison
Run 8 Base model	Delayed 0-order absorption 3 compartments Correlation Cl/V_1 & Q_2/V_2 Proportional error model Random effects: all except Q_3 and V_3	2108	Similar parameter estimates and diagnostic plots as Run 7.

BICc: corrected Bayesian information criteria; RSE: relative standard error; pcVPC: prediction-corrected visual-predictive check.

Source: CAAA000A1/CAAA000A12301/mas_1/model/pgm_001/02-PopPK/Runs.Submission/Runs.Summary.syc

The best structural model that has been selected is a three-compartment model with a delayed 0-order absorption and linear elimination as illustrated in [Figure 7-8](#).

Figure 7-8 Structural PK model



The following PK parameters were estimated:

- Tlag, the delay before the artificial absorption
- Tk0, the duration of the artificial 0-order absorption
- Cl, the clearance of elimination
- V_1 , the volume of distribution of the first (or central) compartment
- Q_2 , the inter-compartmental clearance from compartment 1 to compartment 2
- V_2 , the volume of distribution of second compartment
- Q_3 , the inter-compartmental clearance from compartment 1 to compartment 3
- V_3 , the volume of distribution of third compartment

The algorithm was not able to estimate random effects on Q_3 and V_3 , and those random effects were thus fixed to 0. IIV from all the other PK parameters were estimated and assumed to follow a log-normal distribution. Correlations between random effects on Cl and V_1 , and on Q_2 and V_2 , were introduced in the base model and estimated to be greater than 0.8 ([Table 7-4](#)).

The residual variability was first modeled using a combined error model (combined2 in Monolix, including both a proportional and an additive parts), but the additive part was poorly estimated with high uncertainty. BICc of the model with a proportional residual variability was slightly higher (2108 vs. 2091), and no difference was noted on the parameter estimates and diagnostic plots. Based on the parsimony principle, it was decided to keep a proportional error model in the base model.

Parameter estimates from the base model are reported in [Table 7-4](#).

Table 7-4 Parameter estimates from the base popPK model

Parameter (Unit)	Fixed effect			IIV			
	Estimate	SE	RSE (%)	CV (%)	Estimate (SD)	SE	RSE (%)
Tlag (h)	0.01	0.006	50	291	1.50	0.38	25
Tk0 (h)	0.05	0.03	58	273	1.46	0.37	26
Cl (L.h ⁻¹)	2.50	0.13	5	29	0.28	0.04	13
V ₁ (L)	11.61	1.29	11	45	0.43	0.07	16
Q ₂ (L.h ⁻¹)	0.52	0.072	14	82	0.72	0.10	15
V ₂ (L)	29.29	4.49	15	96	0.81	0.12	14
Q ₃ (L.h ⁻¹)	11.73	2.15	18	0	0 FIX	NA	NA
V ₃ (L)	11.40	0.76	7	0	0 FIX	NA	NA
Correlation parameters							
Correlation Cl/V ₁	0.82	0.08	10			NA	
Correlation Q ₂ /V ₂	0.87	0.05	6			NA	
Residual error model parameter							
Proportional error (%)	13.96	0.01	8			NA	

CV: coefficient of variation; IIV: inter-individual variability; NA: not applicable; RSE: relative standard error; SD: standard deviation; SE: standard error; 0 FIX: fixed variability to 0.

CV (%) was calculated using $\sqrt{e^{SD^2} - 1} \cdot 100\%$.

SD corresponds to the estimated omega from Monolix.

Source: CAAA000A1/CAAA000A12301/mas_1/model/pgm_001/02-PopPK/Runs.Submission/Run8 mlxtran

Output: CAAA000A1/CAAA000A12301/mas_1/model/pgm_001/02-PopPK/Runs.Submission/Run8/populationParameters.txt

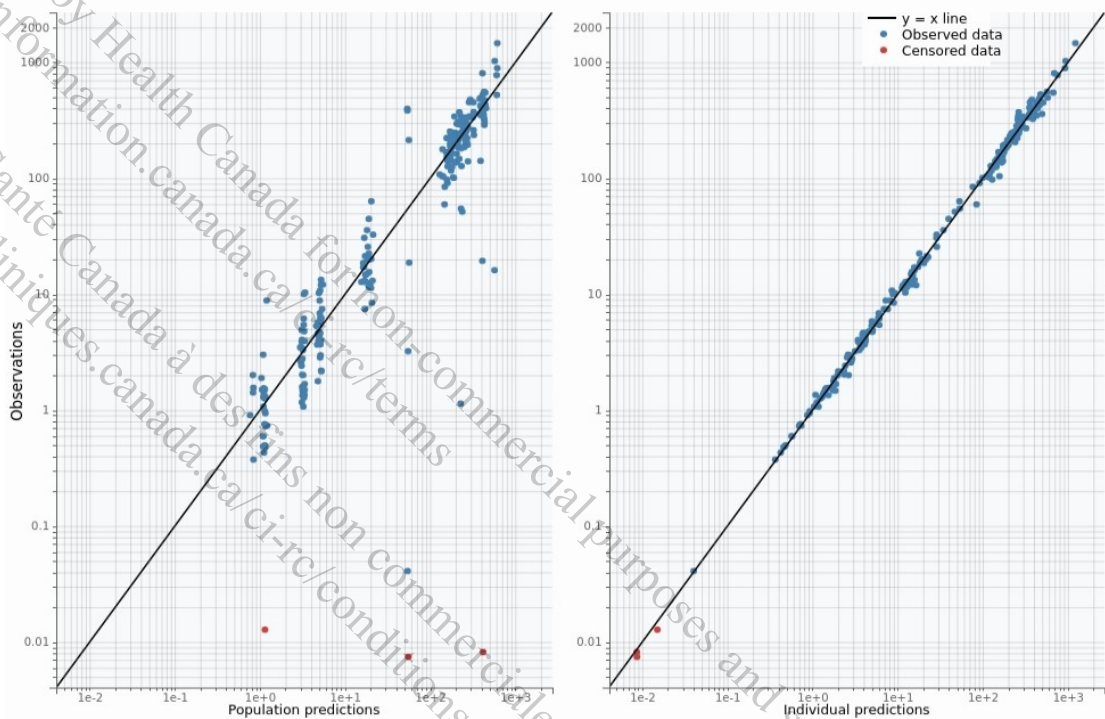
All parameters from the base model were well estimated, with relatively low RSE, except for Tlag and Tk0. Population clearance and central volume of distribution were estimated at 2.50 L.h⁻¹ and 11.61 L, respectively, with moderate variability (CV% = 29% and 45% respectively). Q₂ and V₂ were estimated at 0.52 L.h⁻¹ and 29.29 L, respectively, with relatively high variability (CV% = 82% and 96% respectively). Q₃ and V₃ were estimated at 11.73 L.h⁻¹ and 11.40 L.

Tlag and Tk0, reproducing an artificial delayed absorption after the start of dose administration, were estimated at 0.01 h and 0.05 h, respectively. These parameters had the highest RSE values, which can be explained by their high variability, also consistent with the large variability observed in the infusion times.

The residual proportional error of the model was estimated at a low value (13.96%).

All diagnostic plots suggested that the base model described the data adequately. The observed concentration vs. model predictions (population and individual) plots are presented in [Figure 7-9](#), and demonstrated a reasonable agreement between data and model predictions. The other diagnostic plots from the base model are reported in [Appendix 1.1](#).

Figure 7-9 Observed concentrations vs. population prediction or individual prediction on log scale from the base popPK model



Blue dots are the concentrations above the LOQ and red dots the simulated concentrations below the LOQ. The black line is the identity line.

Source: CAAA000A1/CAAA000A12301/mas_1/model/pgm_001/02-

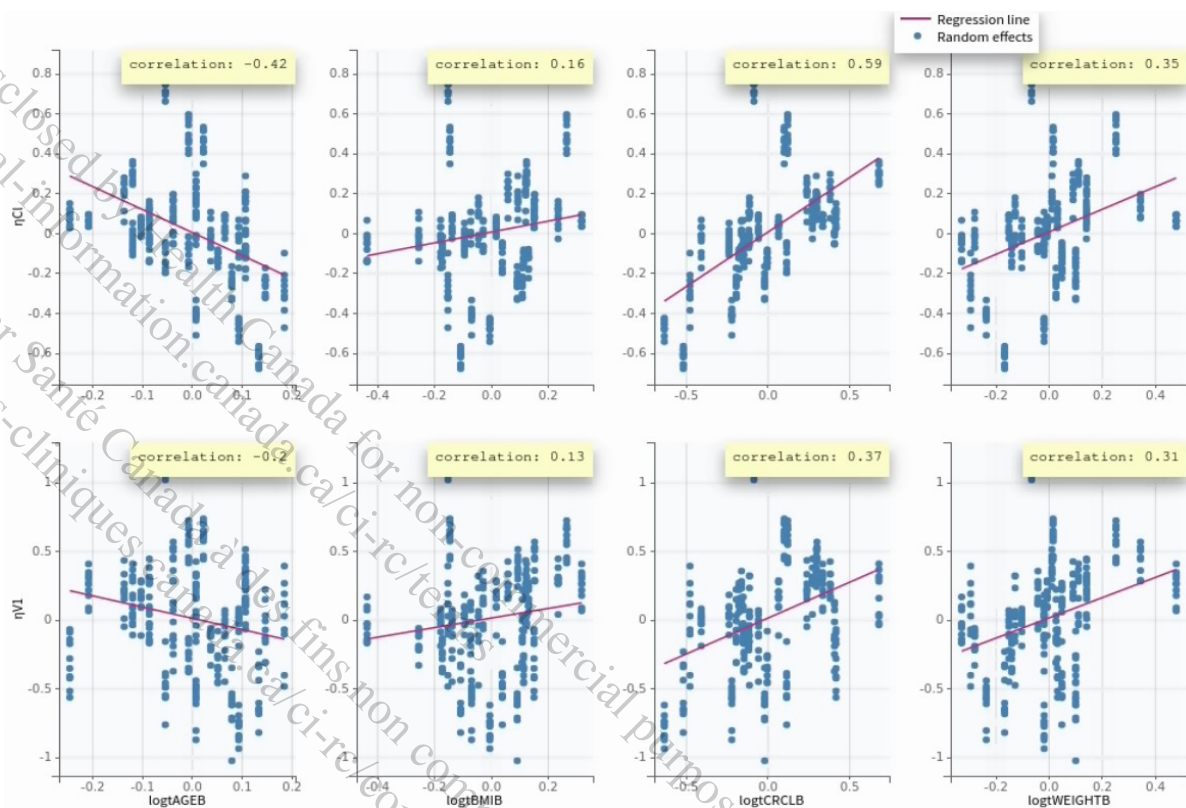
PopPK/Runs.Submission/Run8.mltran

Output: CAAA000A1/CAAA000A12301/mas_1/model/pgm_001/02-

PopPK/Runs.Submission/Run8/ChartsFigures/obspred_LIDV_0_0.png

7.1.4 Covariate selection

Post-hoc random effects of the key model parameters (i.e. Cl and V₁) from the base model was plotted against all covariates of interest, as illustrated in [Figure 7-10](#). Each covariate was log-transformed and centered on the weighted mean. The figure displays the estimators of the individual random effects using simulated parameters from the conditional distributions (10 simulated parameters per individual). These estimators lead to more reliable results compared to the conditional mode or mean, as they represent the uncertainty of the individual's parameter value.

Figure 7-10 Post-hoc random effects from the base popPK model vs. covariates of interest

Post-hoc random effects were simulated from the conditional distributions. Covariates were normalized by the weighted mean value and log-transformed. The weighted mean for age, weight, CrCl_{BL} and BMI, calculated by Monolix, were 66.4 years, 88.5 kg, 101.5 mL/min and 28.2 kg/m², respectively. Red lines correspond to the regression lines and the correlation values represent the Pearson correlation coefficients.

Source: CAAA000A1/CAAA000A12301/mas_1/model/pgm_001/02-PopPK/Runs.Submission/Run8 mlxtran
Output: CAAA000A1/CAAA000A12301/mas_1/model/output_001/02-PopPK/Run8.Monolix/Covariates1.PNG

The covariates showing the strongest correlation with the random effect on Cl are CrCl_{BL}, age and weight, with Pearson correlation coefficient of 0.59, 0.42 and respectively 0.35. Correlations were also detected between the random effect on V_d and CrCl_{BL} as well as weight (Pearson correlation coefficient of 0.37 and respectively 0.31).

By definition, CrCL_{BL} is derived from age and weight, as described in [Section 5.3.1](#); this dependence was also illustrated based on the observed data ([Figure 7-7](#)). Thus, these 3 covariates had to be tested separately, and it was not possible to build a formal full model, including all potential relationships.

An alternative stepwise approach has been applied for covariate selection, as summarized in [Table 7-5](#). Only parameter-covariate relationships with a correlation coefficient ≥ 0.3 ([Figure 7-10](#)) were evaluated and selection criteria were based on BICc, significance of Wald test and reduction of variability, as described in [Section 6.1.7](#).

Table 7-5 Models for covariate selection

Model name	Description	BICc	Result / Comparison
Run 8 Base model	No covariate	2108	CV% of CI=29% CV% of V ₁ =45%
Run 10	CrCl _{BL} on CI	2099	Significant CrCl _{BL} effect on CI (p=0.00014) CV% of CI=23% CV% of V ₁ =45 %
Run 11	Age on CI	2102	Non-significant age effect on CI (p=0.3) CV% of CI=25% CV% of V ₁ =45 %
Run 12	WT _{BL} on CI	2109	Non-significant WT _{BL} effect on CI (p=0.4) CV% of CI=27% CV% of V ₁ =44 %
Run 13	CrCl _{BL} on V ₁	2108	Non-significant CrCl _{BL} effect on V ₁ (p=0.2) CV% of CI=29% CV% of V ₁ =49 %
Run 14	WT _{BL} on V ₁	2111	Non-significant WT _{BL} effect on V ₁ (p=0.4) CV% of CI=29% CV% of V ₁ =42 %
Run 15	CrCl _{BL} on CI + CrCl _{BL} on V ₁	2097	Significant CrCl _{BL} effect on CI (p=0.00004) Non-significant CrCl _{BL} effect on V ₁ (p=0.06) CV% of CI=22% CV% of V ₁ =42 %
Run 16 Final model	CrCl _{BL} on CI + WT _{BL} on V ₁	2098	Significant CrCl _{BL} effect on CI (p=0.000007) Significant WT _{BL} effect on V ₁ (p=0.02) CV% of CI=22% CV% of V ₁ =42 %
Run 17	WT _{BL} on CI + CrCL _{BL} on V ₁	2112	Non-significant WT _{BL} effect on CI (p=0.9) Non-significant CrCl _{BL} effect on V ₁ (p=0.2) CV% of CI=29% CV% of V ₁ =50 %
Run 18	Age on CI + WT _{BL} on V ₁	2101	Significant Age effect on CI (p=0.0002) Non-significant WT _{BL} effect on V ₁ (p=0.2) CV% of CI=25% CV% of V ₁ =42 %
Run 19	Age on CI + CrCl _{BL} on V ₁	2104	Significant Age effect on CI (p=0.005) Non-significant CrCl _{BL} effect on V ₁ (p=0.7) CV% of CI=25% CV% of V ₁ =47 %
Run 20	WT _{BL} on CI + WT _{BL} on V ₁	2108	Significant WT _{BL} effect on CI (p=0.04) Non-significant WT _{BL} effect on V ₁ (p=0.06) CV% of CI=26 % CV% of V ₁ =42 %

Model name	Description	BICc	Result / Comparison
Run 21	Run 16 - No correlation between Cl and V ₁	2116	Remaining trend of strong correlation between random effects of Cl and V ₁ . No remaining trend of covariate effect.

BICc: corrected Bayesian information criteria; p: p-value associated with Wald test; WT_{BL}: baseline weight.

CV (%) was calculated using $\sqrt{e^{SD^2} - 1} \cdot 100\%$.
Covariates were normalized by the weighted mean value and log-transformed. The weighted mean for age, WT_{BL} and CrCl_{BL}, calculated by Monolix, were 66.4 years, 88.5 kg and 101.5 mL/min, respectively.

Source: CAAA000A1/CAAA000A12301/mas_1/model/pgm_001/02-PopPK/Runs/Submission/Runs.Summary.syc

Based on p-values from Wald test and BICc, CrCl_{BL} was found to be statistically significant on Cl (Run 10). Adding CrCl_{BL} on V₁ (Run 15) reduced the BICc, but the covariate was not statistically significant, IIV was not reduced and no improvement in GOFs was noted. Adding WT_{BL} on V₁ (Run 16) led to similar BICc, but reduced the IIV and was statistically significant based on Wald test. The Run 16 was considered as the final model, which is further described in [Section 7.1.5](#).

Increasing CrCl_{BL} was associated with higher Cl, and increasing WT_{BL} with higher V₁. CrCl_{BL} reduced the CV% of Cl from 29% in the base model (Run 8) to 22% in the final model (Run 16). WT_{BL} reduced the CV% of V₁ from 45% in the base model to 42% in the final model.

Post-hoc random effects of Q₂ and V₂ from the base model were also plotted against covariates ([Appendix 1.1, Figure 11-6](#)) for exploratory purpose, but no correlation was identified to potentially explain their high variability (CV% = 82% and 96% respectively in the base model).

The use of the automatic covariate model building algorithm COSSAC, implemented in Monolix, was also explored. But the algorithm did not converge, with an error message due to a possible outlier, a BLOQ value observed (i.e. 0.015 kBq/mL in the popPK dataset) during the infusion for the individual 584617-1266, as illustrated on [Figure 7-6](#).

7.1.5 Final model: description

The final model is therefore a three-compartment model with a delayed 0-order absorption and linear elimination as previously illustrated in [Figure 7-8](#). As per the pre-defined criteria for the covariate selection, CrCl_{BL} effect on Cl and WT_{BL} effect on V₁ were retained in the final model.

The control stream (.mlxtran) from the final popPK model is provided in the [Appendix 2](#). Data specifications of columns used in Monolix for the final popPK model are summarized in [Appendix 4](#).

7.1.6 Final model: parameter estimates

The parameter estimates of the final model are presented in [Table 7-6](#).

Table 7-6 Parameter estimates from the final popPK model

Parameter (Unit)	Fixed effect			IIV			
	Estimate	SE	RSE (%)	CV (%)	Estimate (SD)	SE	RSE (%)
Tlag (h)	0.01	0.006	48	291	1.50	0.35	23
TK0 (h)	0.06	0.03	54	264	1.44	0.36	25
Cl (L.h ⁻¹)	2.50	0.11	4	22	0.22	0.03	14
CrCl _{BL} effect on Cl	0.46	0.10	22	NA	NA	NA	NA
V ₁ (L)	11.53	1.16	10	42	0.40	0.06	15
WT _{BL} effect on V ₁	0.75	0.33	45	NA	NA	NA	NA
Q ₂ (L.h ⁻¹)	0.52	0.07	13	80	0.70	0.10	14
V ₂ (L)	29.34	4.42	15	93	0.79	0.11	14
Q ₃ (L.h ⁻¹)	12.00	2.11	18	0	0 FIX	NA	NA
V ₃ (L)	11.51	0.67	6	0	0 FIX	NA	NA
Correlation parameters							
Correlation Cl/V ₁	0.84	0.08	10	NA			
Correlation Q ₂ /V ₂	0.86	0.05	6	NA			
Residual error model parameter							
Proportional error (%)	13.96	1	7	NA			

CrCl_{BL}: baseline creatinine clearance; CV: coefficient of variation; IIV: inter-individual variability; NA: not applicable; RSE: relative standard error; SD: standard deviation; SE: standard error; WT_{BL}: baseline weight; 0 FIX: fixed variability to 0.

CV (%) was calculated using $\sqrt{e^{SD^2} - 1} \cdot 100\%$.

SD corresponds to the estimated omega from Monolix. Covariates were normalized by the weighted mean value and log-transformed. The weighted mean for WT_{BL} and CrCl_{BL}, calculated by Monolix, were 88.5 kg and 101.5 mL/min, respectively.

Source: CAAA000A1/CAAA000A12301/mas_1/model/pgm_001/02-PopPK/Runs.Submission/Run16 mlxtran

Output: CAAA000A1/CAAA000A12301/mas_1/model/pgm_001/02-PopPK/Runs.Submission/Run16/populationParameters.txt

All parameters from the final model were estimated with reasonable precision, with RSE of 45% at most, except for Tlag and Tk0.

For a typical subject with CrCl_{BL}=101.5 mL/min and WT_{BL}=88.5 kg, the clearance was estimated to be 2.50 L.h⁻¹ and V₁ was estimated to be 11.53 L. V₂ and V₃ were estimated at 29.34 L and 11.51 L, respectively. Q₂ and Q₃ were estimated at 0.52 L.h⁻¹ and 12.00 L.h⁻¹, respectively.

Variabilities on Cl and V₁ were moderate (CV% = 22% and 42% respectively), while variabilities on Q₂ and V₂ were estimated at relatively high values (CV% = 80% and 93% respectively).

Tlag and Tk0, reproducing an artificial delayed absorption after the start of administration, were estimated at 0.01 h and 0.06 h, respectively. These parameters had the highest RSE values, which can be explained by their high variability, also consistent with the large variability observed in the infusion times.

The residual proportional error of the model was estimated at a low value (13.96%).

CrCl_{BL} had a significant impact on Cl. More specifically, a decrease of CrCl_{BL} by 40%, such as a decrease from 101.5 mL/min to 60.9 mL/min, will lead to an average decrease of Cl by 21%.

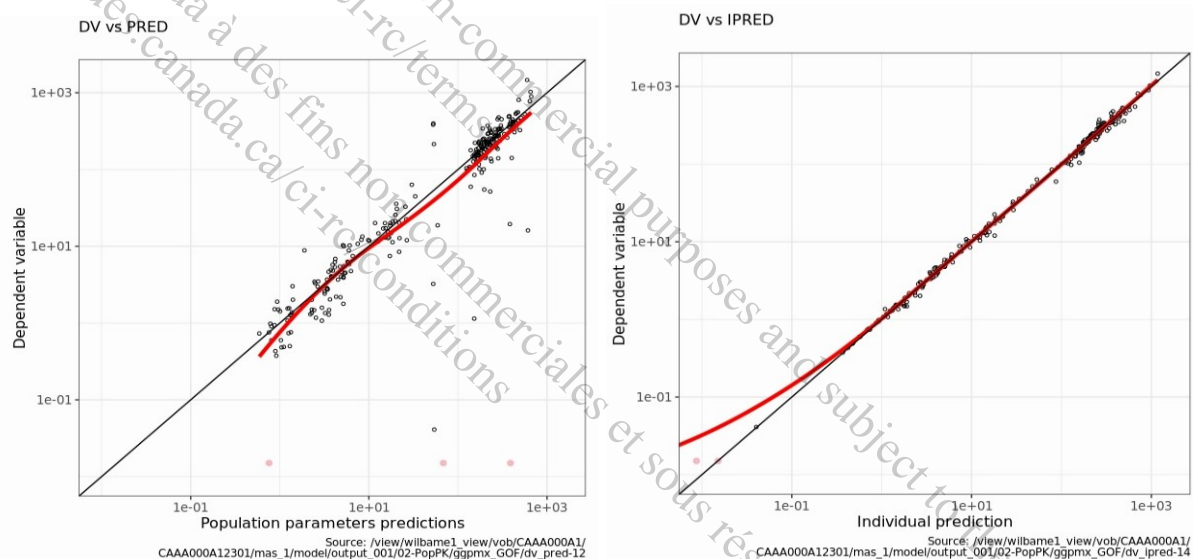
WT_{BL} had a significant impact on V₁. More specifically, a decrease of WT_{BL} by 23%, such as a decrease from 88.5 kg to 68.1 kg, will lead to an average decrease of V₁ by 18%.

Impact of covariates on PK exposure metrics, AUCinf and Cmax, were explored with simulations and summarized in [Section 7.1.8](#).

7.1.7 Final model: evaluation

All diagnostic plots ([Appendix 1.2](#)) suggested that the final popPK model described the data adequately. The plots of observed concentration vs. model predictions (population and individual) are presented in [Figure 7-11](#), and demonstrated a reasonable agreement between data and model predictions.

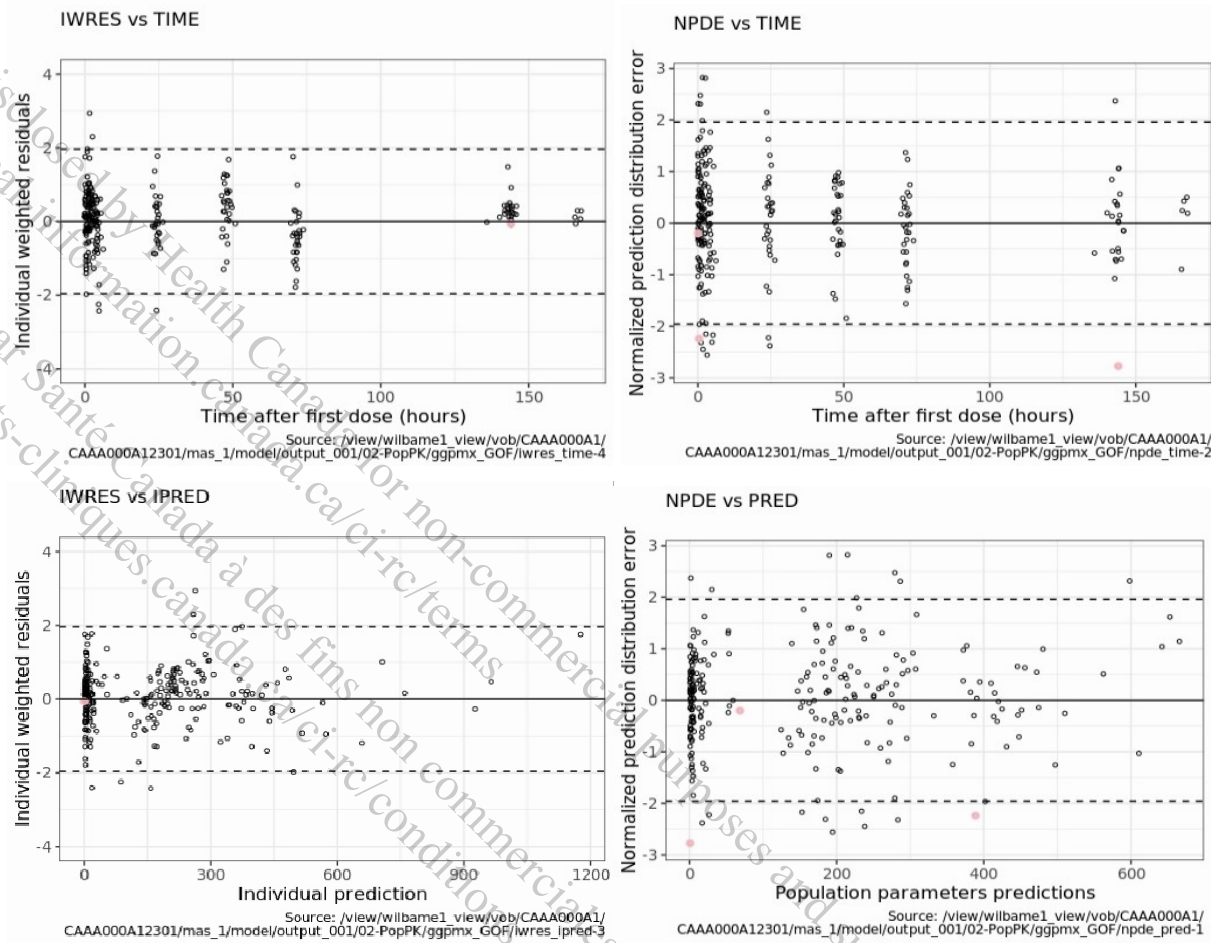
Figure 7-11 Observed concentrations vs. population prediction (PRED) or individual prediction (IPRED) on log scale for the final popPK model



Black dots are the concentrations above the LOQ and red dots the concentration below the LOQ. The black line is the identity line and the red curve a smooth line. The dependent variable is the concentration in kBq/mL.

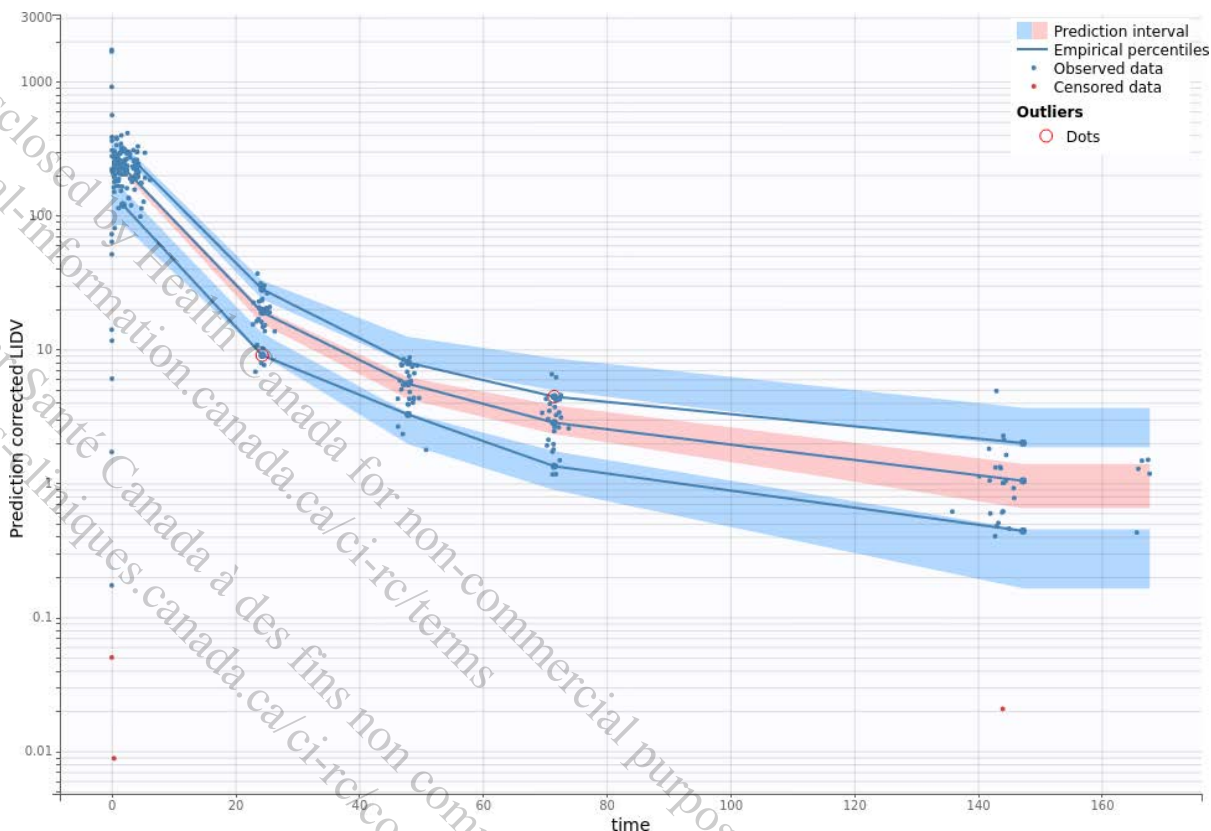
The residual plots are presented in [Figure 7-12](#). In general, the residuals (IWRES and NPDE) are symmetrical around the zero line, suggesting no trends in variability with either time or concentration.

Figure 7-12 Residual diagnostics from the final popPK model



Black dots correspond to the values above the LOQ and red dots the values below the LOQ.

The pcVPC from Figure 7-13 shows the good predictive ability of the final popPK model.

Figure 7-13 pcVPC from the final popPK model

The time corresponds to the time after start of infusion, in hours. LIDV corresponds to the concentration in kBq/mL. Solid lines display observed 10th, 50th, 90th percentiles. Blue/Pink regions show 90% prediction interval around the percentiles. Blue dots are the concentrations above the LOQ and red dots the simulated concentrations below the LOQ.

Source: CAAA000A1/CAAA000A12301/mas_1/model/pgm_001/02-PopPK/Runs.Submission/Run16/ChartsFigures/vpc_LIDV_0_0.png

All the other goodness-of-fit plots are presented in [Appendix 1.2](#).

Sensitivity analyses were performed on the final model and demonstrated the robustness of the algorithm convergence and the stability on parameter estimates. Convergence assessment from several runs using different randomly generated initial values of fixed effects, as well as different seeds is available in [Appendix 1.2 \(Figure 11-13\)](#).

7.1.8 Simulations

The final popPK model was used to simulate the effect of CrCl_{BL} and WT_{BL} on radioactivity-blood PK exposure, specifically on AUC_{inf} and Cmax. A typical subject was considered as having CrCl_{BL}=101.5 mL/min and WT_{BL}=88.5 kg.

Two external tables of covariates were created and imported in Simulx GUI:

- Table of 30 individuals with observed CrCl_{BL} values and WT_{BL} fixed to the typical value (CAAA000A1/CAAA000A12301/mas_1/simulation/pgm_001/Task05-Simul.CRCL.txt);

- Table of 30 individuals with observed WT_{BL} values and CrCl_{BL} fixed to the typical value (CAAA000A1/CAAA000A12301/mas_1/simulation/pgm_001/Task05-Simul.WT.txt).

Simulations of 500 individuals were performed for each external table. All simulated patients received a common dose of 7.4 GBq at time 0. Covariates were randomly sampled with replacement from the previously created tables. Concentrations and cumulative AUC were simulated from the time of start of infusion up to the scheduled time of the second administration (i.e. 6 weeks after the first administration). Inter-individual variability from the final popPK model were used, and residual error was fixed to 0.

Simulated patients were then categorized into renal impairment categories, based on CrCl_{BL} values, and into baseline weight categories, as described on [Table 7-7](#). As the main route of excretion for [¹⁷⁷Lu]Lu-PSMA-617 is renal, sufficient renal function (CrCl ≥ 50 mL/min) was an eligibility criteria for patients to be enrolled in the PSMA-617-01 study. Thus, there was no patients with severe renal impairment (CrCl_{BL} < 30 mL/min) in this study, and no simulations was performed for the severe renal impairment category.

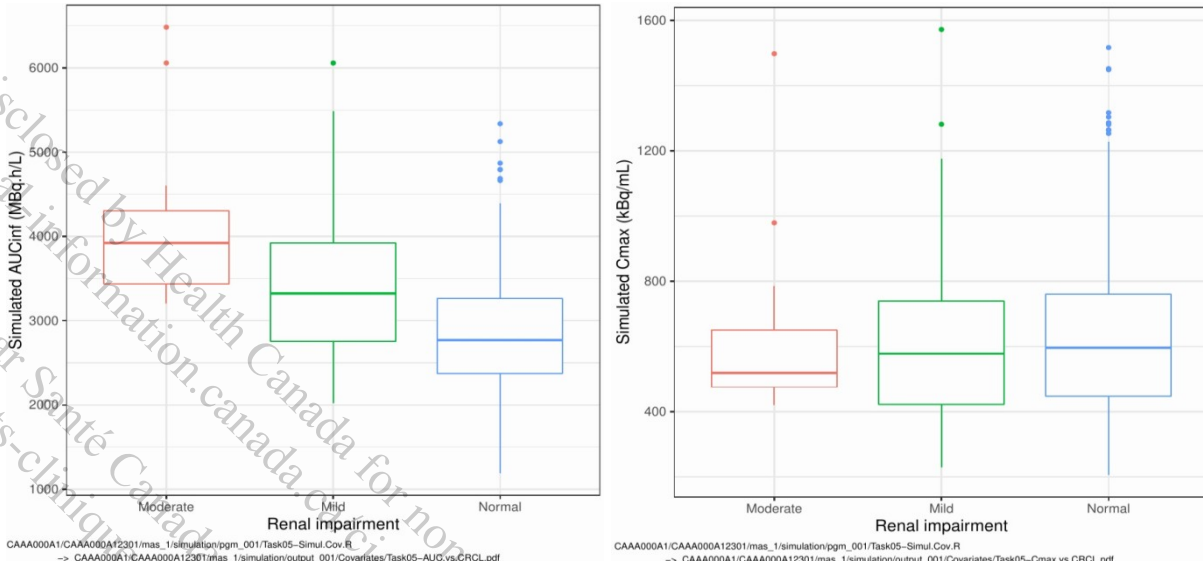
Table 7-7 Summary of observed data by renal impairment and weight categories

Category	Observed number of patients (%)	Observed value Median (1 st quartile – 3 rd quartile)
Renal impairment		
Moderate: 30 mL/min ≤ CRCL _{BL} < 60 mL/min	1 (3.3%)	54.0 mL/min (NA)
Mild: 60 mL/min ≤ CRCL _{BL} < 90 mL/min	10 (33.3%)	82.7 mL/min (70.8 – 86.3)
Normal: CRCL _{BL} ≥ 90 mL/min	19 (63.3%)	114.9 mL/min (100.6 – 139.9)
Weight category		
WT _{BL} < 88.5 kg	15 (50%)	78.0 kg (72.5 – 86.0)
WT _{BL} ≥ 88.5 kg	15 (50%)	98.0 kg (92.3 – 102.1)

CrCl_{BL}: baseline creatinine clearance; NA: not applicable; WT_{BL}: baseline weight.

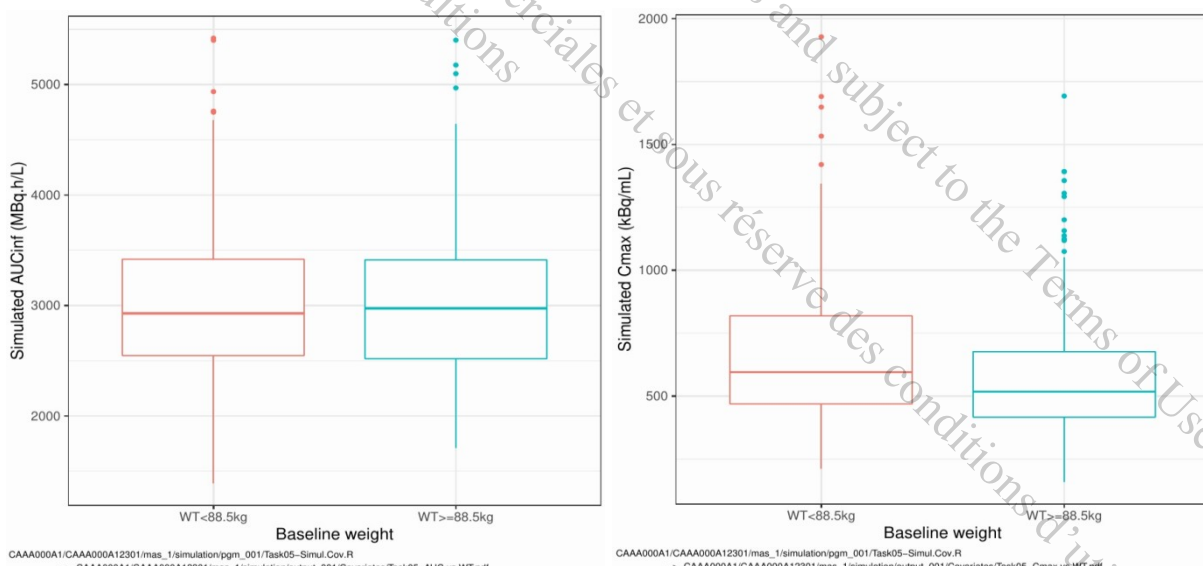
Source: CAAA000A1/CAAA000A12301/mas_1/simulation/pgm_001/Task05-Simul.Cov.R
Output: CAAA000A1/CAAA000A12301/mas_1/simulation/output_001/Covariates/Task05-Summary.CRCL.csv & Task05-Summary.WT.csv

AUCinf and Cmax were derived for each one of the 500 simulated individuals and their distribution was plotted by renal impairment category (normal, mild, moderate) in [Figure 7-14](#). A strong impact of renal impairment can be noted on AUCinf, with higher exposure in the moderate and mild categories compared to the normal category. However, as only one patient in the sub-study was observed in the moderate renal impairment category, with a CrCl_{BL} value of 54.0 mL/min, simulations from this category were only based on this value. Renal impairment did not show any significant effect on Cmax.

Figure 7-14 Box plot of simulated AUCinf and Cmax by renal impairment category

Simulations of 500 individuals were performed with covariates randomly sampled with replacement from the observed values. Only one individual had a moderate renal impairment ($\text{CrCl}_{\text{BL}}=54 \text{ mL/min}$). For each box plot, the top horizontal line is the 3rd quartile, the middle line is the median and the bottom line is the 1st quartile.

Figure 7-15 did not show any significant impact of WT_{BL} on either Cmax or AUCinf. The lack of impact on AUCinf is expected given the lack of effect of WT_{BL} on clearance.

Figure 7-15 Box plot of simulated AUCinf and Cmax by WT_{BL} 

Simulations of 500 individuals were performed with covariates randomly sampled with replacement from the observed values. For each box plot, the top horizontal line is the 3rd quartile, the middle line is the median and the bottom line is the 1st quartile.

Simulated AUCinf and Cmax were summarized for each baseline renal impairment and baseline weight categories in Table 7-8. Simulations showed a 42% and 20% increase in median of

simulated AUC_{inf} for moderate and mild renal impairment respectively vs. for normal renal function. It should be noted that simulations of moderate renal impairment are based only on one patient (CrCl_{BL}=54 mL/min). There was no significant effect of either renal impairment or weight categories on Cmax.

Table 7-8 Summary of simulated AUC_{inf} and Cmax by baseline renal impairment and baseline weight categories

PK metrics	Simulated group	Min	1 st Quartile	Median	3 rd Quartile	Max
Baseline renal impairment						
AUC _{inf} (MBq.h/L)	Moderate	3202	3436	3924	4304	6482
	Mild	2019	2753	3323	3923	6057
	Normal	1192	2371	2767	3262	5337
Cmax (kBq/mL)	Moderate	420	476	519	651	1498
	Mild	228	422	578	739	1572
	Normal	206	447	597	760	1517
Baseline weight						
AUC _{inf} (MBq.h/L)	WT _{BL} < 88.5 kg	1391	2546	2930	3420	5420
	WT _{BL} ≥ 88.5 kg	1710	2517	2974	3412	5402
Cmax (kBq/mL)	WT _{BL} < 88.5 kg	211	469	595	820	1928
	WT _{BL} ≥ 88.5 kg	159	416	517	676	1693

CrCl_{BL}: baseline creatinine clearance; WT_{BL}: baseline weight.

Source: CAAA000A1/CAAA000A12301/mas_1/simulation/pgm_001/Task05-Simul.Cov.R

Output: CAAA000A1/CAAA000A12301/mas_1/simulation/output_001/Covariates/Task05-Summary.AUC.CRCL.csv & Task05-Summary.AUC.WT.csv & Task05-Summary.Cmax.CRCL.csv & Task05-Summary.Cmax.WT.csv

Note that correlations between CrCl_{BL} and WT_{BL} were not considered for the simulations.

7.1.9 Derivation of patients' model-based PK exposure metrics

Individual patients' data, including dosing information, WT_{BL} and CrCl_{BL} values were used to predict longitudinal concentrations during the first cycle (up to the individual second administration) for the 30 sub-study patients. Missing information on the date of the second cycle from 3 individuals were imputed to the planned duration of 1 cycle (6 weeks). From these predicted concentrations, Cmax and AUC_{inf} on Cycle 1 were derived, and subsequently used for E-R analyses. A summary of individual predicted Cmax and AUC_{inf} is provided in [Table 7-9](#).

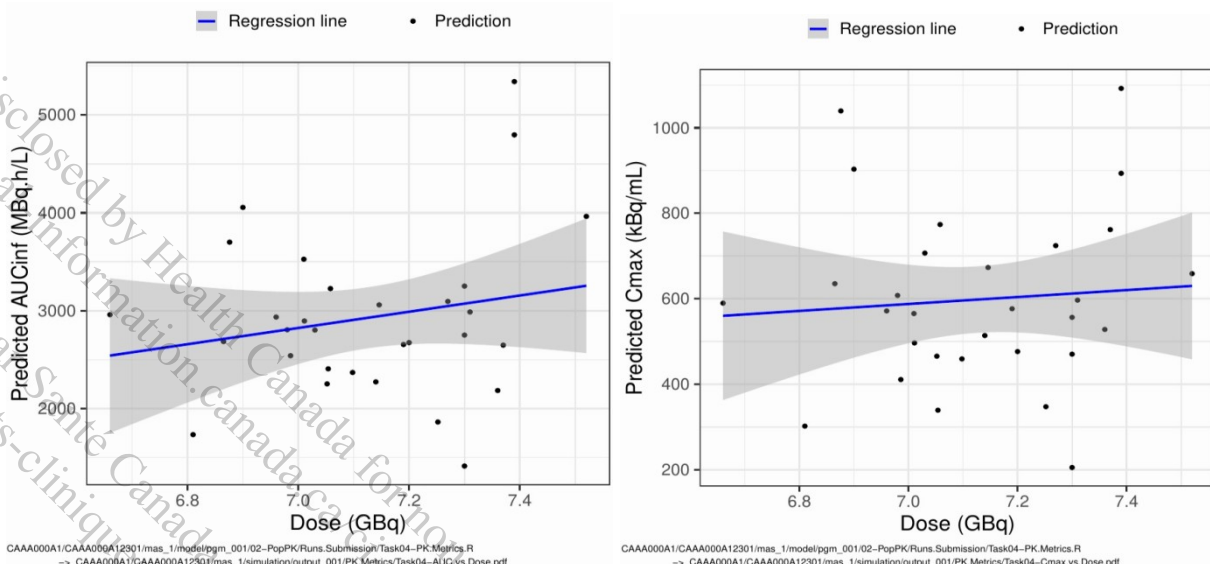
Table 7-9 Summary of predicted individual PK exposure metrics

PK metrics	Min	1 st quartile	Median	Mean	3 rd quartile	Max
AUC _{inf} (MBq.h/L)	1414	2440	2804	2928	3193	5341
Cmax (kBq/mL)	205.3	471.9	574.1	598.1	698.5	1092.2

Source: CAAA000A1/CAAA000A12301/mas_1/simulation/pgm_001/Task04-PK.Metrics.R

Output: CAAA000A1/CAAA000A12301/mas_1/simulation/output_001/PK.Metrics/Sum.PK.Metrics.csv

Individual predicted AUC_{inf} and Cmax were plotted against injected dose and did not show any clear trend of correlation, as illustrated in [Figure 7-16](#).

Figure 7-16 Predicted AUCinf and Cmax vs. injected dose

The blue lines are the regression lines with the 95% confidence intervals in grey.

7.2 E-R analyses results

The programs used to generate E-R analyses are listed in [Table 7-10](#).

Table 7-10 Programs used to generate E-R analyses

Description	File name	GPSII location
Exposure-Dosimetry analyses	Task01-PK-Dosimetry.R	CAAA000A1/pk/pk_1/pgm/pkpd/
Exposure/Dosimetry-Toxicity analyses	Task02-PK-Toxicity.R	CAAA000A1/pk/pk_1/pgm/pkpd/

In the following sections:

- “injected activity” corresponds to the administered [¹⁷⁷Lu]Lu-PSMA-617 dose;
- Exposure metrics include:
 - “AUCinf”, i.e. the individual radioactivity-blood AUCinf predicted from the popPK model;
 - “Cmax”, i.e. the individual radioactivity-blood Cmax predicted from the popPK model.

7.2.1 Exposure-dosimetry analyses

Effect of exposure on [¹⁷⁷Lu]Lu-PSMA-617 dosimetry in critical organs (i.e. kidney, bone marrow, salivary glands and lacrimal glands) during the first cycle of treatment in mCRPC patients were explored.

7.2.1.1 Description of the observed data

In the PK-Dosimetry dataset, all the response (dosimetry in critical organs) and exposure metrics, demographics and CrCl_{BL} were considered as continuous variables. The number of

bone lesions at baseline was not collected as a continuous variable, and thus was only available as an ordinal variable.

Dosimetry assessments for each organ of interest (bone marrow, kidney, lacrimal glands and salivary glands) were available in 29 patients from the PSMA-617-01 sub-study. Dosimetry results from patient 584617-1266 were not available due to patient discontinuation from the study. For this patient, only a single planar image was collected which was not sufficient for completion of the dosimetry analysis.

Table 7-11 summarizes the dosimetry values (in Gy) calculated on Cycle 1 per organs, and [Figure 7-17](#) illustrates their distributions. The highest dosimetry values were observed in lacrimal glands (median [range] =14.67 Gy [8.15, 22.02]). Lower dosimetry values were observed in salivary glands (median [range] =3.78 Gy [1.52, 10.76]), kidney (median [range]=2.72 Gy [1.57, 6.03], and bone marrow (median [range]=0.21 Gy [0.14, 1.00]. One patient (ID 453610-8791) had a very high bone marrow dosimetry compared to the others.

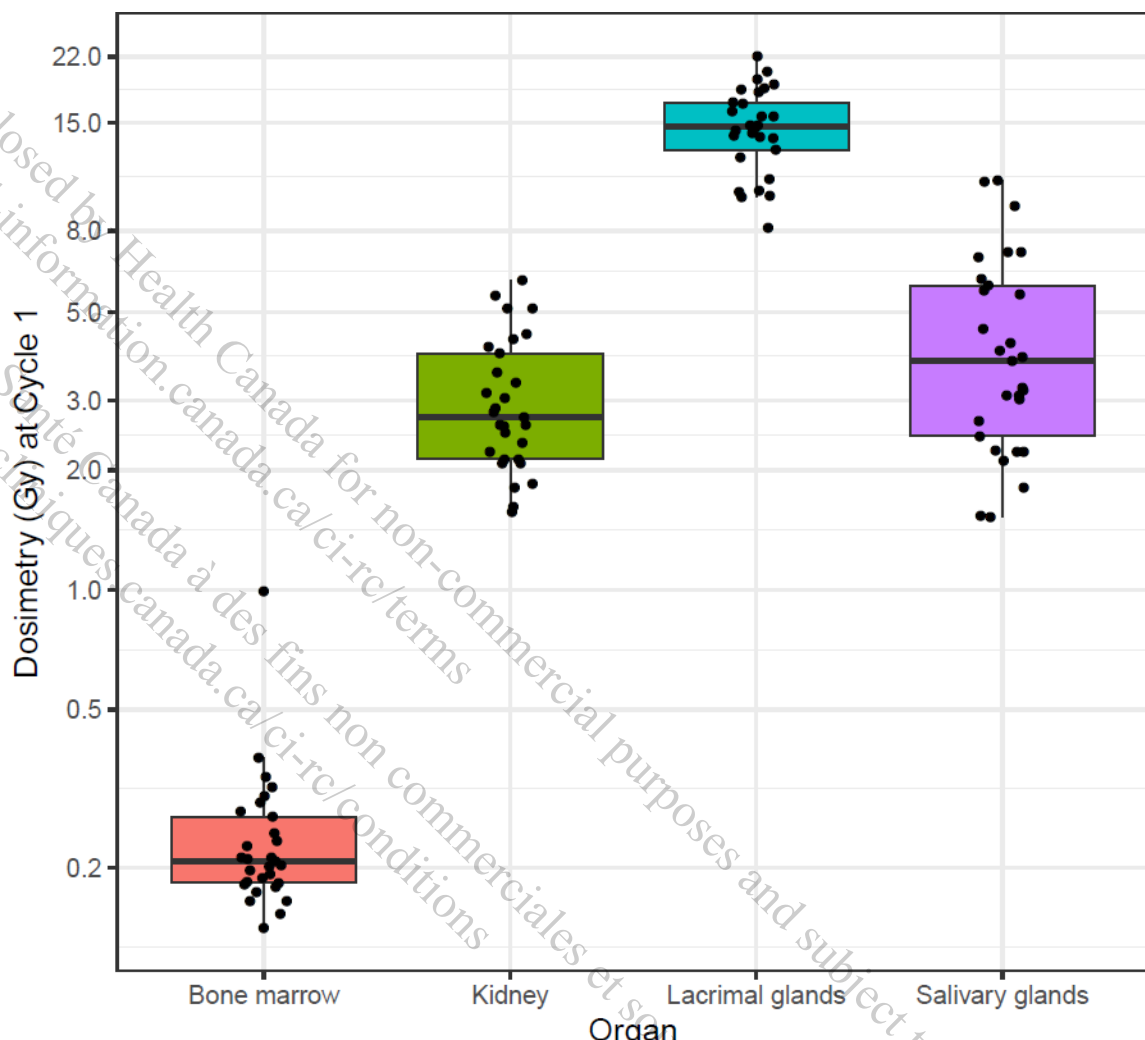
Table 7-11 Summary of dosimetry values (Gy) per organs on Cycle 1

Organ	Min	1 st quartile	Median	Mean	3 rd quartile	Max	SD	CV%
Bone marrow	0.14	0.18	0.21	0.25	0.27	1.00	0.15	62
Kidney	1.57	2.13	2.72	3.10	3.93	6.03	1.22	39
Lacrimal glands	8.15	12.81	14.67	14.75	16.87	22.02	3.43	23
Salivary glands	1.52	2.44	3.78	4.47	5.83	10.76	2.61	58

CV%: coefficient of variation calculated as SD/Mean*100%.

Source: CAAA000A1/pk/pk_1/pgm/pkpd/Task01-PK-Dosimetry.R

Output: CAAA000A1/pk/pk_1/reports/pkpd/Task01-Summary.dosimetry.csv

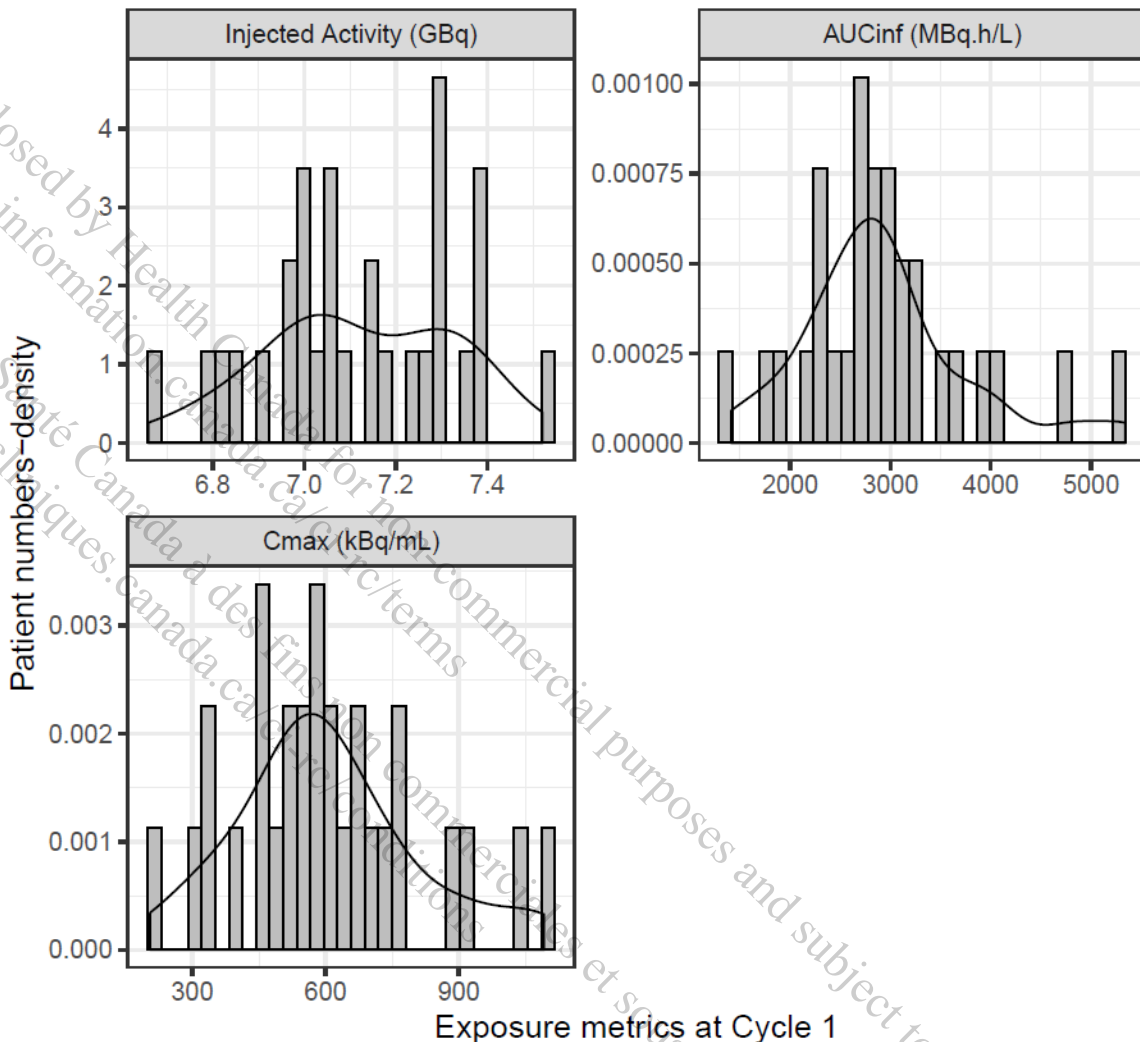
Figure 7-17 Boxplot of dosimetry values per organ on Cycle 1 (N=29)

CAAA000A1/pk/pk_1/pgm/pkpd/Task01-PK-Dosimetry.R
-> CAAA000A1/pk/pk_1/reports/pkpd/Task01-Dosimetry.boxplot.pdf

The y-axis is in log-scale. For each box plot, the top horizontal line is the 3rd quartile, the middle line is the median and the bottom line is the 1st quartile

Density histograms of dosimetry values per organ as well as individual values are presented in [Appendix 5.2](#).

The distributions of the exposure metrics (i.e. injected activity, predicted AUC_{inf} and C_{max} in blood) at Cycle 1 are shown in [Figure 7-18](#).

Figure 7-18 Distribution of the exposure metrics at Cycle 1 (N=29)

The individual baseline characteristics are summarized in [Table 7-12](#). In order to balance the number of subjects across the “number of bone lesions” categories for covariate exploration in the E-R analyses, subjects were grouped into 3 categories: with ≤ 20 bone lesions, with > 20 bone lesions, or as missing.

Table 7-12 Summary of individual baseline characteristics

Baseline characteristics	Summary					
	Continuous variables					
	Min	1 st quartile	Median	Mean	3 rd quartile	Max
Age (years)	52.00	63.00	67.00	66.93	73.00	80.00
Weight (kg)	63.80	78.00	88.00	89.46	97.00	143.00
BMI (kg/m ²)	18.24	24.60	28.09	28.33	31.64	38.79
CrCl _{BL} (mL/min)	53.98	85.27	96.11	105.67	129.23	200.98

Baseline characteristics		Summary	
		Ordinal variable - number of patients (%)	
Number of bone lesions: 1	1 (3%)	≤20	13 (45%)
2-4	4 (14%)	>20	13 (45%)
5-9	8 (28%)	Missing	3 (10%)
>20	13 (45%)		
Missing	3 (10%)		

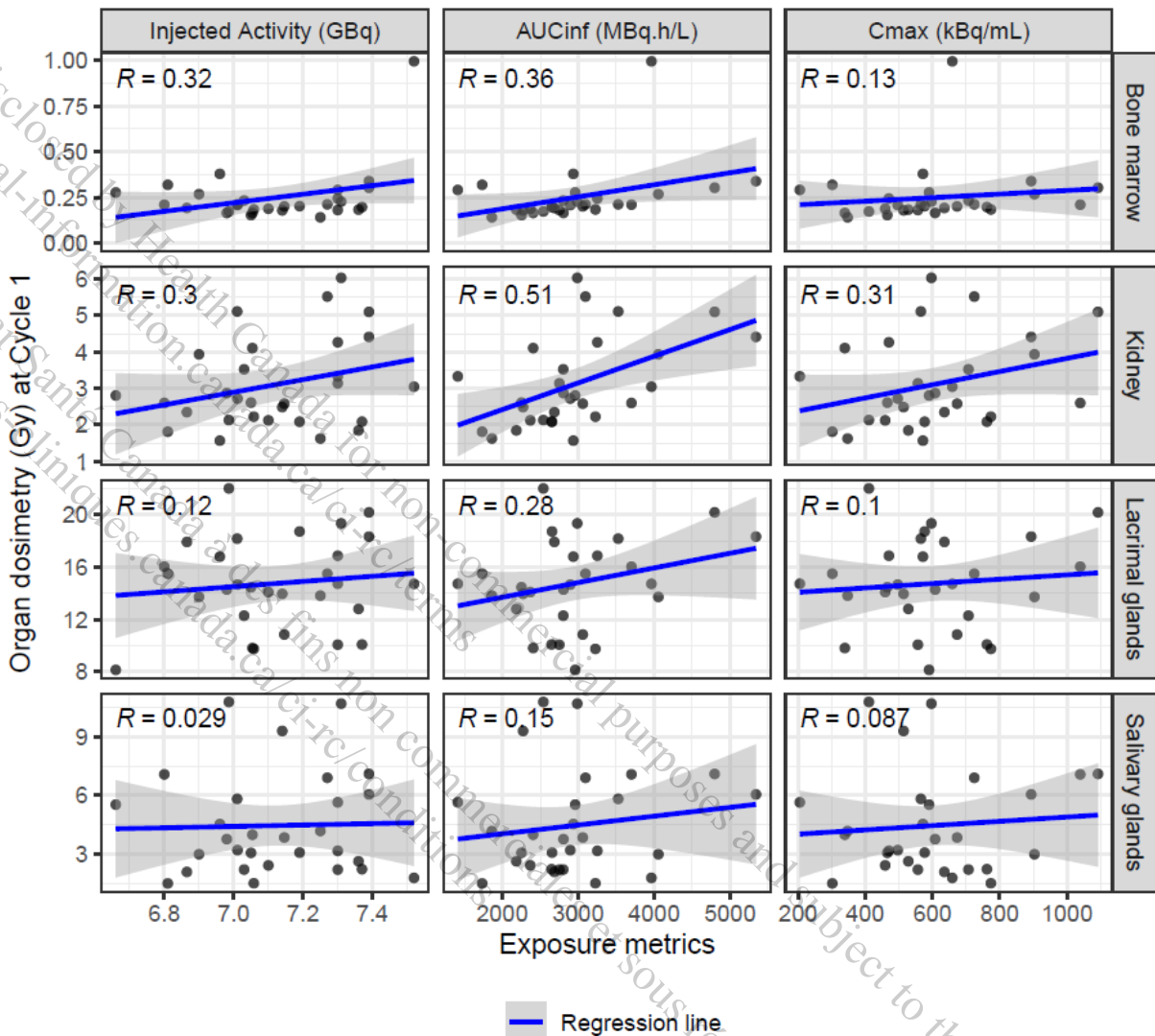
BMI: body mass index. CrCl_{BL}: baseline creatinine clearance.

Source: CAAA000A1/pk/pk_1/pgm/pkpd/Task01-PK-Dosimetry.R

Outputs: CAAA000A1/pk/pk_1/reports/pkpd/Task01-Summary.cov.cont.csv & Task01-Summary.cov.cat.csv

7.2.1.2 Exposure-Dosimetry results

Relationships between exposure and dosimetry from organs at risk at Cycle 1 were explored. Scatterplots along with Pearson correlation coefficient (R) are represented in Figure 7-19. The strongest correlation was observed between blood AUCinf and kidney dosimetry (R=0.51). The Pearson correlation coefficients also suggested some degrees of correlation between blood AUCinf and dosimetry in bone marrow (R=0.36) and in lacrimal glands (R=0.28), between Cmax and kidney dosimetry (R=0.31), as well as between injected activity and dosimetry in bone marrow (R=0.32) and in kidney (R=0.3).

Figure 7-19 Correlations between exposure and organ dosimetry at Cycle 1 (N=29)

CAAA000A1/pk/pk_1/pgm/pkpd/Task01-PK-Dosimetry.R

-> CAAA000A1/pk/pk_1/reports/pkpd/Task01-Dosimetry.vs.Exposure.pdf

The blue lines are the regression lines with the 95% confidence intervals in grey. R=Pearson correlation coefficient.

Linear regression was performed for each exposure-dosimetry relationship, and corresponding p-values are reported in Table 7-13. Results show that AUCinf in blood is a statistically significant predictor of kidney dosimetry ($p=0.005$).

Table 7-13 p-values from linear regression between exposure metrics and dosimetry

Exposure metrics	Organ dosimetry			
	Bone marrow	Kidney	Lacrimal glands	Salivary glands
Injected activity	0.09	0.12	0.53	0.88
AUCinf in blood	0.05	0.005*	0.15	0.45
Cmax in blood	0.50	0.11	0.60	0.66

*Significant p-value ($p<0.05$).

Source: CAAA000A1/pk/pk_1/pgm/pkpd/Task01-PK-Dosimetry.R

Output: CAAA000A1/pk/pk_1/reports/pkpd/Task01-Linear.reg.Exposure.csv

Results from the linear regression between AUCinf and kidney dosimetry were reported in [Table 7-14](#). This analysis suggests that an increase in AUCinf by 1000 MBq.h/L would lead to an increase in kidney dosimetry by 0.7 Gy.

Table 7-14 Results from the linear regressions between AUCinf and kidney dosimetry

Parameter	Estimate	95% CI	p-value
Intercept	0.95	[-0.55 – 2.45]	0.20
AUCinf effect	0.0007	[0.0002 – 0.0012]	0.005*

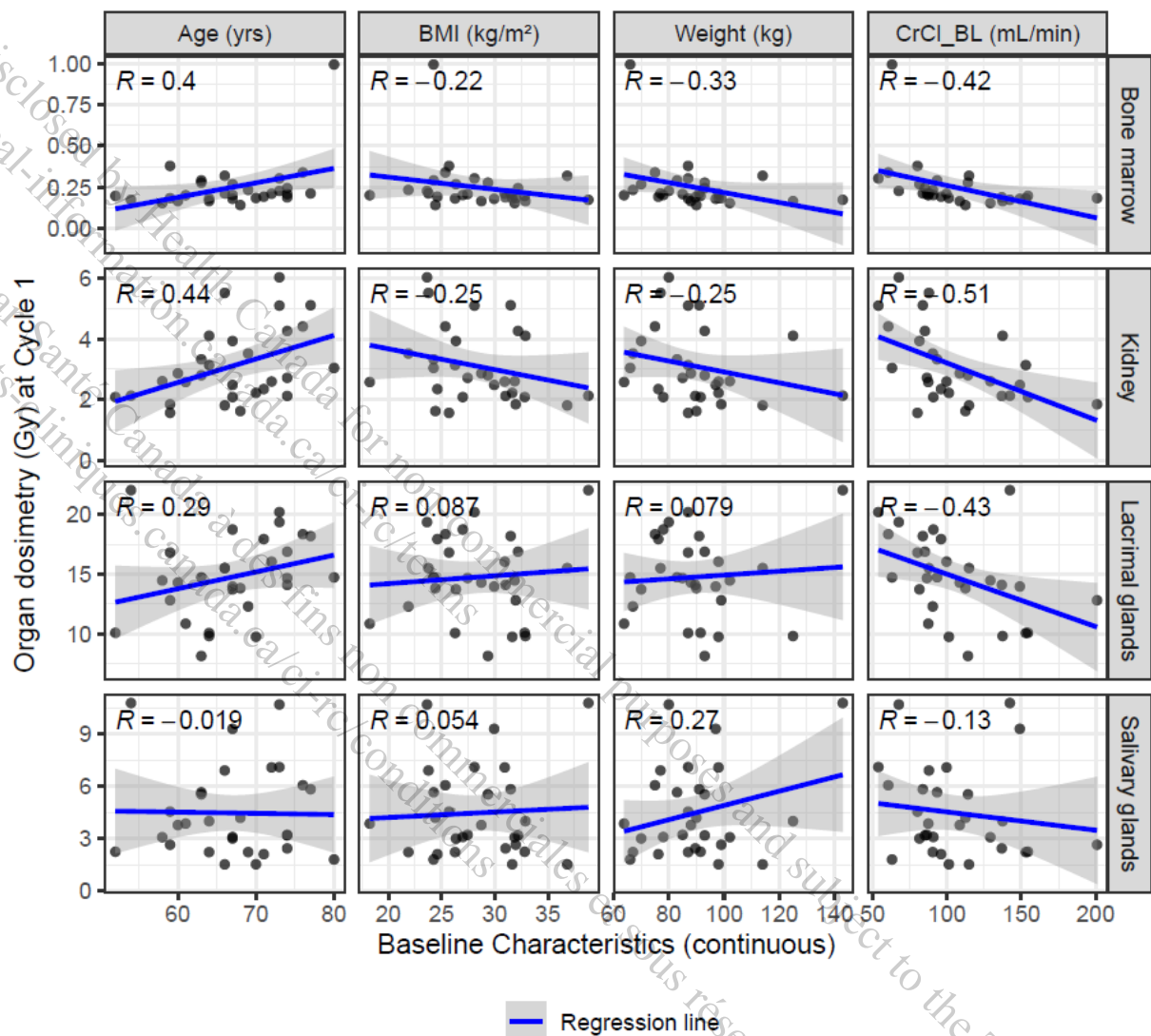
*Significant p-value ($p<0.05$). CI: confidence interval.

Source: CAAA000A1/pk/pk_1/pgm/pkpd/Task01-PK-Dosimetry.R

Output: CAAA000A1/pk/pk_1/reports/pkpd/Task01-Linear.reg.AUC.Kidney.csv

Due to the small number of subjects (N=29), no covariate inclusion, other than exposure metrics, was evaluated in any linear regression. In addition, as CrCl_{BL} was included as a covariate on Cl in the popPK model, with a significant effect on AUCinf, it would be a confounding factor in the linear regression on kidney dosimetry vs. AUCinf.

Correlations between organ dosimetry and continuous baseline characteristics were only graphically explored, as illustrated in [Figure 7-20](#). The strongest correlation was observed between kidney dosimetry and CrCl_{BL} ($R=-0.51$). The dosimetry in bone marrow and lacrimal gland dosimetry also appear to be correlated to CrCl_{BL}, and a correlation with age was detected for kidney and bone marrow dosimetry.

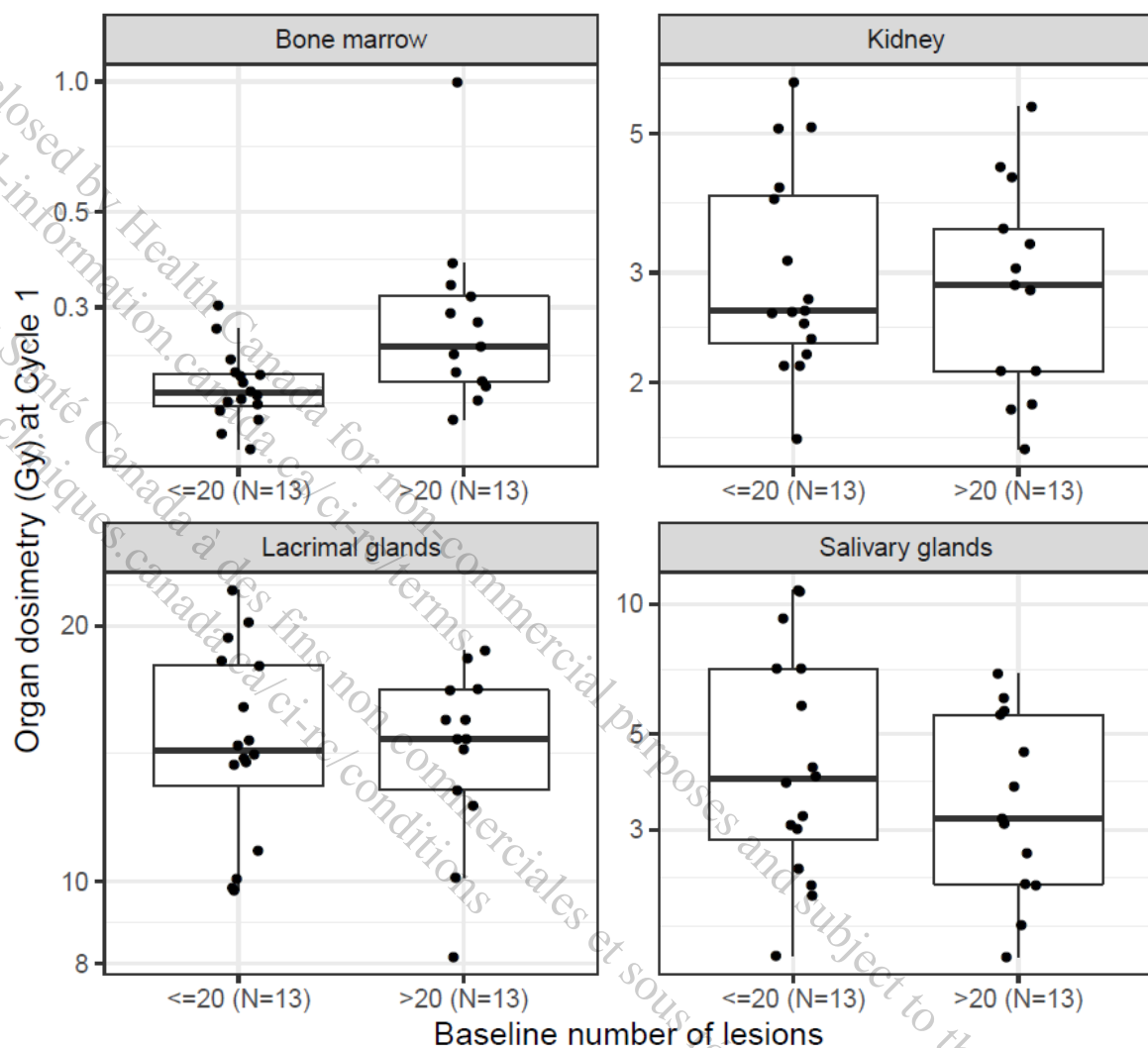
Figure 7-20 Correlations between organ dosimetry and continuous baseline characteristics (N=29)

CAAA000A1/pk/pk_1/pgm/pkpd/Task01-PK-Dosimetry.R
-> CAAA000A1/pk/pk_1/reports/pkpd/Task01-Dosimetry.vs.Baseline.Cont.pdf

The blue lines are the regression lines with the 95% confidence intervals in grey.

The AUCinf effect on kidney dosimetry, mentioned above, may be confounded by CrCL_{BL}, as it has both an effect on the independent (AUCinf) and dependent (kidney dosimetry) variables.

Figure 7-21 showed a trend toward higher bone marrow dosimetry values in patients with a large number of bone lesions (>20 bone lesions). The 3 patients with missing number of bone lesions were excluded from the plot.

Figure 7-21 Correlations between organ dosimetry and baseline number of bone lesions (N=26)

CAAA000A1/pk/pk_1/pgm/pkpd/Task01-PK-Dosimetry.R
-> CAAA000A1/pk/pk_1/reports/pkpd/Task01-Dosimetry.vs.Baseline.Cat.pdf

The y-axis is in log-scale. The 3 patients with missing number of bone lesions were excluded from the plot. For each box plot, the top horizontal line is the 3rd quartile, the middle line is the median and the bottom line is the 1st quartile.

Finally, kidney dosimetry was further explored as a function of renal impairment, based on categorization of CrCl_{BL} values as described on Table 7-15. Observed median kidney dosimetry in patients with mild renal impairment was 1.7 fold higher compared to the median in patients with normal renal function (4.1 Gy vs. 2.4 Gy, respectively).

Table 7-15 Summary of kidney dosimetry by renal impairment category

Renal impairment category	Number of patients (%)	Observed kidney dosimetry (Gy) - Median (1 st quartile – 3 rd quartile)
Moderate: 30 mL/min ≤ CRCL _{BL} < 60 mL/min	1 (3.4%)	5.10 (NA)

Renal impairment category	Number of patients (%)	Observed kidney dosimetry (Gy) - Median (1 st quartile – 3 rd quartile)
Mild: $60 \text{ mL/min} \leq \text{CRCL}_{\text{BL}} < 90 \text{ mL/min}$	10 (34.5%)	4.10 (2.80 – 4.94)
Normal: $\text{CRCL}_{\text{BL}} \geq 90 \text{ mL/min}$	18 (62.1%)	2.42 (2.10 – 2.85)

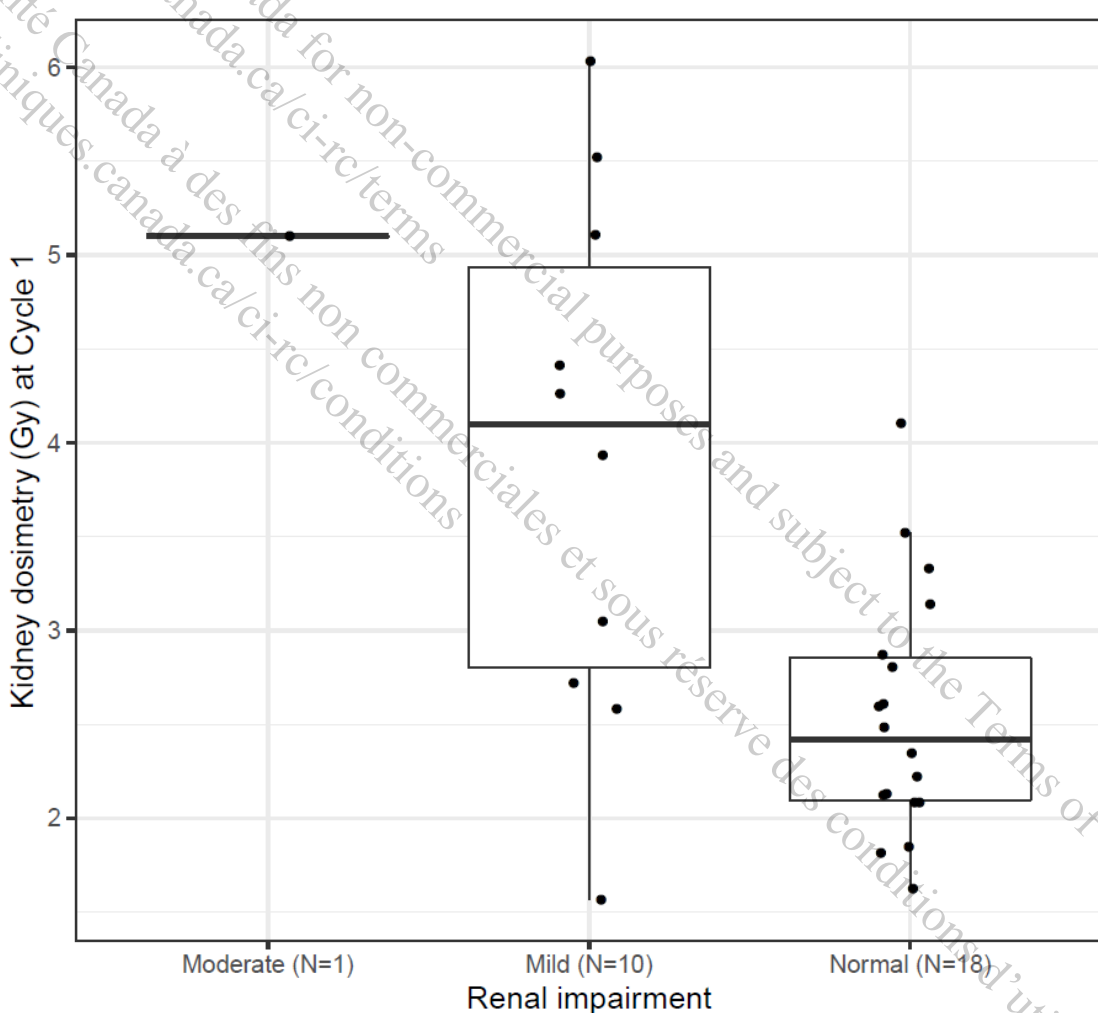
CrCl_{BL} : baseline creatinine clearance; NA: not applicable.

Source: CAAA000A1/pk/pk_1/pgm/pkpd/Task01-PK-Dosimetry.R

Output: CAAA000A1/pk/pk_1/reports/pkpd/Task01-Sum.Kidney.Renal.imp.csv

Kidney dosimetry distribution by renal impairment category was also plotted in [Figure 7-22](#).

Figure 7-22 Correlation between kidney dosimetry and renal impairment category (N=29)



CAAA000A1/pk/pk_1/pgm/pkpd/Task01-PK-Dosimetry.R
-> CAAA000A1/pk/pk_1/reports/pkpd/Task01-Kidney.dosim.Renal.imp.pdf

For each box plot, the top horizontal line is the 3rd quartile, the middle line is the median and the bottom line is the 1st quartile.

7.2.2 Exposure/Dosimetry-toxicity analyses

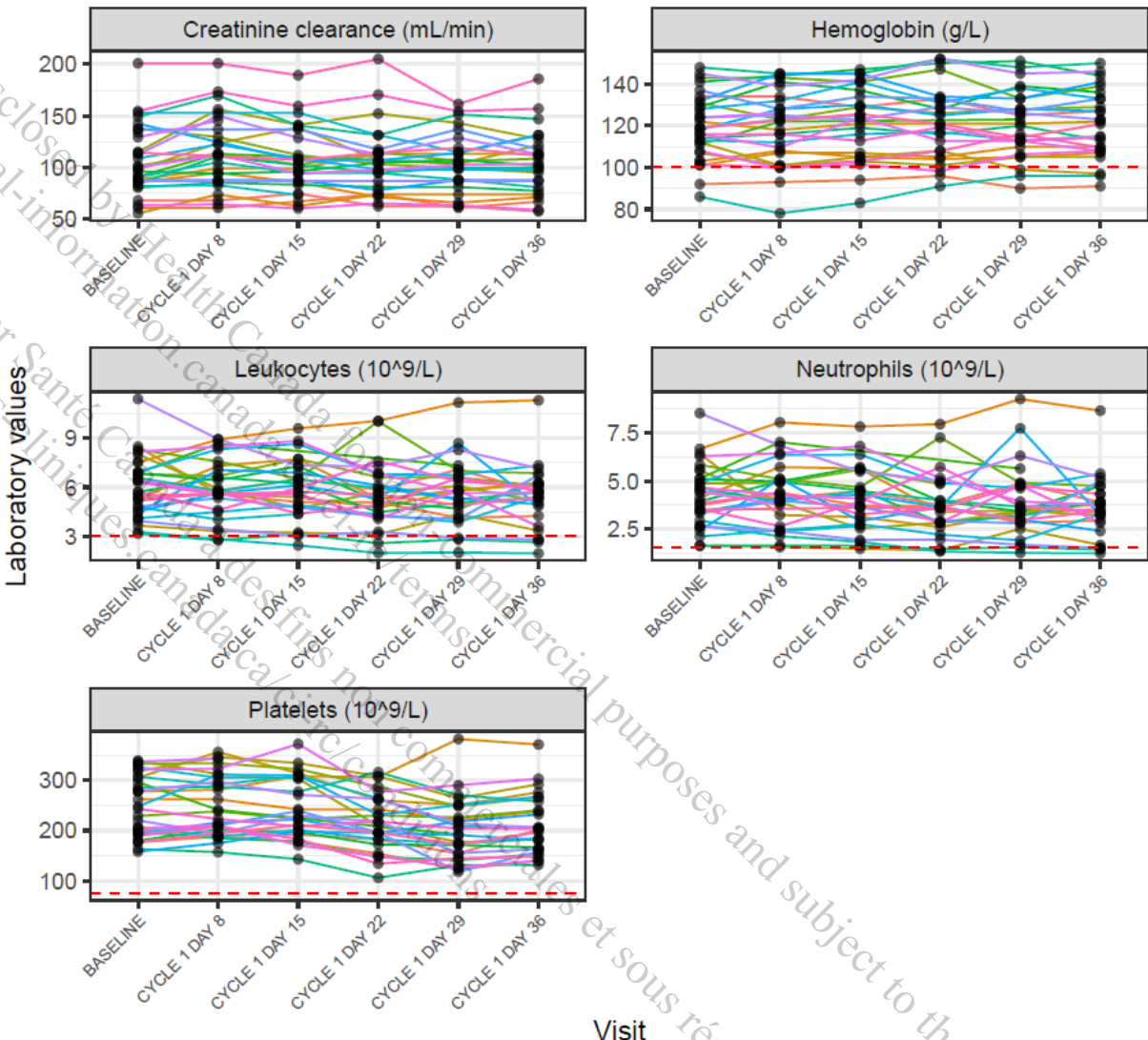
Relationships between exposure/dosimetry and acute toxicity related to kidney, bone marrow, salivary and lacrimal glands during the first cycle of treatment with [¹⁷⁷Lu]Lu-PSMA-617 in mCRPC patients were explored. Due to the limited number of patients and adverse events, only descriptive plots were generated.

CrCl, as a surrogate of renal function, and renal adverse events were explored to evaluate the risk related to kidneys. Hemoglobin, leukocyte, neutrophil and platelet counts together with their associated adverse events (i.e. anemia, leukopenia, neutropenia and thrombocytopenia) were explored as indicators for hematological toxicity.

7.2.2.1 Description of the observed data

In the PK/Dosimetry-Toxicity datasets, occurrence of toxicity and their associated grades were considered as categorical variables and laboratory values as continuous variables. All the exposure metrics were considered as continuous variables.

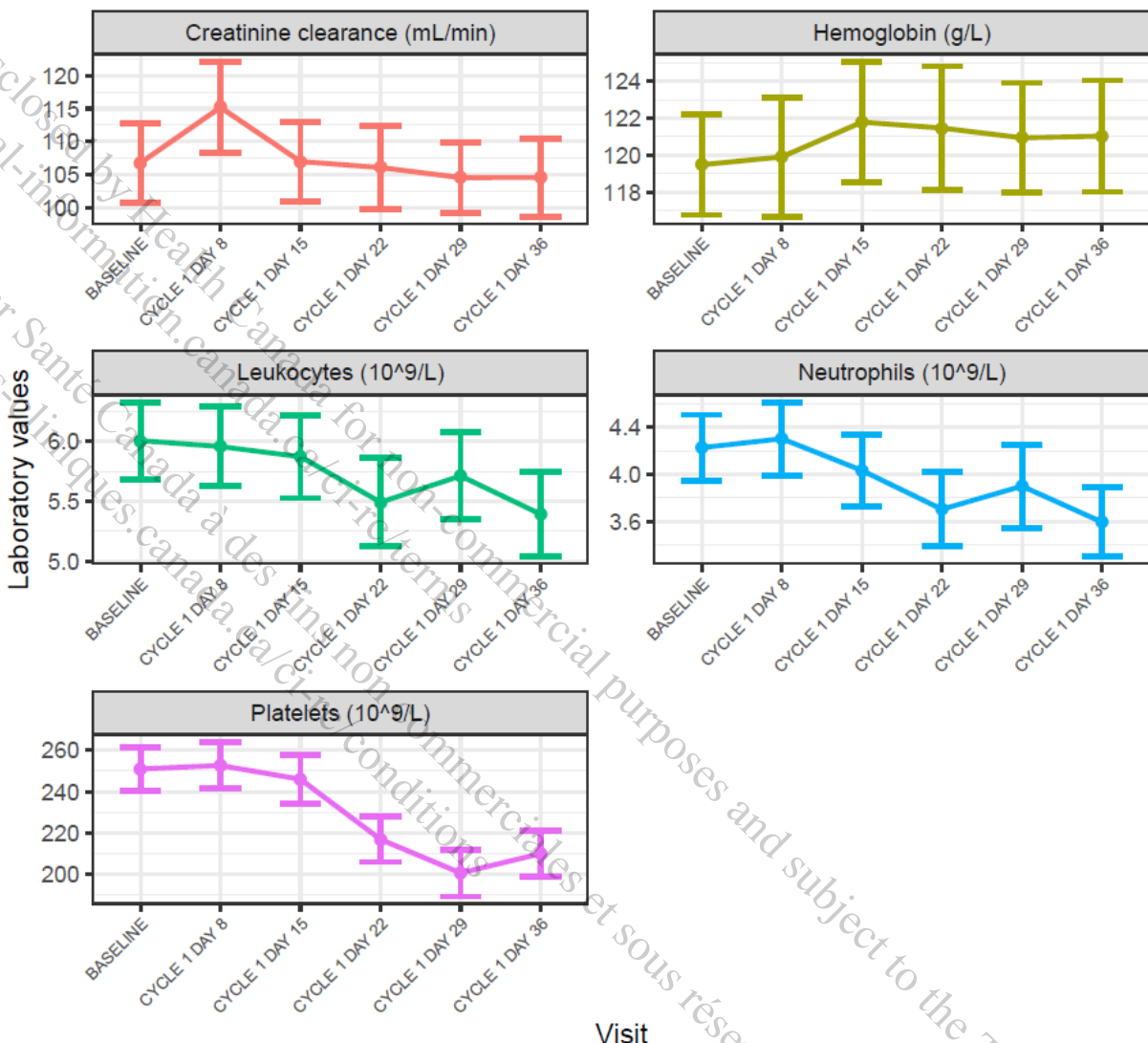
Longitudinal laboratory data during Cycle 1 were first explored from a total of 30 patients, as illustrated in [Figure 7-23](#). The majority of the individuals had one baseline and 5 post-baseline observations available per type of laboratory assessment. Spaghetti plots showed that only few individuals reached the threshold for hematological adverse event of CTCAE Grade ≥ 2 related to hemoglobin, leukocytes, neutrophils or platelets. Those patients were the ones with low baseline levels for the associated laboratory values.

Figure 7-23 Spaghetti plots of laboratory values at Cycle 1 (N=30)

CAAA000A1/pk/pk_1/pgm/pkpd/Task02-PK-Toxicity.R
-> CAAA000A1/pk/pk_1/reports/pkpd/Task02-Lab.Spaghetti.plot.pdf

The horizontal dashed lines correspond to the CTCAE Grade ≥ 2 for anemia, leukopenia, neutropenia and thrombocytopenia respectively.

Mean ($\pm 95\%CI$) longitudinal laboratory profiles are plotted in [Figure 7-24](#). It showed an initial peak in CrCl (representative of kidney function) observed from baseline to Day 8, before a slight decrease from baseline. Hemoglobin levels remain consistent over the course of the first treatment cycle. A decrease in leukocytes, neutrophils and platelets was observed starting from 8 days after treatment start.

Figure 7-24 Mean (± 95% CI) longitudinal laboratory profiles throughout Cycle 1 (N=30)

CAAA000A1/pk/pk_1/pgm/pkpd/Task02-PK-Toxicity.R
-> CAAA000A1/pk/pk_1/reports/pkpd/Task02-Lab.Longit.Mean.CI.pdf

The adverse events related to the organs at risk during Cycle 1 are summarized in [Table 7-16](#). A total of 6 (20%) sub-study patients experienced a worsening from baseline of at least one hematological adverse events of CTCAE Grade ≥ 2 . The most common of those adverse events were anemia, observed in 17% of the sub-study patients. On Cycle 1, none of the sub-study patients had thrombocytopenia of CTCAE Grade ≥ 2 .

None of the patients from the sub-study experienced any lacrimal and renal toxicity at Cycle 1. A total of 2 (7%) patients had a salivary gland adverse event at Cycle 1, limited to Grade 1 (CAAA000A1/pk/pk_1/pgm/pkpd/Task02-PK-Toxicity.Rout - Lines 966-969).

Table 7-16 Summary of adverse events from the organs at risk during Cycle 1 (N=30)

Adverse event	Number of patients (%)	
	Based on PK/Dosimetry-Toxicity-Lab dataset	
Thrombocytopenia (CTCAE Grade ≥ 2) ^a	0 (0%)	
Anemia (CTCAE Grade ≥ 2) ^a	5 (17%)	
Leukopenia (CTCAE Grade ≥ 2) ^a	3 (10%)	
Neutropenia (CTCAE Grade ≥ 2) ^a	3 (10%)	
Worsening from baseline of at least one hematological adverse event (CTCAE Grade ≥ 2)	6 (20%)	
Based on PK/Dosimetry-Toxicity-AE dataset		
Renal toxicity (any CTCAE Grade)	0 (0%)	
Salivary gland adverse event (any CTCAE Grade)	2 (7%)	
Lacrimal gland adverse event (any CTCAE Grade)	0 (0%)	

^a These numbers reflect study outcome irrespective of patients' baseline value.

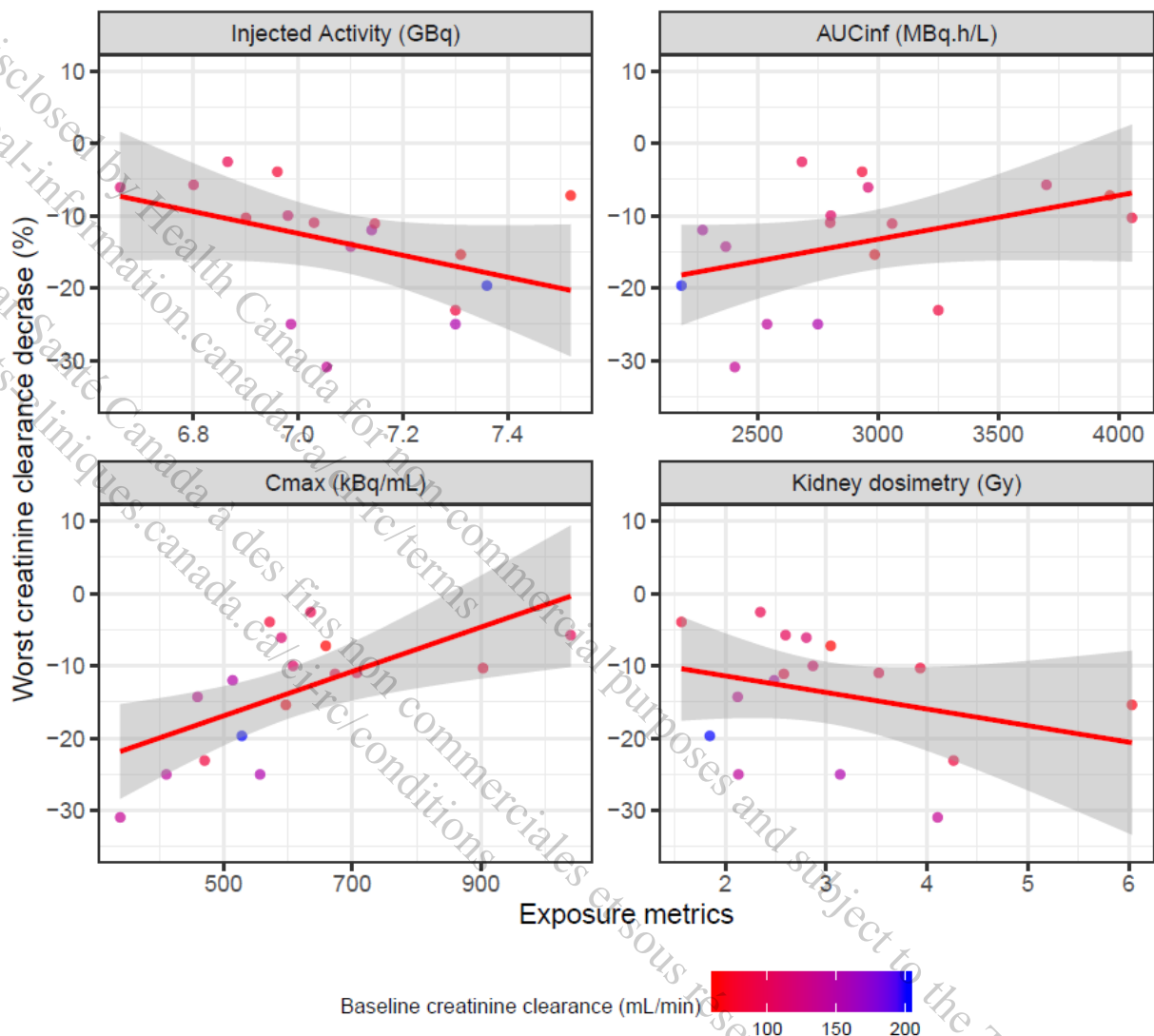
Source: CAAA000A1/pk/pk_1/pgm/pkpd/Task02-PK-Toxicity.R

Output: CAAA000A1/pk/pk_1/reports/pkpd/Task02-AE.summary.csv

7.2.2.2 Exposure/Dosimetry-Toxicity results

First, exposure/dosimetry-toxicity analyses explored the worst decrease from baseline in CrCl, reflecting renal function, and the worst decrease from baseline in platelet count, the most radiation-sensitive hematological laboratory assessment. Among the sub-study patients with post-baseline assessments, 17 (59%) showed a decrease from baseline in CrCl and 25 (86%) experienced a decrease in platelet count during Cycle 1 (Appendix 5.3).

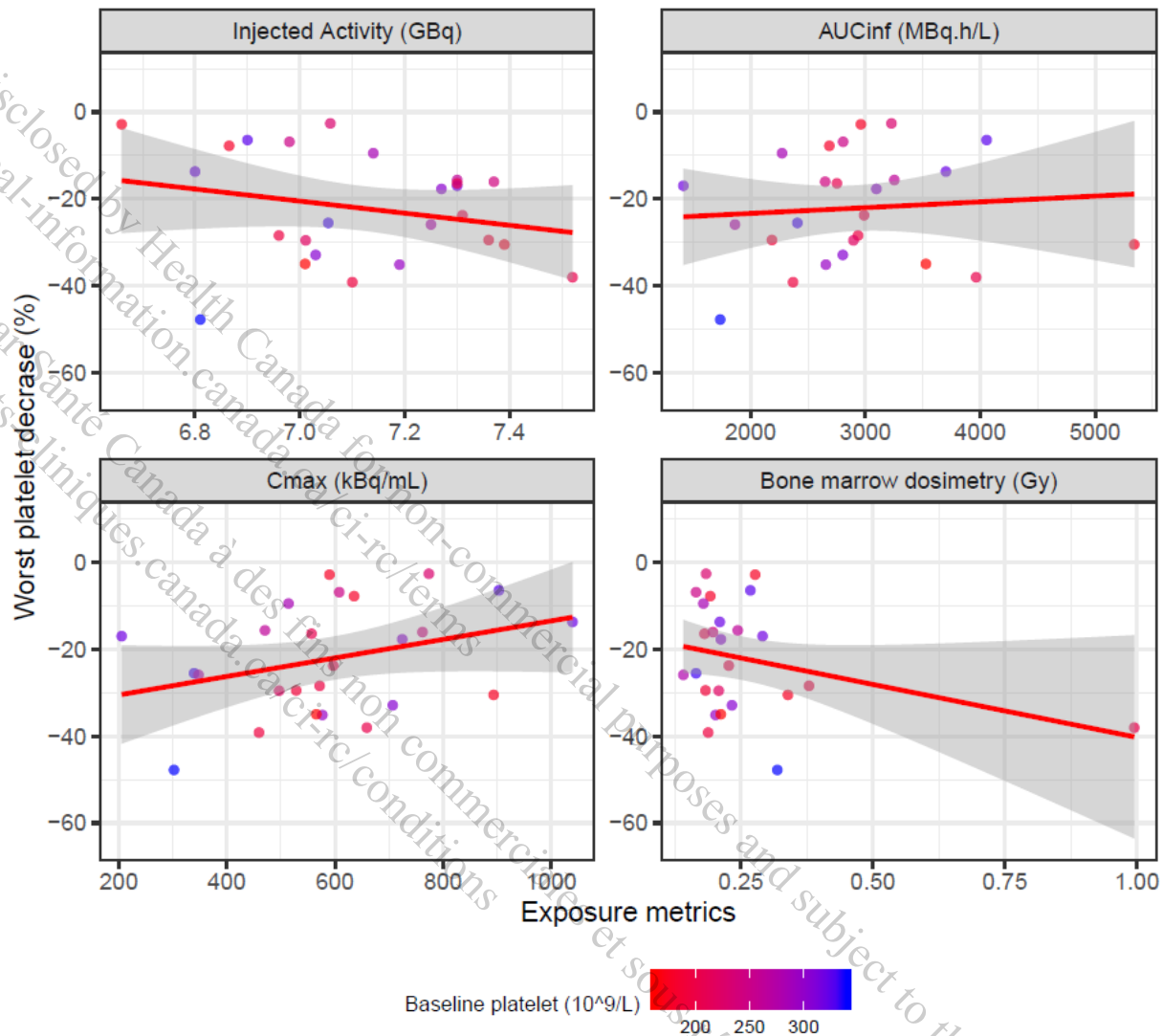
The worst individual CrCl decrease (% change from baseline) at Cycle 1 was plotted against each exposure metrics for each one of the 17 patients who had a decrease in CrCl from baseline, as shown in Figure 7-25. Higher injected activity and higher kidney dosimetry tend to be associated with larger decrease in CrCl change from baseline. The positive trend between worst CrCl decrease and exposure in blood (AUCinf and Cmax) may be due to the limited sample size, the variability in the data and the presence of outliers.

Figure 7-25 Worst individual CrCl decrease from baseline vs. exposure metrics (N=17)

CAAA000A1/pk/pk_1/pgm/pkpd/Task02-PK-Toxicity.R
-> CAAA000A1/pk/pk_1/reports/pkpd/Task02-Worst.CRCL.vs.Exposure.pdf

The red lines are the regression lines with the 95% confidence intervals in grey.

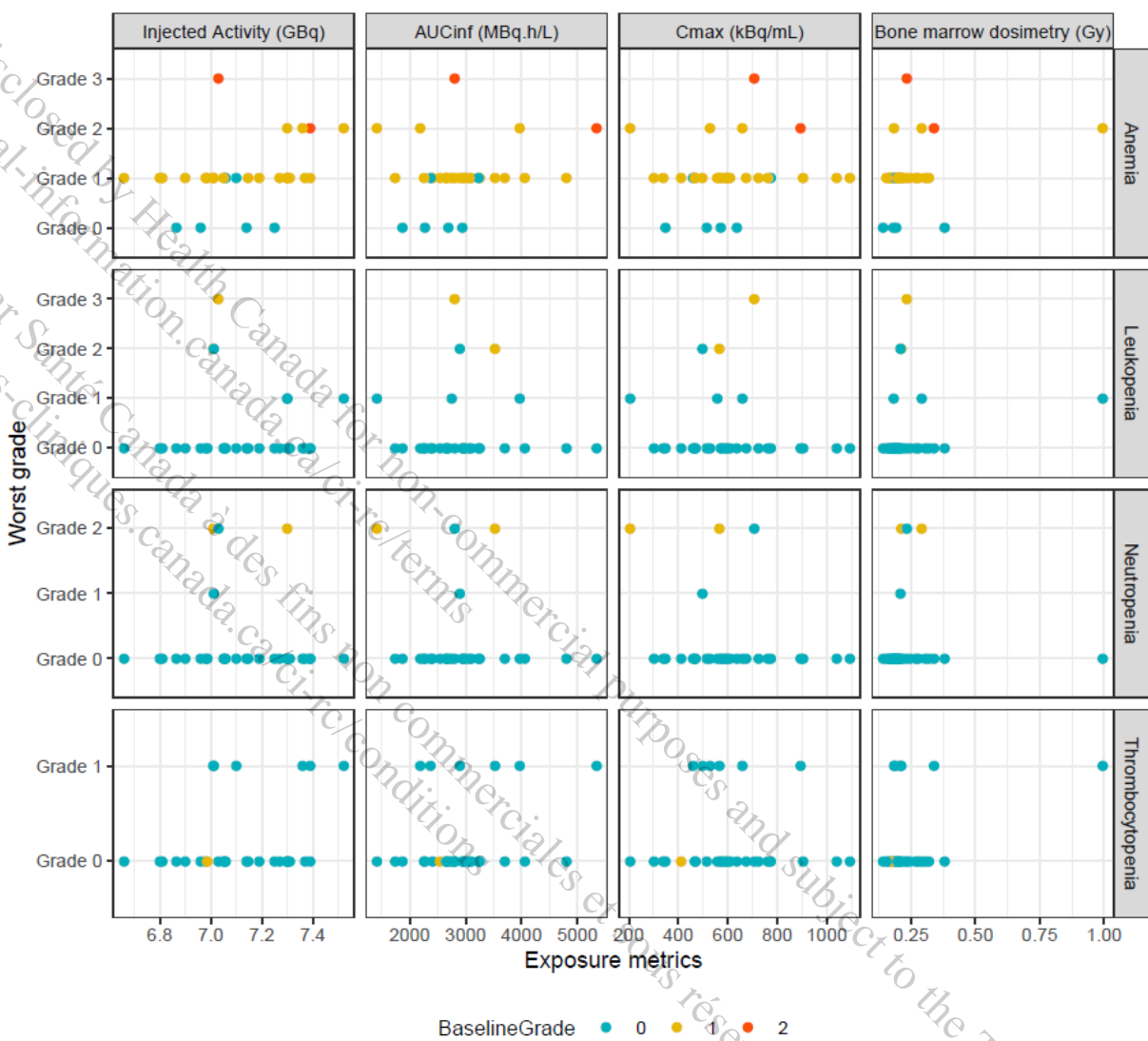
Among the 25 individuals with a decrease from baseline in platelet count, the worst individual platelet decrease (% change from baseline) at Cycle 1 was plotted against each exposure metrics, as shown in [Figure 7-26](#). No clear and consistent trend can be detected between worst platelet count decrease and exposure.

Figure 7-26 Worst individual platelet count decrease vs. exposure metrics (N=25)

CAAA000A1/pk/pk_1/pgm/pkpd/Task02-PK-Toxicity.R
-> CAAA000A1/pk/pk_1/reports/pkpd/Task02-Worst.PLT.vs.Exposure.pdf

The red lines are the regression lines with the 95% confidence intervals in grey.

Then, relationships between the worst hematological toxicity grades during Cycle 1 and exposure metrics were explored in [Figure 7-27](#). No consistent trend across the 4 exposure metrics can be detected.

Figure 7-27 Worst hematological toxicity grades after first injection and during Cycle 1 vs. exposure metrics

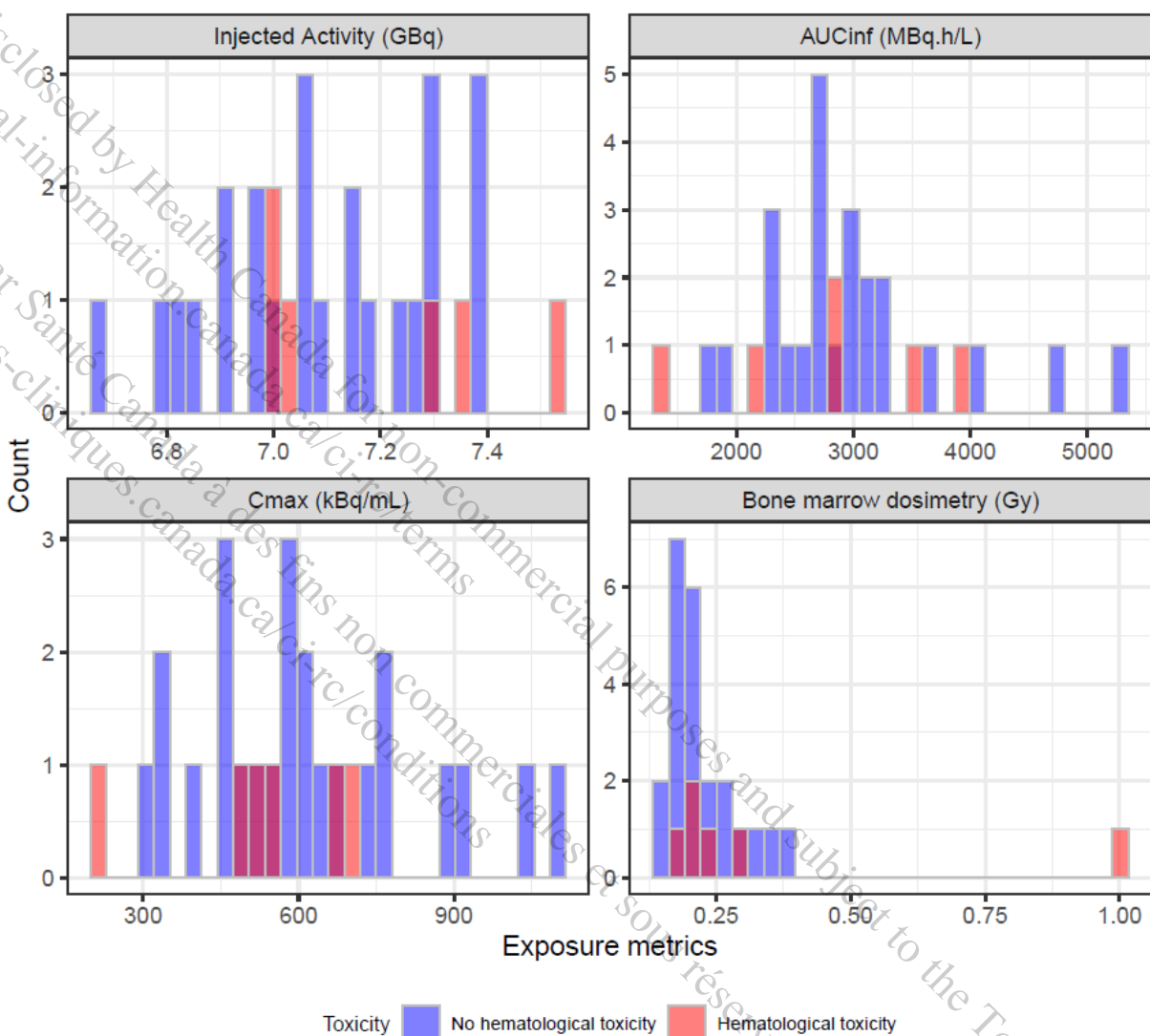
CAAA000A1/pk/pk_1/pgm/pkpd/Task02-PK-Toxicity.R
-> CAAA000A1/pk/pk_1/reports/pkpd/Task02-Worst.Hemato.Grade.vs.Exposure.pdf

The patient with missing dosimetry value has been excluded from the bone marrow dosimetry subplot.

Occurrence of any hematological adverse events and exposure metrics were explored: Figure 7-28 shows the distribution of each exposure metrics with different color for whether or not patients experienced at least one hematological adverse event of CTCAE Grade ≥ 2 , and whether this represented a worsening from baseline (in red). It can be observed that the patient with a high bone marrow dosimetry suffered from a hematological adverse event with Grade ≥ 2 (anemia). No clear trend could be noted.

Figure 7-28

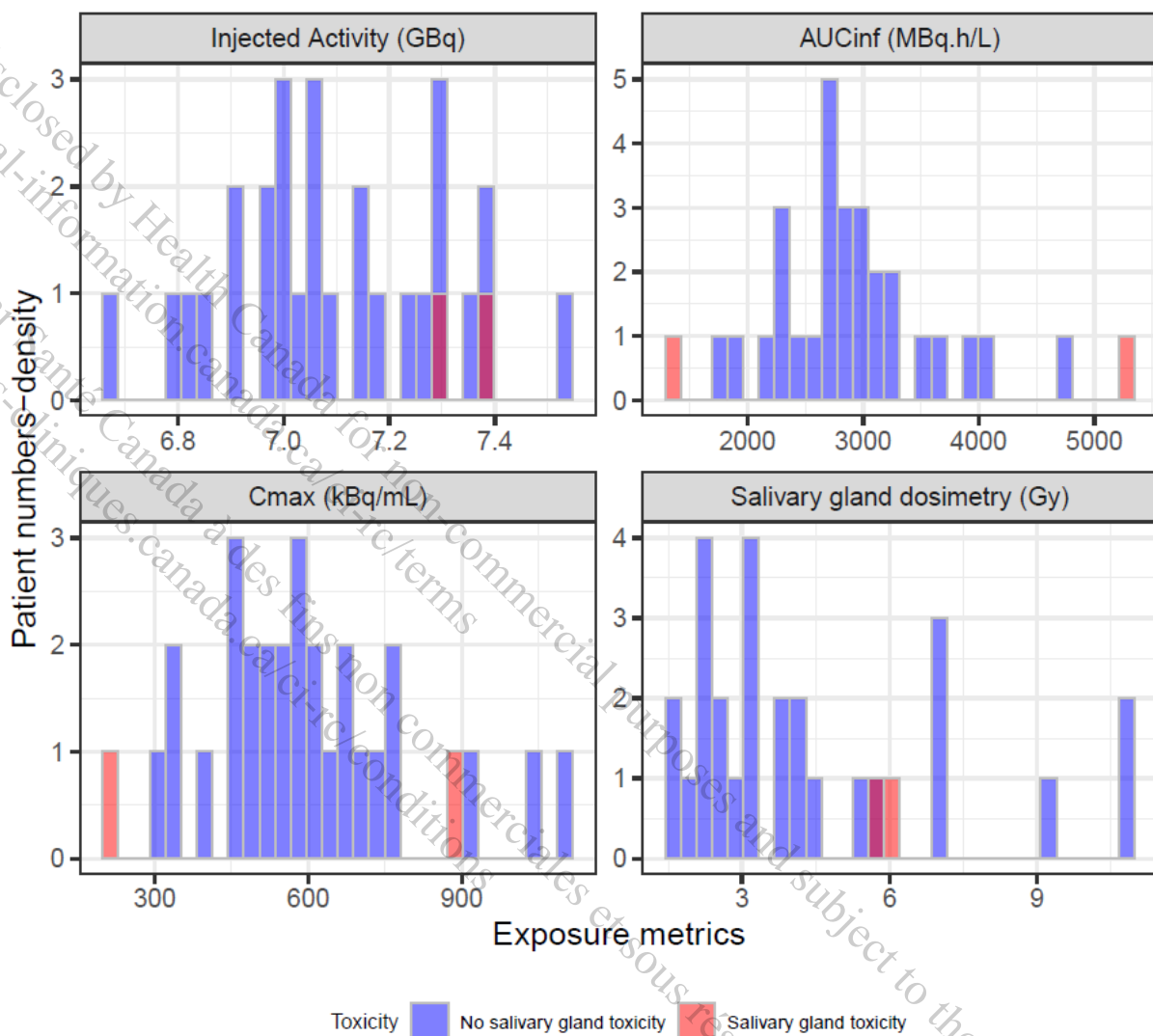
Distribution of exposure metrics in relation to patients experiencing a worsening from baseline of at least one hematological adverse event of Grade ≥ 2



CAAA000A1/pk/pk_1/pgm/pkpd/Task02-PK-Toxicity.R
-> CAAA000A1/pk/pk_1/reports/pkpd/Task02-Hemato2.Hist.Exposure.pdf

The patient with missing dosimetry value has been excluded from the distribution of bone marrow dosimetry. The bars colored in dark-red correspond to the overlay of both groups.

Finally, Figure 7-29 shows the distribution of each exposure metrics with patients experiencing at least one salivary gland toxicity (any grade) highlighted in red. No consistent trend across the 4 exposure metrics can be observed.

Figure 7-29 Distribution of exposure metrics in relation to patients experiencing any salivary gland toxicity

CAAA000A1/pk/pk_1/pgm/pkpd/Task02-PK-Toxicity.R
-> CAAA000A1/pk/pk_1/reports/pkpd/Task02-Salivary.tox.Hist.Exposure.pdf

The patient with missing dosimetry value has been excluded from the distribution of salivary gland dosimetry. The bars colored in dark-red correspond to the overlay of both groups.

8 Discussion

8.1 Population PK modeling

The PK of radioactivity-blood [¹⁷⁷Lu]Lu-PSMA-617 concentrations was characterized based on data from the PSMA-617-01 sub-study. The final structural model was a three-compartment model with a delayed 0-order absorption and linear elimination. All key parameters were estimated with reasonable precision, and the diagnostic plots suggested a good description and prediction of the data.

Tlag and Tk0, reproducing an artificial delayed absorption after the start of administration, were estimated with relatively high RSE(%) (48% and 54% respectively). They still remain acceptable, and can be explained by their high variability (CV% = 291% and 264% respectively), also consistent with the large variability observed in the infusion times (range: 0.017 h to 1.783 h). Addition of both Tlag and Tk0 in the structural model was required to provide a good description of individual PK profiles, particularly those with low concentrations observed at the first post-dose sample.

Variabilities on Q₂ and V₂ were estimated at relatively high values (CV% = 80% and 93% respectively), but none of the available covariates was found to explain them.

Out of the baseline covariates tested (age, WT_{BL}, BMI and CrCl_{BL}) for their potential effects on [¹⁷⁷Lu]Lu-PSMA-617 popPK parameters, the final model retained CrCl_{BL} on Cl and WT_{BL} on V₁. The effect of CrCl_{BL} on Cl is pharmacologically plausible as kidneys are the main route of excretion for this compound. Increasing CrCl_{BL} resulted in increased Cl, and subsequently in lower exposure. Simulations showed a 42% and 20% increase in median of simulated AUCinf for moderate and mild renal impairment respectively vs. for normal renal function. These findings should be interpreted with caution since the population included only one patient with moderate renal impairment (CrCl_{BL}=54 mL/min). It should be noted that the study did not include any patient with severe renal impairment and thus no conclusion can be made for this population.

Although WT_{BL} was also found as a significant covariate on V₁, this did not result in any significant effect on [¹⁷⁷Lu]Lu-PSMA-617 exposure (i.e. Cmax), supporting the use of a fixed dosing.

PopPK results and covariate findings need to be interpreted with caution as these analyses are based on a limited number of patients (N=30). It should also be noted that only Cycle 1 PK profile was available, and inter-occasion variability is thus unknown for this compound. Finally, clinical implication of covariate effect is difficult to interpret as no clear relationship has been established between blood exposure and clinical efficacy and safety.

8.2 Exposure-response analyses

8.2.1 Exposure-Dosimetry

Injected activity and blood PK exposure were evaluated as predictors of dosimetry in the organs at risk, namely kidney, bone marrow, salivary glands and lacrimal glands during Cycle 1. Exposure-dosimetry analyses showed that only AUCinf in blood was a statistically significant predictor of kidney dosimetry (p=0.005). However, the relationship between AUCinf and kidney dosimetry may not be a causal relationship as it is confounded by CrCl_{BL}. Indeed, CrCl_{BL} has a strong effect on AUCinf, and is also highly negatively correlated with kidney dosimetry. As such, it remains challenging to make any conclusion on the exposure effect.

The Pearson correlation coefficients also suggested some degrees of positive correlations between blood AUCinf and dosimetry in bone marrow (R=0.36), and in lacrimal glands (R=0.28), between Cmax and kidney dosimetry (R=0.31), as well as between injected activity and dosimetry in bone marrow (R=0.32) and in kidney (R=0.3). However, none of these relationships were statistically significant in a linear regression.

Physiological characteristics, demographics and baseline factors tend to be correlated with organ dosimetry. Higher CrCl_{BL} was associated with lower values of kidney, bone marrow and lacrimal gland dosimetry. Older subjects were associated with higher values of kidney and bone marrow dosimetry. Of note, this may be confounded by the negative correlation between age and CrCl_{BL}.

Correlation with categorical baseline characteristics showed a trend toward higher bone marrow dosimetry values in patients with a large number of bone lesions (>20). It may be explained by the presence of extensive bone metastases in the mCRPC population.

Correlation between kidney dosimetry at Cycle 1 and baseline renal impairment category showed a trend toward higher kidney dosimetry values in patients with mild or moderate renal impairment compared to those with normal renal function. Results for the moderate impairment category needs to be considered with caution given that only one patient with moderate renal impaired was enrolled in the PSMA-617-01 sub-study, with kidney dosimetry within the distribution observed for mild impairment. No information was available for severe renal impairment.

Exposure-Dosimetry and correlations with baseline characteristics for [¹⁷⁷Lu]Lu-PSMA-617 have not been reported in the literature. However, few authors explored relationships between baseline factors and the uptake of the pre-therapeutic imaging tracer ([⁶⁸Ga]Ga-PSMA-11). Gaertner et al. found that patients with high tumor load showed a significant reduction of tracer uptake in kidney and in lacrimal and salivary glands (Gaertner et al 2017). In our analyses, no trend was noted between these organ dosimetry and number of bone lesions. Violet et al. reported reduced salivary and kidney uptake in patients with a higher tumor burden. The parotid uptake also reduced with increasing body mass and body surface area (Violet et al 2019).

The current exposure-dosimetry analyses are limited by the small sample size (N=29).

8.2.2 Exposure/Dosimetry-Toxicity

Descriptive longitudinal analyses during Cycle 1 showed an impact of [¹⁷⁷Lu]Lu-PSMA-617 on hematological laboratory assessments, with a decrease in leukocytes, neutrophils and platelets starting from 8 days after treatment administration. Specifically, 86% of patients presented a decrease from baseline in platelet count. Only 20% of the sub-study patients experienced a worsening from baseline of at least one hematological adverse events of CTCAE Grade ≥ 2 . And those patients were the ones with low baseline hematological laboratory values. No hematological recovery was observed during Cycle 1. Assessments at later time points are needed to better evaluate the cumulative treatment effect on the hematological toxicity.

CrCl, reflecting kidney function, reached an initial peak observed on Day 8, before a slight decrease from baseline. Although 59% of patients presented a decrease from baseline in CrCl, none of them had any renal adverse event of CTCAE Grade ≥ 2 . Indeed, based on literature data, the onset of the toxic response to radiation exposure in the kidneys may not be present in the acute setting, but appear as a delayed response.

In addition, none of the sub-study patients experienced any lacrimal gland toxicity and only 2 patients had a salivary gland adverse event during Cycle 1, limited to Grade 1.

Effect of injected activity, blood exposure and organ dosimetry were evaluated on acute toxicity related to the organs at risk during Cycle 1. Higher injected activity and higher kidney dosimetry

tend to be associated with larger decrease from baseline in CrCl. No consistent trend was detected in the relationships between platelet count decrease, hematological adverse events of CTCAE Grade ≥ 2 and salivary gland toxicities with exposure metrics.

The unexpected trend observed with blood PK exposure (AUCinf and Cmax) may be due to the limited sample size, the large variability in the data and the presence of outliers.

Exposure/Dosimetry-Toxicity analyses are limited by the small sample size (N=30) and the number of adverse events. In addition, the current work explored only Cycle 1 data, and additional assessments are needed at the end of all cycles to account for the risk of cumulative doses.

9 Conclusions

A popPK modeling and E-R analyses on organ dosimetry and acute toxicity were proposed to support the [¹⁷⁷Lu]Lu-PSMA-617 submission in mCRPC patients.

1. Key results from the popPK modeling of radioactivity-blood PK of [¹⁷⁷Lu]Lu-PSMA-617 were:
 - The final structural model was a three-compartment model with a delayed 0-order absorption and linear elimination.
 - PopPK parameter estimates were $Cl=2.50 \text{ L.h}^{-1}$, $V_1=11.53 \text{ L}$, $Q_2=0.52 \text{ L.h}^{-1}$, $V_2=29.34 \text{ L}$, $Q_3=12.00 \text{ L.h}^{-1}$ and $V_3=11.51 \text{ L}$ for a typical subject (with $CrCl_{BL}=101.5 \text{ mL/min}$ and $WT_{BL}=88.5 \text{ kg}$).
 - The inter-individual variabilities on Cl and V_1 were moderate ($CV\% = 22\%$ and 42% respectively), while variabilities on Q_2 and V_2 were estimated at relatively high values ($CV\% = 80\%$ and 93% respectively).
 - Tlag and Tk0, reproducing an artificial delayed absorption after the start of administration, were estimated at 0.01 h and 0.06 h with high variability ($CV\% = 291\%$ and 264% respectively).
 - The residual proportional error of the model was estimated at a low value (13.96%).
 - $CrCl_{BL}$ had a statistically significant impact on Cl, with a decrease of $CrCl_{BL}$ by 40%, such as a decrease from 101.5 mL/min to 60.9 mL/min , leading to an average decrease of Cl by 21%. An increase in $CrCl_{BL}$ was subsequently associated with a lower AUCinf: simulations showed a 42% and 20% increase in median of simulated AUCinf for moderate and mild renal impairment respectively vs. for normal renal function. There was no significant effect on Cmax.
 - WT_{BL} had a statistically significant impact on V_1 , with a decrease of WT_{BL} by 23%, such as a decrease from 88.5 kg to 68.1 kg , leading to an average decrease of V_1 by 18%. There was no significant effect of WT_{BL} on exposure.
2. Key results from the Exposure-Dosimetry analyses at Cycle 1 were:
 - There was no consistent association between exposure metrics (i.e. injected activity, AUCinf, Cmax) and dosimetry in the organs at risk, namely kidney, bone marrow, salivary glands and lacrimal glands.

- Only AUC_{inf} in blood was a statistically significant predictor of kidney dosimetry ($p=0.005$), but confounded by CrCl_{BL}.
 - Renal impairment (mild/moderate vs. normal) showed a trend toward higher kidney dosimetry values.
3. Key results from the descriptive Exposure/Dosimetry-Toxicity analyses at Cycle 1 were:
- Longitudinal laboratory profiles showed a decrease in leukocytes, neutrophils and platelets starting from 8 days after treatment administration.
 - Higher injected activity and higher kidney dosimetry tend to be associated with larger decrease from baseline in CrCl.
 - No consistent trend was detected in the relationships between platelet count decrease, hematological adverse events and salivary gland toxicities with exposure metrics.

10 References

References are available upon request.

Delker A, Fendler WP, Kratochwil C, et al (2016) Dosimetry for (177) Lu-DKFZ-PSMA-617: a new radiopharmaceutical for the treatment of metastatic prostate cancer. Eur J Nucl Med Mol Imaging; 43(1):42-51.

Gaertner F C, Halabi K, Ahmadzadehfari H, et al (2017) Uptake of PSMA-ligands in normal tissues is dependent on tumor load in patients with prostate cancer. Oncotarget; 8(33):55094-103.

Kabasakal L, Toklu T, Yeyin N, et al (2017) Lu-177-PSMA-617 Prostate-Specific Membrane Antigen Inhibitor Therapy in Patients with Castration-Resistant Prostate Cancer: Stability, Bio-distribution and Dosimetry. Mol Imaging Radionucl Ther; 26(2):62-8.

Kamaldeep, Wanage G, Sahu SK, et al (2020) Examining Absorbed Doses of Indigenously Developed ¹⁷⁷Lu-PSMA-617 in Metastatic Castration-Resistant Prostate Cancer Patients at Baseline and During Course of Peptide Receptor Radioligand Therapy. Cancer Biother Radiopharmac; 36(3):292-304.

Kratochwil C, Giesel F, Stefanova M, et al (2016) PSMA-targeted radionuclide therapy of metastatic castration-resistant prostate cancer with 177Lu-labeled PSMA-617. J Nucl Med; 57(8):1170-6.

Maffey-Steffan, J, Scarpa L, Svirydenka A, et al (2020) The ⁶⁸Ga/¹⁷⁷Lu-theragnostic concept in PSMA-targeting of metastatic castration-resistant prostate cancer: impact of post-therapeutic whole-body scintigraphy in the follow-up. Eur J Nucl Med Mol Imaging; 47(3):695-712.

Scarpa L, Buxbaum S, Kendler D, et al (2017) The ⁶⁸Ga/¹⁷⁷Lu-theragnostic concept in PSMA-targeting of castration-resistant prostate cancer: correlation of SUV_{max} values and absorbed doses estimates. Eur J Nucl Med Mol Imaging; 44(5):788-800.

Violet J, Jackson P, Ferdinandus J, et al (2019) Dosimetry of (177)Lu-PSMA-617 in metastatic castration-resistant prostate cancer: correlations between pretherapeutic imaging and whole-body tumor dosimetry with treatment outcomes. J Nucl Med; 60(4):517-23.

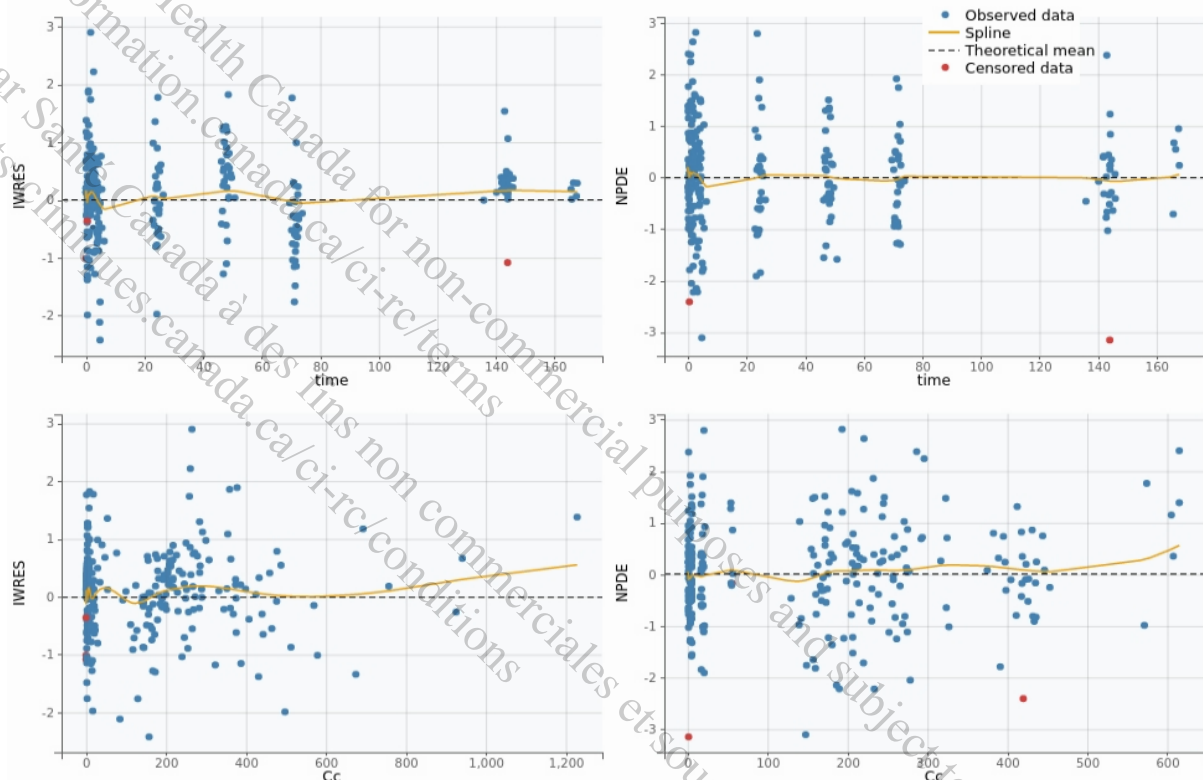
Yadav MP, Ballal S, Tripathi M, et al (2017) Post-therapeutic dosimetry of 177Lu-DKFZ-PSMA-617 in the treatment of patients with metastatic castration-resistant prostate cancer. Nucl Med Commun; 38(1):91-8.

11 Appendices

11.1 Appendix 1: Goodness-of-fit plots

11.1.1 Appendix 1.1: Goodness-of-fit plots from the base popPK model

Figure 11-1 IWRES/NPDE vs. time/population predictions from the base popPK model

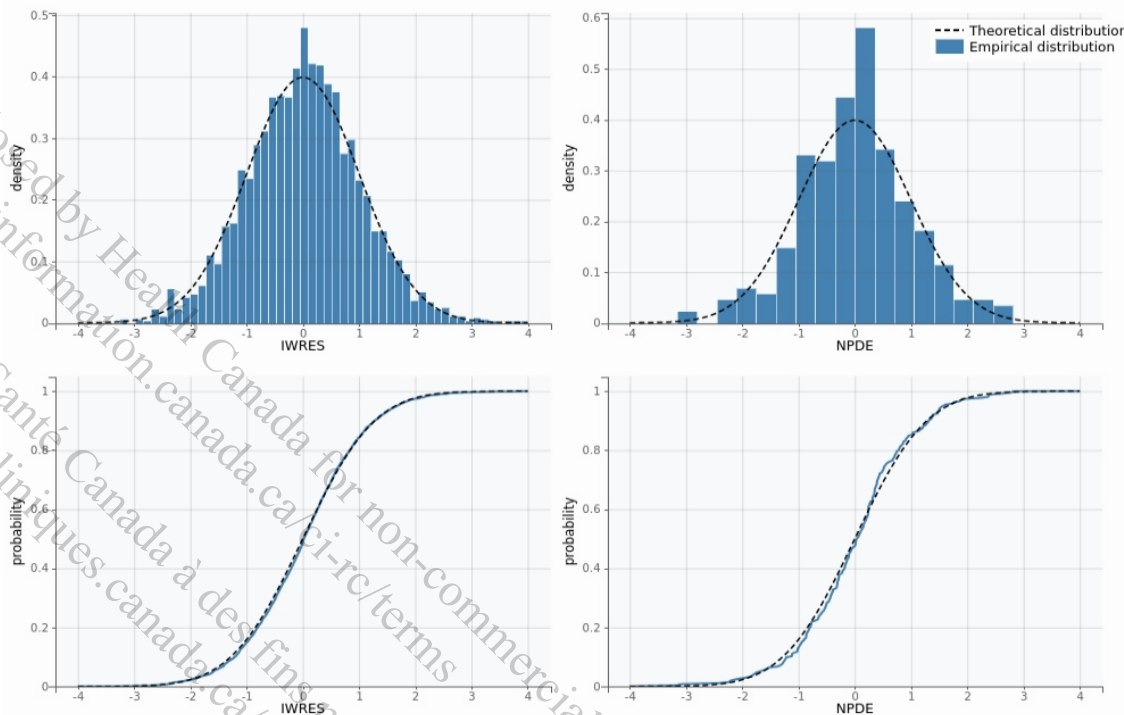


Blue dots are the concentrations above the LOQ and red dots the simulated concentrations below the LOQ. Orange curves correspond to the splines.

Source: CAAA000A1/CAAA000A12301/mas_1/model/pgm_001/02-PopPK/Runs/Submission/Run8.mlxtran

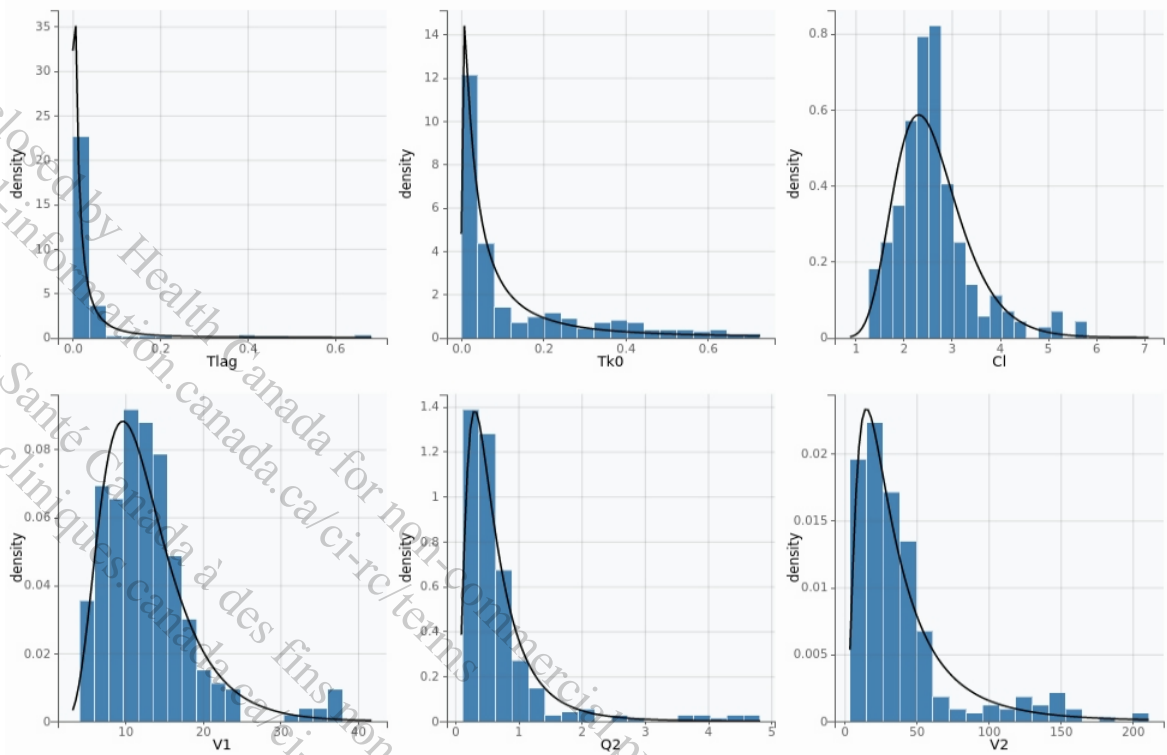
Output: CAAA000A1/CAAA000A12301/mas_1/model/pgm_001/02-PopPK/Runs/Submission/Run8/ChartsFigures/residualsscatter_LIDV_0_0.png

Figure 11-2 IWRES/NPDE distributions from the base popPK model

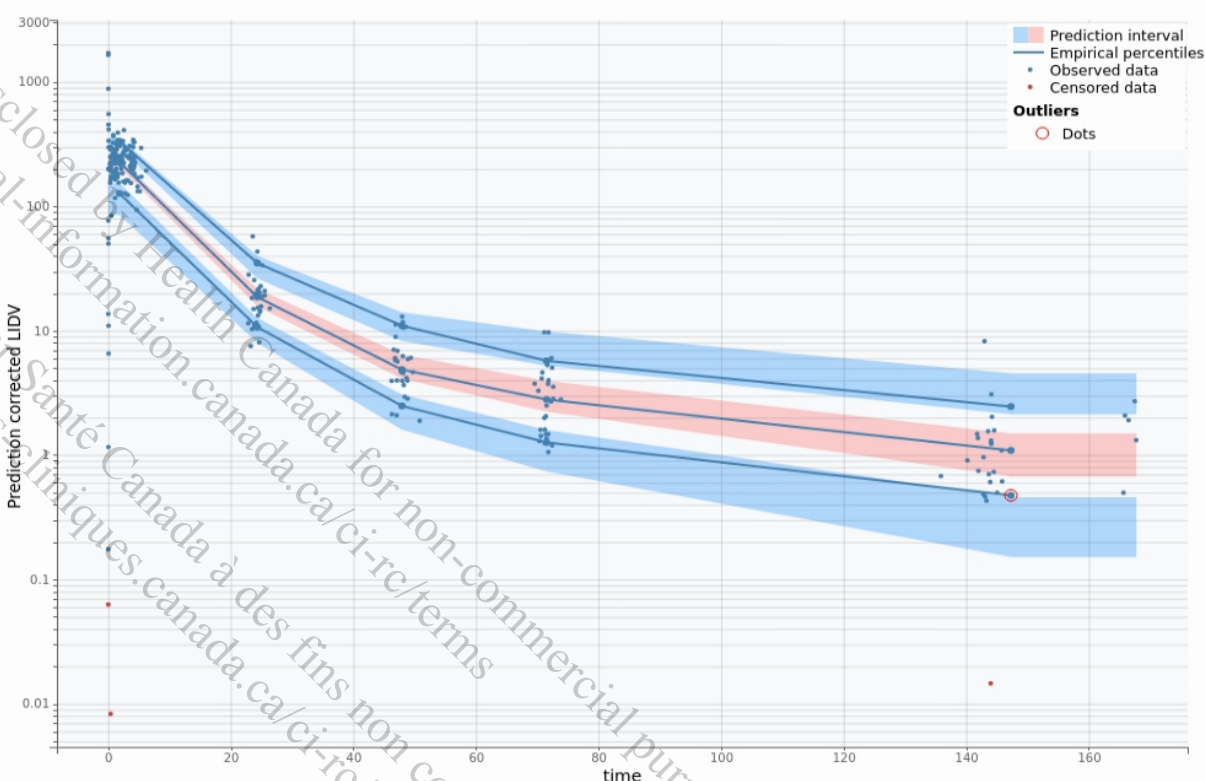


Source: CAAA000A1/CAAA000A12301/mas_1/model/pgm_001/02-
PopPK/Runs.Submission/Run8 mlxtran
Output: CAAA000A1/CAAA000A12301/mas_1/model/pgm_001/02-
PopPK/Runs.Submission/Run8/ChartsFigures/residualsdistribution_LIDV_0_0.png

Figure 11-3 Parameter distribution from the base popPK model



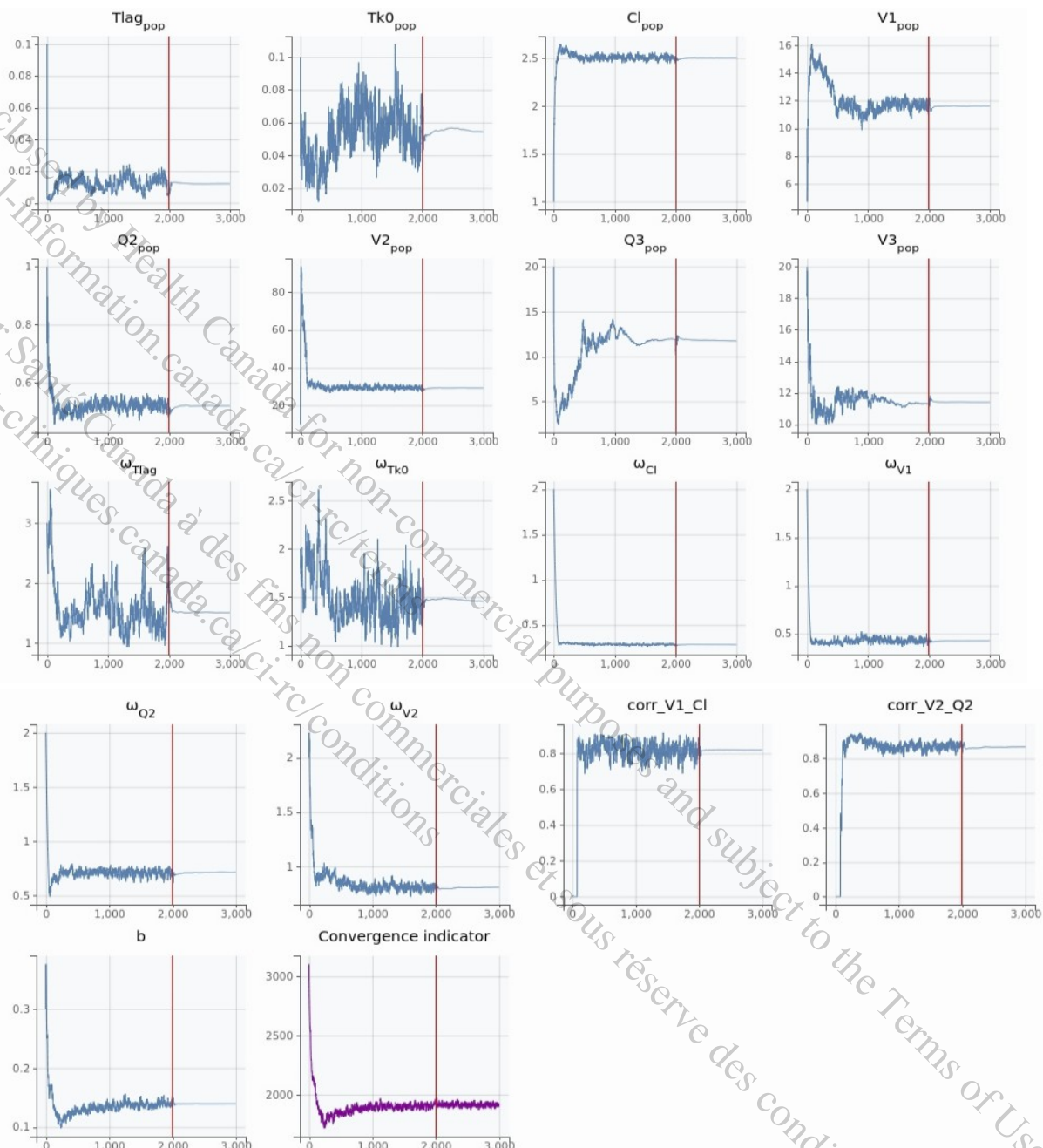
Source: CAAA000A1/CAAA000A12301/mas_1/model/pgm_001/02-
PopPK/Runs.Submission/Run8 mlxtran
Output: CAAA000A1/CAAA000A12301/mas_1/model/pgm_001/02-
PopPK/Runs.Submission/Run8/ChartsFigures/parameterdistribution_0_0.png

Figure 11-4 pcVPC from the base popPK model

The time corresponds to the time after start of infusion, in hours. LIDV corresponds to the concentration in kBq/mL. Solid lines display observed 10th, 50th, 90th percentiles. Blue/Pink regions show 90% prediction interval around the percentiles. Blue dots are the concentrations above the LOQ and red dots the simulated concentrations below the LOQ.

Source: CAAA000A1/CAAA000A12301/mas_1/model/pgm_001/02-PopPK/Runs/Submission/Run8 mlxtran

Output: CAAA000A1/CAAA000A12301/mas_1/model/pgm_001/02-PopPK/Runs/Submission/Run8/ChartsFigures/vpc_LIDV_0_0.png

Figure 11-5 SAEM convergence from the base popPK model

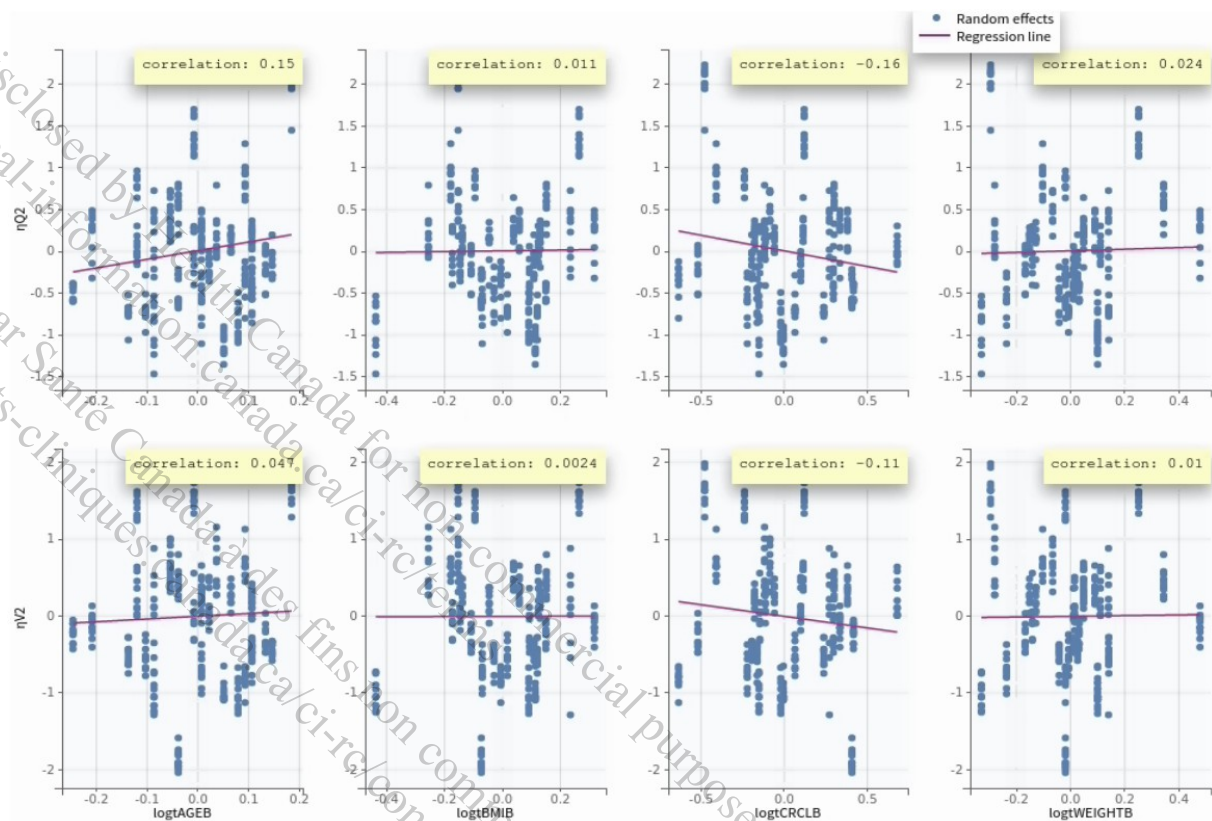
The x- and y-axis correspond to the iteration number and the parameter value, respectively. The vertical red line is the limit between the exploratory and the smoothing phases from the SAEM algorithm.

Source: CAAA000A1/CAAA000A12301/mas_1/model/pgm_001/02-

PopPK/Runs/Submission/Run8 mlxtran

Output: CAAA000A1/CAAA000A12301/mas_1/model/pgm_001/02-

PopPK/Runs/Submission/Run8/ChartsFigures/saemresults_0_0.png & saemresults_0_1.png

Figure 11-6 Post-hoc random effects for Q₂ and V₂ against covariates from the base popPK model

Post-hoc random effects were simulated from the conditional distributions. Covariates were normalized by the weighted mean value and log-transformed. Covariates were normalized by the weighted mean value and log-transformed. The weighted mean for age, weight, CrCl_{BL} and BMI, calculated by Monolix, were 66.4 years, 88.5 kg, 101.5 mL/min and 28.2 kg/m², respectively.

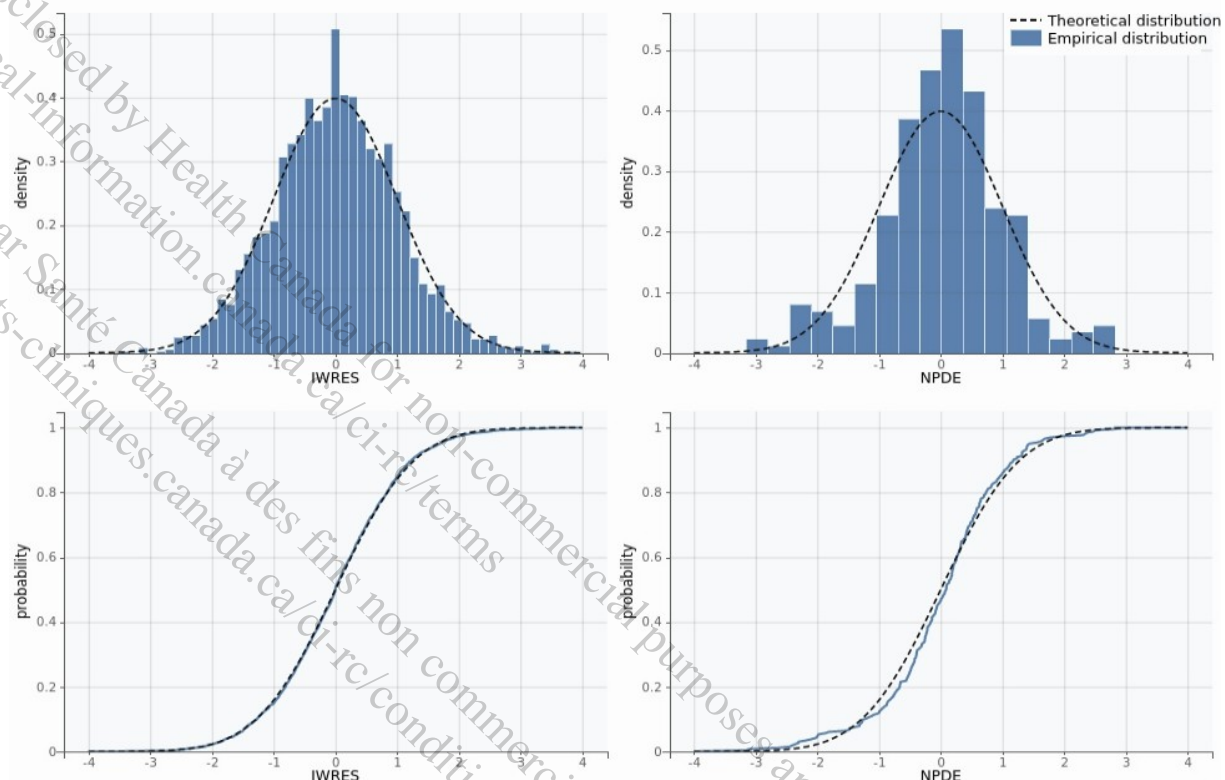
Red lines correspond to the regression lines and the correlations represent the Pearson correlation coefficients

Source: CAAA000A1/CAAA000A12301/mas_1/model/pgm_001/02-PopPK/Runs.Submission/Run8 mlxtran

Output: CAAA000A1/CAAA000A12301/mas_1/model/output_001/02-PopPK/Run8.Monolix/Covariates2.PNG

11.1.2 Appendix 1.2: Additional goodness-of-fit plots from the final popPK model

Figure 11-7 IWRES/NPDE distribution from the final popPK model



Source: CAAA000A1/CAAA000A12301/mas_1/model/pgm_001/02-PopPK/Runs.Submission/Run16 mlxtran
Output: CAAA000A1/CAAA000A12301/mas_1/model/pgm_001/02-PopPK/Runs.Submission/Run16/ChartsFigures/residualsdistribution_LIDV_0_0.png

Figure 11-8 Random effect distribution and shrinkage from the final popPK model

EBE distribution

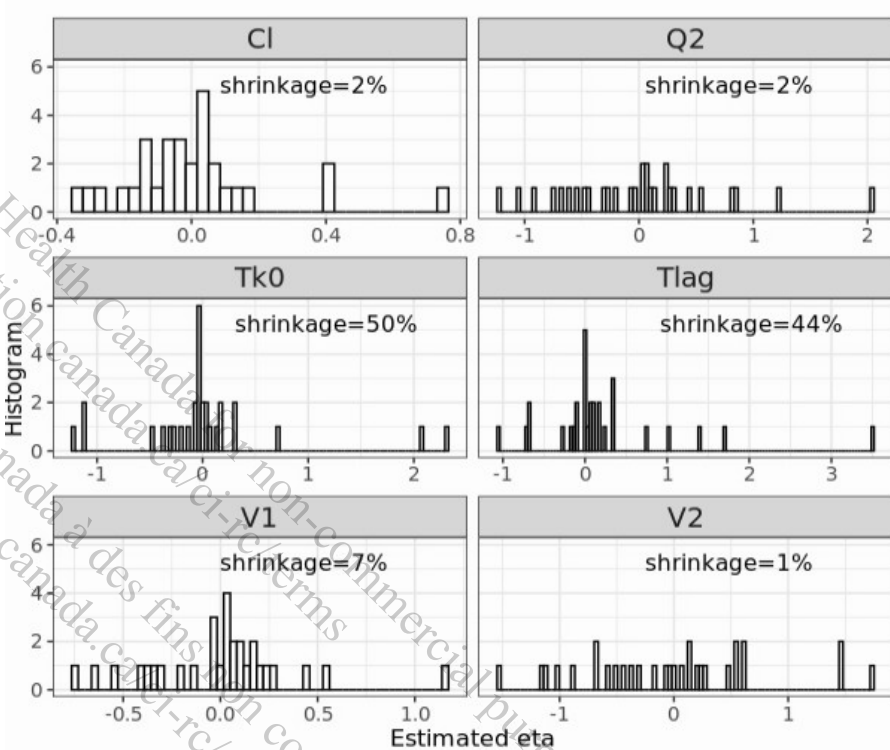
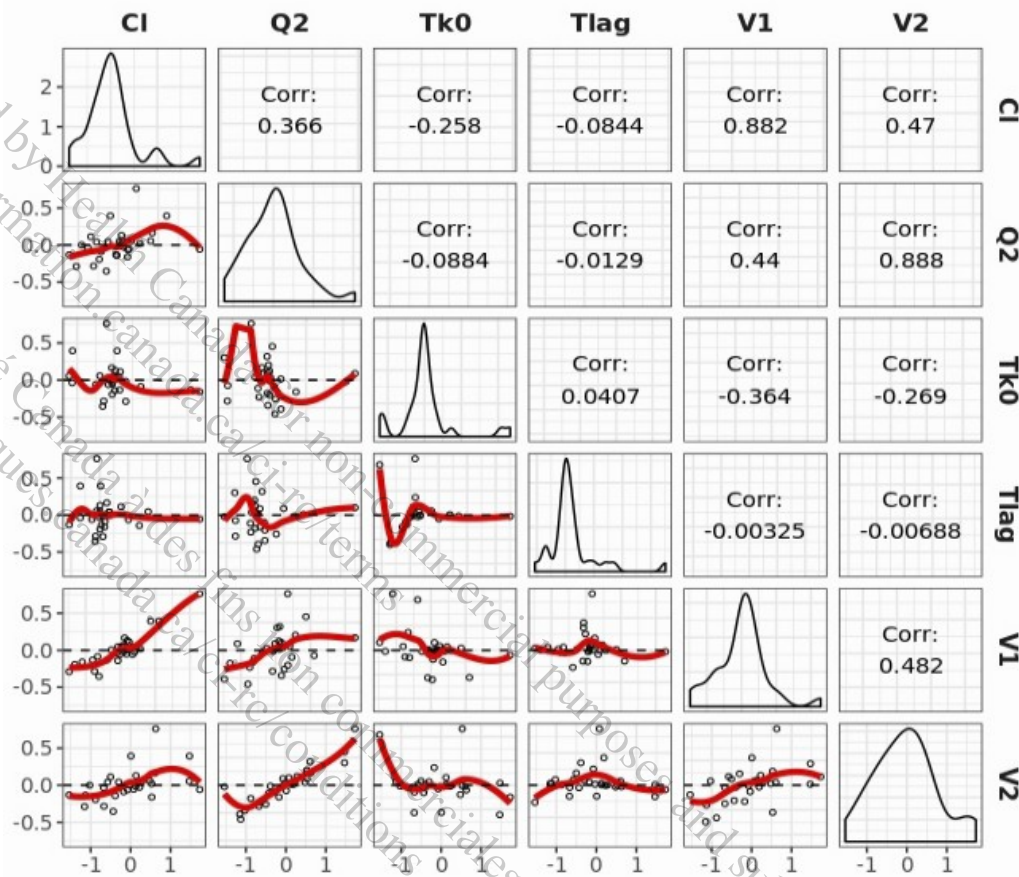
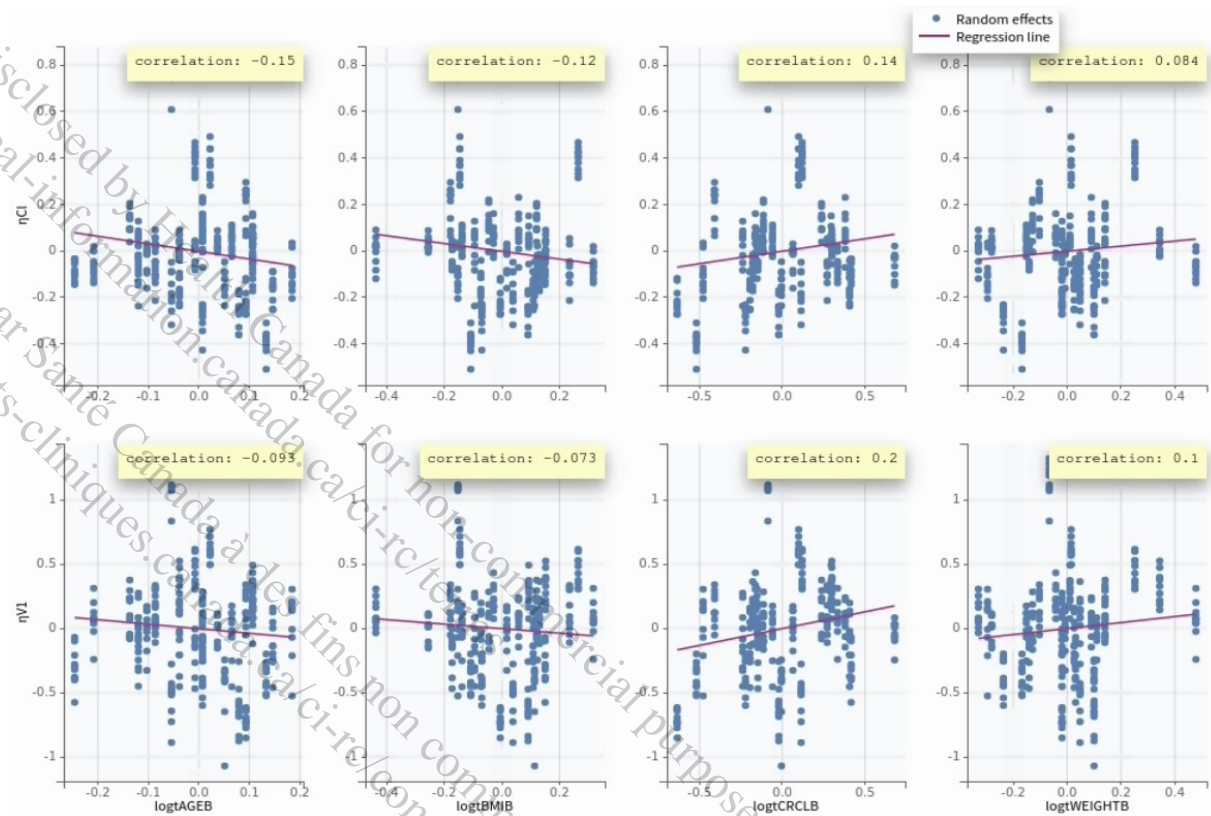
Source: /view/wilbarne1_view/vob/CAAA000A1/
CAAA000A12301/mas_1/model/output_001/02-PopPK/ggpmx_GOF/eta_hist-9

Figure 11-9 Distribution and correlation of random effects from the final popPK model

Correlations of random effects



Source: /view/wilbamel_view/vob/CAAA000A1/CAA000A12301/mas_1/model/output_001/02-PopPK/ggpmx_GOF/eta_matrix-10

Figure 11-10 Post-hoc random effects from the final popPK model vs. covariates of interest

Post-hoc random effects were simulated from the conditional distributions.

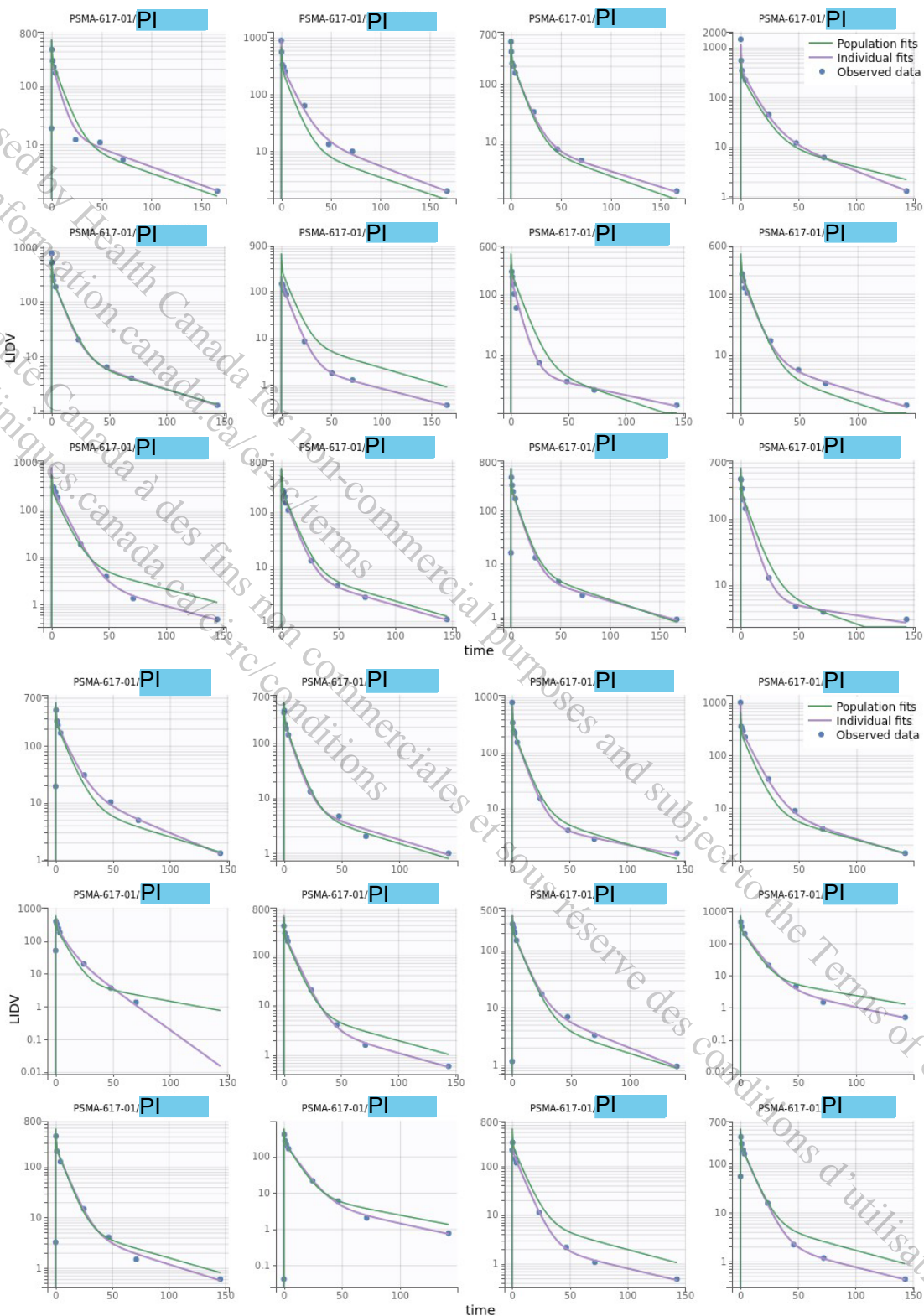
Source: CAAA000A1/CAAA000A12301/mas_1/model/pgm_001/02-

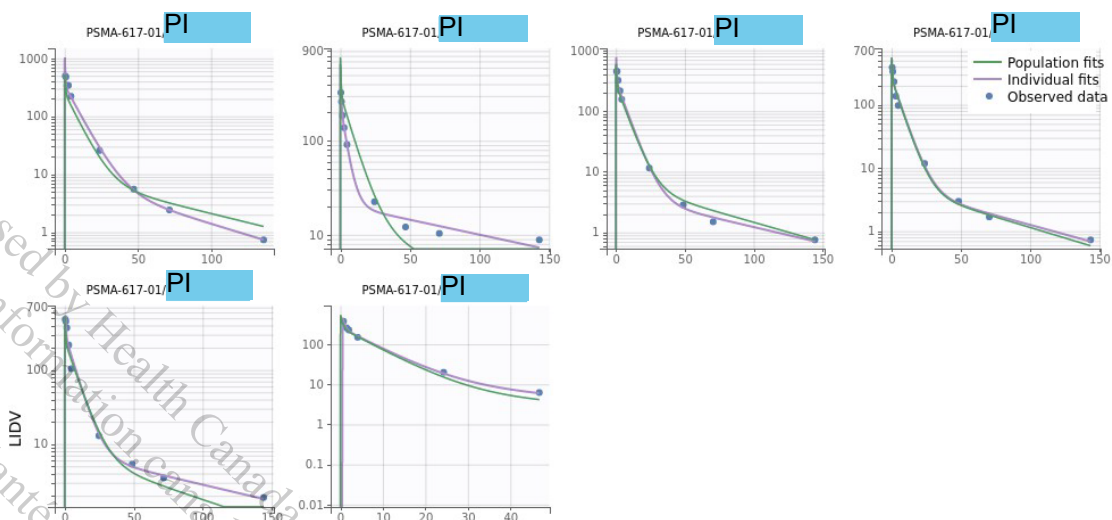
PopPK/Runs.Submission/Run16 mlxtran

Output: CAAA000A1/CAAA000A12301/mas_1/model/pgm_001/02-

PopPK/Runs.Submission/Run16/ChartsFigures/Covariates1.PNG

Figure 11-11 Individual fits from the final popPK model



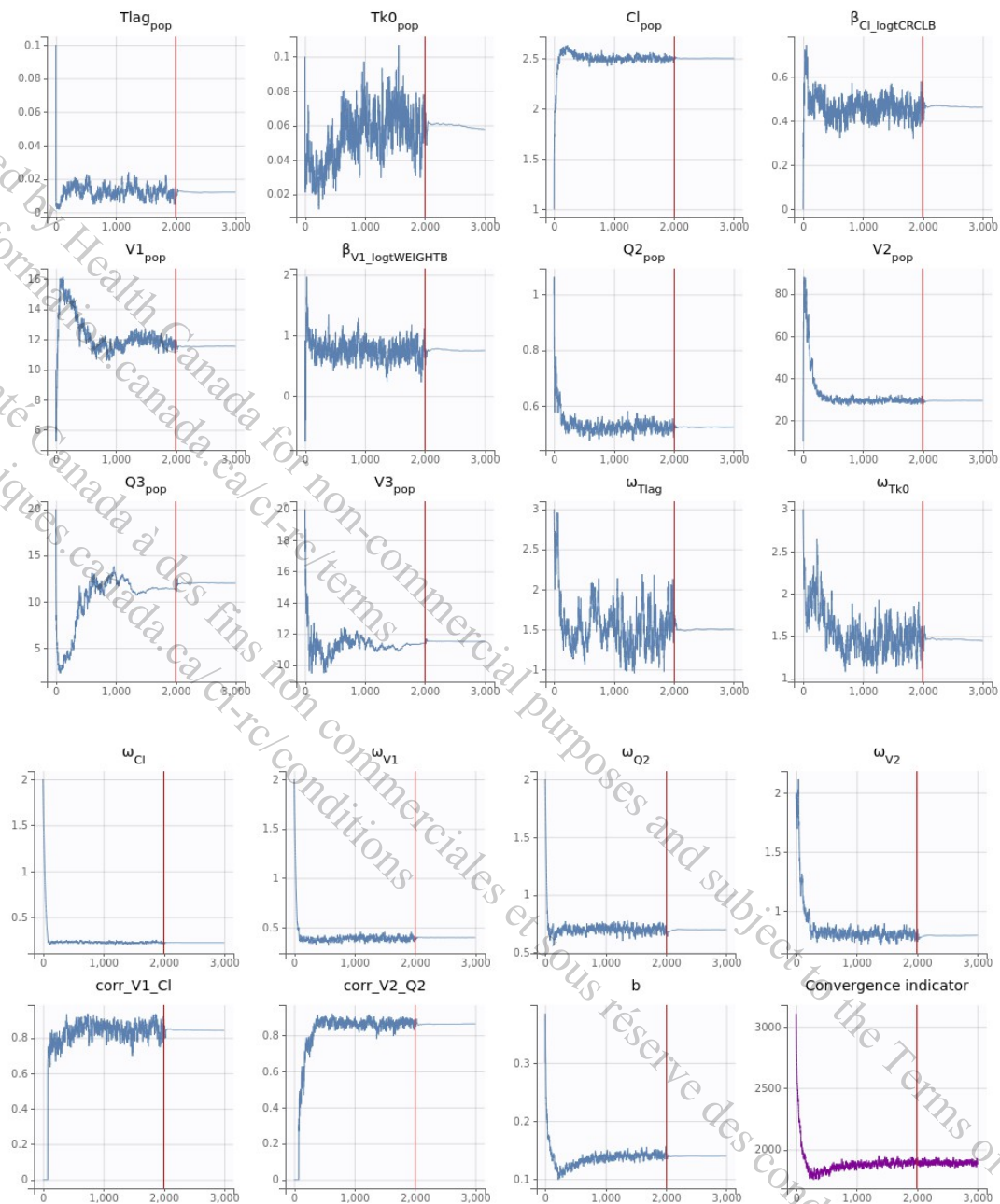


Source: CAAA000A1/CAAA000A12301/mas_1/model/pgm_001/02-

PopPK/Runs.Submission/Run16.mlxtran

Output: CAAA000A1/CAAA000A12301/mas_1/model/pgm_001/02-

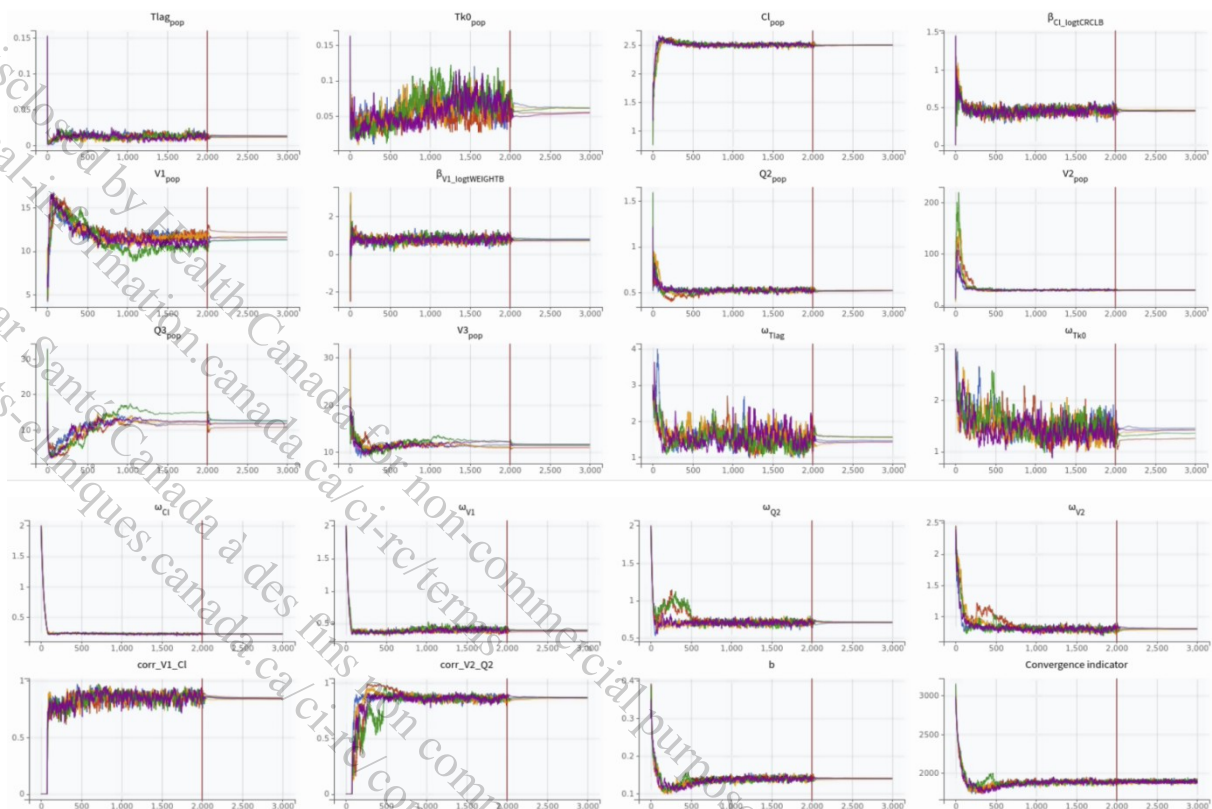
PopPK/Runs.Submission/Run16/ChartsFigures/indfits_LIDV_0_0.png & indfits_LIDV_0_1.png & indfits_LIDV_0_2.png

Figure 11-12 SAEM convergence from the final popPK model

The x- and y-axis correspond to the iteration number and the parameter value, respectively. The vertical red line is the limit between the exploratory and the smoothing phases from the SAEM algorithm.

Source: CAAA000A1/CAAA000A12301/mas_1/model/pgm_001/02-PopPK/Runs.Submission/Run16.mlxtran

Output: CAAA000A1/CAAA000A12301/mas_1/model/pgm_001/02-PopPK/Runs.Submission/Run16/ChartsFigures/saemresults_0_0.png & saemresults_0_1.png

Figure 11-13 Convergence assessment plot from the sensitivity analysis on the final popPK model

The x- and y-axis correspond to the iteration number and the parameter value, respectively. The vertical red line is the limit between the exploratory and the smoothing phases from the SAEM algorithm.

Source: CAAA000A1/CAAA000A12301/mas_1/model/pgm_001/02-
PopPK/Runs/Submission/Run16.mlxtran

Output: CAAA000A1/CAAA000A12301/mas_1/model/pgm_001/02-
PopPK/Runs/Submission/Run16/ChartsFigures/Conv.assessment1.PNG & Conv.assessment2.PNG

11.2 Appendix 2: Model control streams from the final popPK model (Run16.mlxtran)

The final popPK model file is located in:
CAAA000A1/CAAA000A12301/mas_1/model/pgm_001/02-
PopPK/Runs/Submission/Run16.mlxtran.

```
<DATAFILE>
[FILEINFO]
file='../../../../data/output_001/mt78062.csv@@/main/14'
delimiter = comma
header = {STUDYIDN, ID, USUBJID, TIME, NOMTIME, TIMEUNIT, AMT, LIDV, YTYPE, EVDT, ADM, CMT,
NAME, EVENTU, MDV, CENS, EVID, IGNOREN, IGNORE, AGEB, AGE0, WEIGHTB, WEIGHT0, HEIGHTB,
HEIGHT0, SEXN, SEX, RACEN, RACE, ETHNICN, ETHNIC, TRTN, TRT, TAD, LDOS, STUDYID, VISIT,
VISNAME, LNDV, TINF, LOQ, LIMIT, BMIB, BMI0, BSAGGB, BSAGGO, GFRMDRDB, GFRMDRD0, CRCLB,
CRCL0, TIMEC2}
```

[CONTENT]

USUBJID = {use=identifier}
TIME = {use=time}
AMT = {use=amount}
LIDV = {use=observation, name=LIDV, type=continuous}
MDV = {use=missingdependentvariable}
CENS = {use=censored}
EVID = {use=eventidentifier}
IGNOREN = {use=ignoredline}
AGEB = {use=covariate, type=continuous}
WEIGHTB = {use=covariate, type=continuous}
LIMIT = {use=limit}
BMIB = {use=covariate, type=continuous}
CRCLB = {use=covariate, type=continuous}

<MODEL>

[COVARIATE]

input = {CRCLB, AGEB, BMIB, WEIGHTB}

EQUATION:

logtCRCLB = log(CRCLB/101.533)
logtAGEB = log(AGEB/66.4383)
logtBMIB = log(BMIB/28.1866)
logtWEIGHTB = log(WEIGHTB/88.4644)

[INDIVIDUAL]

input = {Cl_pop, omega_Cl, V1_pop, omega_V1, V2_pop, omega_V2, Q2_pop, omega_Q2, Q3_pop, V3_pop, Tk0_pop, omega_Tk0, Tlag_pop, omega_Tlag, corr_V1_C1, corr_V2_Q2, logtCRCLB, beta_Cl_logtCRCLB, logtWEIGHTB, beta_V1_logtWEIGHTB}

DEFINITION:

Cl = {distribution=logNormal, typical=Cl_pop, covariate=logtCRCLB, coefficient=beta_Cl_logtCRCLB, sd=omega_Cl}
V1 = {distribution=logNormal, typical=V1_pop, covariate=logtWEIGHTB, coefficient=beta_V1_logtWEIGHTB, sd=omega_V1}
V2 = {distribution=logNormal, typical=V2_pop, sd=omega_V2}
Q2 = {distribution=logNormal, typical=Q2_pop, sd=omega_Q2}
Q3 = {distribution=logNormal, typical=Q3_pop, no-variability}
V3 = {distribution=logNormal, typical=V3_pop, no-variability}
Tk0 = {distribution=logNormal, typical=Tk0_pop, sd=omega_Tk0}
Tlag = {distribution=logNormal, typical=Tlag_pop, sd=omega_Tlag}
correlation = {level=id, r(V1, Cl)=corr_V1_C1, r(V2, Q2)=corr_V2_Q2}

[LONGITUDINAL]

input = {b}

file = 'Model.txt'

DEFINITION:

LIDV = {distribution=normal, prediction=Cc, errorModel=proportional(b)}

<FIT>

data = LIDV
model = LIDV

<PARAMETER>

Cl_pop = {value=1, method=MLE}
Q2_pop = {value=1, method=MLE}
Q3_pop = {value=20, method=MLE}
Tk0_pop = {value=0.1, method=MLE}

```
Tlag_pop = {value=0.1, method=MLE}
V1_pop = {value=10, method=MLE}
V2_pop = {value=10, method=MLE}
V3_pop = {value=20, method=MLE}
b = {value=0.3, method=MLE}
beta_C1_logtCRCLB = {value=0, method=MLE}
beta_V1_logtWEIGHTB = {value=0, method=MLE}
corr_V1_C1 = {value=0, method=MLE}
corr_V2_Q2 = {value=0, method=MLE}
omega_C1 = {value=2, method=MLE}
omega_Q2 = {value=2, method=MLE}
omega_Tk0 = {value=3, method=MLE}
omega_Tlag = {value=3, method=MLE}
omega_V1 = {value=2, method=MLE}
omega_V2 = {value=2, method=MLE}

<MONOLIX>

[TASKS]
populationParameters()
individualParameters(method = {conditionalMean, conditionalMode })
fim(method = StochasticApproximation)
logLikelihood(method = ImportanceSampling)
plotResult(method = {indfits, parameterdistribution, covariancemodeldiagnosis,
covariatemodeldiagnosis, obspred, vpc, residualssscatter, residualsdistribution,
randomeffects, categorizedoutput, saemresults })

[SETTINGS]
GLOBAL:
exportpath = 'Run16'
nbchains = 2
autochains = no

POPULATION:
exploratoryautostop = no
smoothingautostop = no
smoothingiterations = 1000
exploratoryiterations = 2000
simulatedannealingiterations = 1000
variability = firstStage

[COMMENTS]
; Tk0, Tlag, 3 cmt, Corr C1/V1 + Q2/V2, Prop ; Cov
CrCL on C1 and WT on V
```

11.3 Appendix 3: Analysis plan

Modeling Analysis Plan - CAAA617A12301 - available upon request.

11.4 Appendix 4: Data specifications of columns used in Monolix for the final popPK model

Based on the popPK dataset located in:
CAAA000A1/CAAA000A12301/mas_1/data/output_001/mt78062.csv@@/main/14.

Table 11-1 Description of the columns used in Monolix for the final popPK model

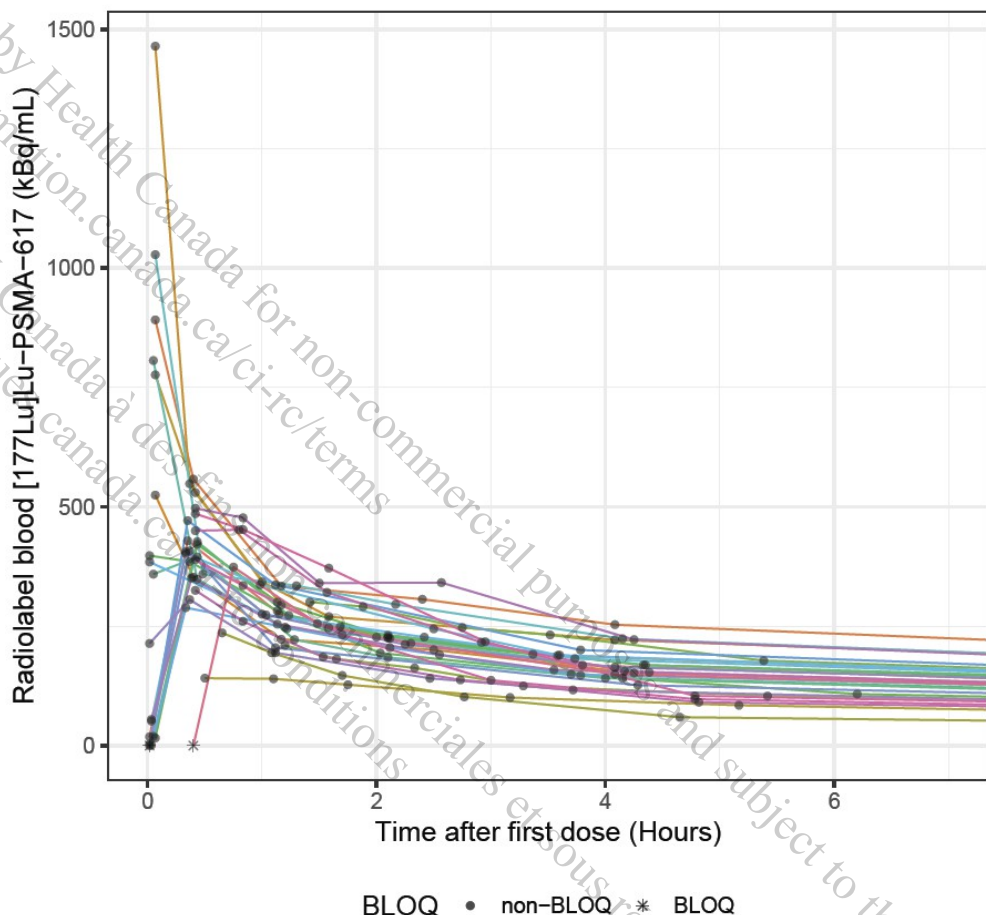
Category	Name	Description
Identification variable	USUBJID	Unique subject identifier

Category	Name	Description
Time variable	TIME	Actual time since first administration (hours)
Event	AMT	Dose given (MBq) 0 = for observation record
Event	LIDV	Dependent variable: radioactivity-blood decay-corrected concentrations Dosing records are replaced by ''.
Time dependent flag	MDV	If values are below or equal to the LOQ, then LIDV needs to be set to LOQ and record is flagged as censored Missing dependent variable: 0 = if observation value is defined 1 = for dose records
Time dependent flag	CENS	Censored data value: 0 = for dosing records 1 = for records below or equal to the LOQ 0 = otherwise (no censoring)
Time dependent flag	EVID	Event identification: 0 = for observation records 1 = for dosing records
Time dependent flag	IGNOREN	Record to be ignored: 0 = Not ignored 1 = Ignored: if LIDV≤LOQ and if the previous and the following LIDV values are > LOQ then IGNOREN=1
Time independent covariate	AGEB	Age at baseline (year)
Time independent covariate	WEIGHTB	Weight at baseline (kg)
Time dependent flag	LIMIT	Lower limit of the censored interval: 0 = value below or equal to the LOQ Equal to " " otherwise
Time independent covariate	BMIB	BMI at baseline (kg.m ²)
Time independent covariate	CRCLB	Creatinine clearance at baseline (mL/min)

11.5 Appendix 5: Additional documentation

11.5.1 Appendix 5.1: Additional descriptive plots and information on PK data

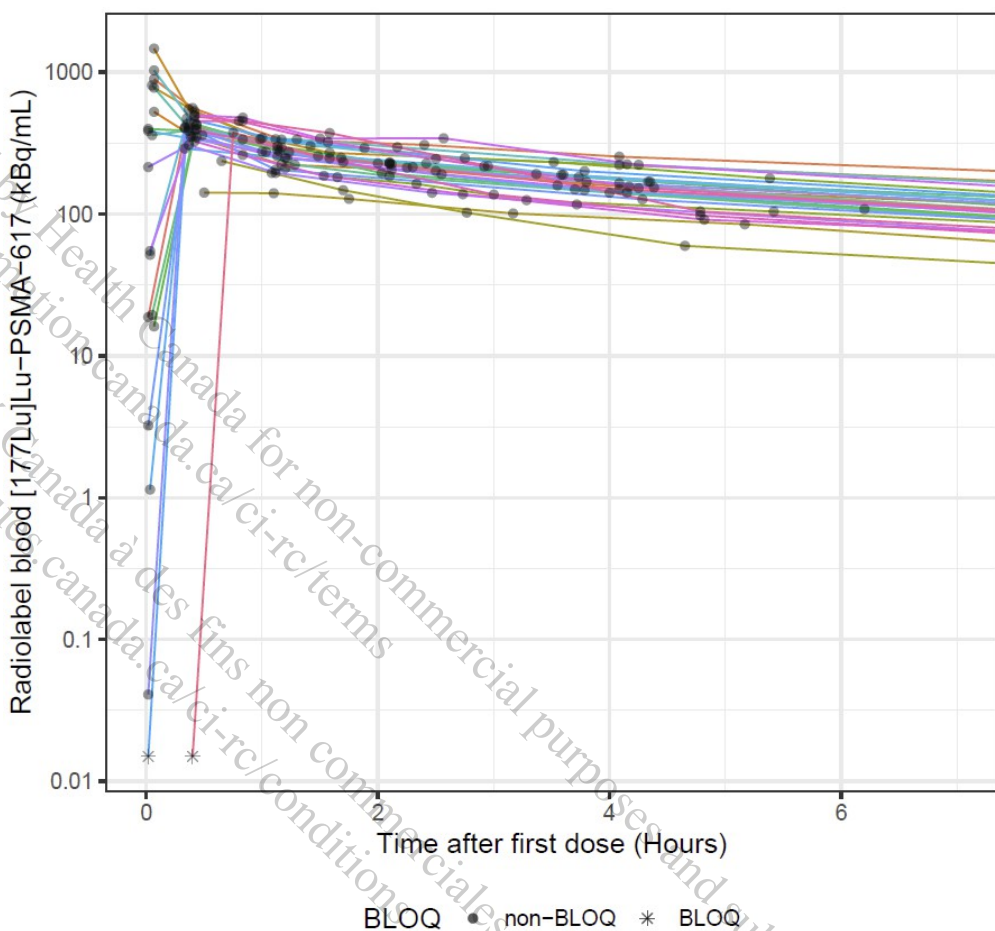
Figure 11-14 Spaghetti plots of observed individual radioactivity-blood PK of [¹⁷⁷Lu]Lu-PSMA-617 limited to the first 7 hours (Linear scale)



CAAA000A1/CAAA000A12301/mas_1/model/pgm_001/01-Data/Task01-Data.exploration.R
-> CAAA000A1/CAAA000A12301/mas_1/model/output_001/01-Data/Task01-Spaghetti.Lin.7h.pdf

The black dots correspond to the observations above the LOQ, and black crosses to the observations below the LOQ. The lines are colored by subjects.

BLOQ: below the limit of quantification.

Figure 11-15 Spaghetti plots of observed individual radioactivity-blood PK of [¹⁷⁷Lu]Lu-PSMA-617 limited to the first 7 hours (Log-linear scale)

CAAA000A1/CAAA000A12301/mas_1/model/pgm_001/01-Data/Task01-Data.exploration.R
-> CAAA000A1/CAAA000A12301/mas_1/model/output_001/01-Data/Task01-Spaghetti.Log.7h.pdf

The black dots correspond to the observations above the LOQ, and black crosses to the observations below the LOQ. The lines are colored by subjects.
BLOQ: below the limit of quantification.

Table 11-2 List of individual durations of infusion and individual actual times of first post-dose sample

Subject ID	Time of first post-dose sample (hours since infusion start)	Duration of infusion (hours)	Observed concentration (kBq/mL)
PSMA-617-01/827264-3893	0.017	0.033	18.741
PSMA-617-01/553179-6374	0.067	0.083	891.543
PSMA-617-01/416092-5299	0.067	0.083	524.65
PSMA-617-01/583036-8857	0.067	0.083	1464.517
PSMA-617-01/150461-4370	0.067	0.083	776.516
PSMA-617-01/015912-2035	0.5	0.75	141.379
PSMA-617-01/871981-6782	0.65	0.733	236.253

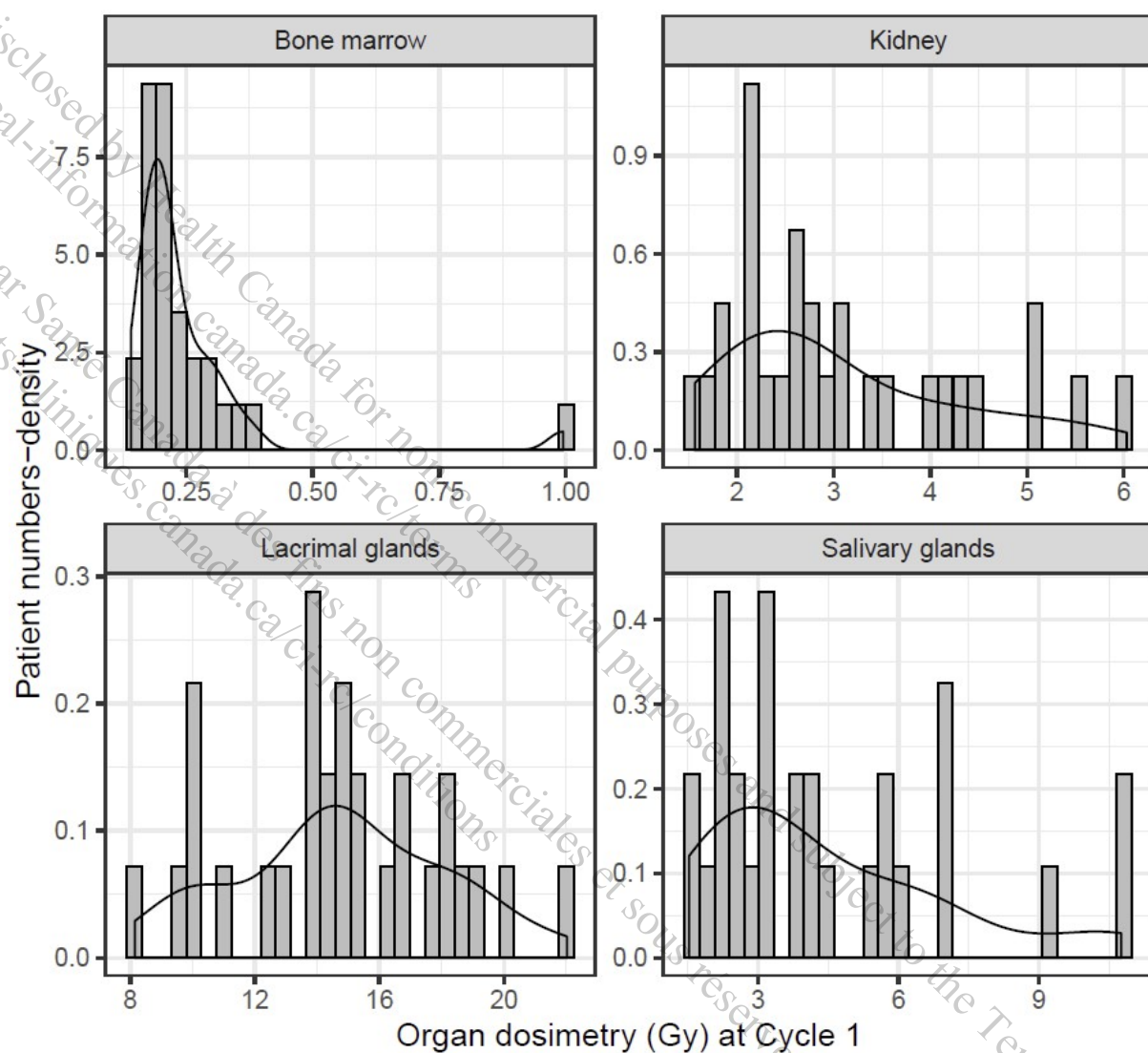
Subject ID	Time of first post-dose sample (hours since infusion start)	Duration of infusion (hours)	Observed concentration (kBq/mL)
PSMA-617-01/987429-4357	1.2	1.283	210.093
PSMA-617-01/990049-9916	1.417	1.517	300.73
PSMA-617-01/972745-5156	1.683	1.783	248.916
PSMA-617-01/557518-3717	0.067	0.1	16.127
PSMA-617-01/194910-2289	0.017	0.033	397.81
PSMA-617-01/377109-1675	0.05	0.1	19.423
PSMA-617-01/464415-9165	0.05	0.1	359.113
PSMA-617-01/684486-8330	0.05	0.1	806.363
PSMA-617-01/839757-2011	0.067	0.15	1028.098
PSMA-617-01/715154-6731	0.033	0.033	51.552
PSMA-617-01/580383-3573	0.017	0.017	384.688
PSMA-617-01/583591-6309	0.033	0.033	1.141
PSMA-617-01/844457-5269	0.017	0.033	0.015*
PSMA-617-01/178947-1630	0.017	0.033	3.231
PSMA-617-01/998629-0229	0.017	0.017	0.041
PSMA-617-01/997578-2516	0.017	0.033	214.011
PSMA-617-01/364862-2840	0.033	0.05	54.812
PSMA-617-01/293940-4656	0.417	0.5	497.053
PSMA-617-01/453610-8791	0.417	0.483	325.186
PSMA-617-01/191543-1376	0.417	0.5	450.062
PSMA-617-01/126164-1612	0.417	0.5	389.54
PSMA-617-01/304762-8689	0.417	0.5	485.584
PSMA-617-01/584617-1266	0.4	0.5	0.015*

*BLOQ values fixed to 0.015.

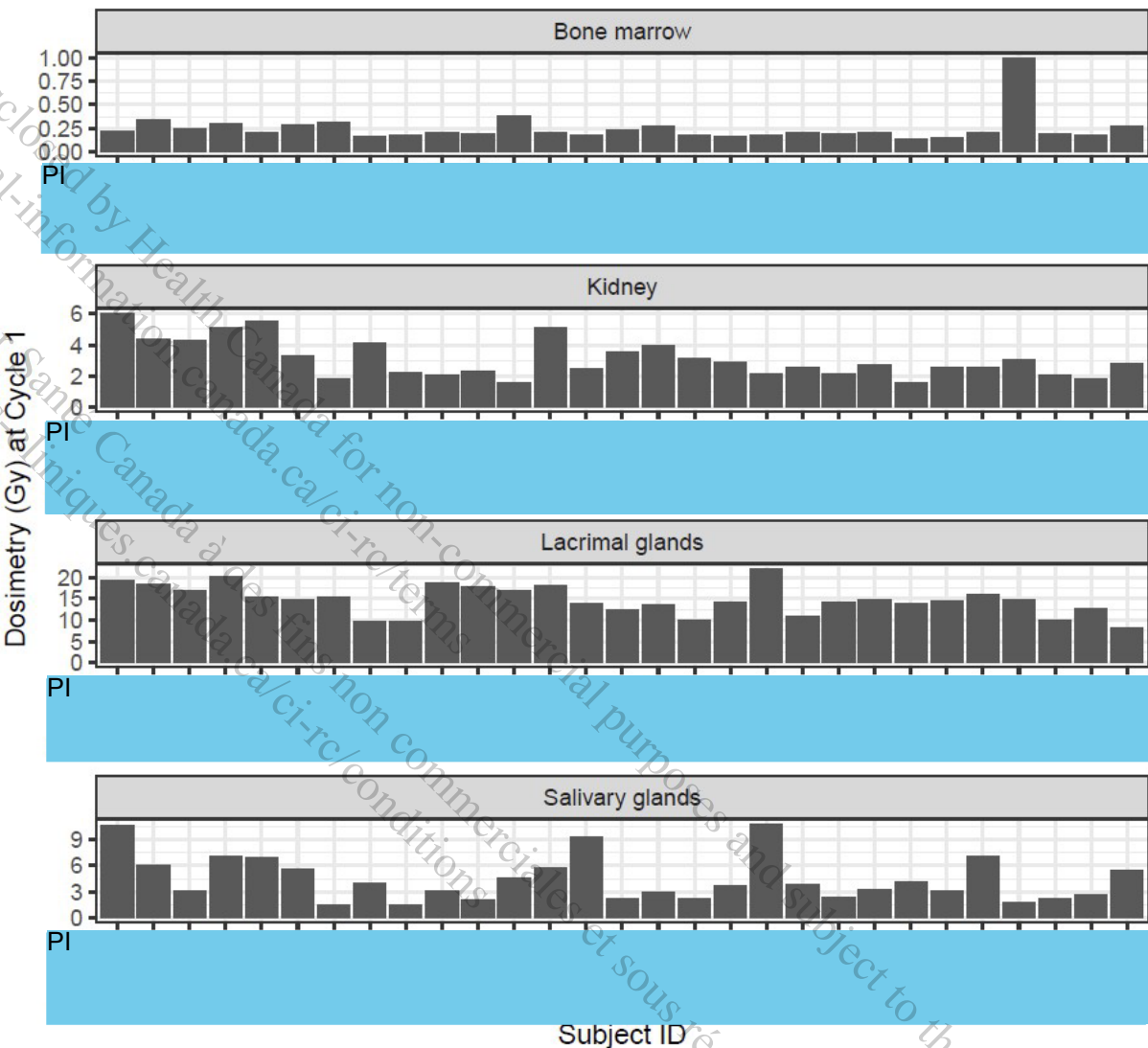
Source: CAAA000A1/CAAA000A12301/mas_1/model/pgm_001/01-Data/Task01-Data.exploration.R
Output: CAAA000A1/CAAA000A12301/mas_1/model/output_001/01-Data/Task01-Infusion.csv

11.5.2 Appendix 5.2: Additional descriptive plots on organ dosimetry

Figure 11-16 Density histograms of dosimetry values per organ at Cycle 1 (N=29)



CAAA000A1/pk/pk_1/pgm/pkpd/Task01-PK-Dosimetry.R
-> CAAA000A1/pk/pk_1/reports/pkpd/Task01-Dosimetry.Hist.pdf

Figure 11-17 Individual dosimetry values per organ at Cycle 1

CAAA000A1/pk/pk_1/pgm/pkpd/Task01-PK-Dosimetry.R
-> CAAA000A1/pk/pk_1/reports/pkpd/Task01-Dosimetry.by.USUBJID.pdf

11.5.3 Appendix 5.3: Additional documentation on toxicity

Table 11-3 Number of individuals with a decrease from baseline in CrCl and platelet count during Cycle 1

	Number of individuals (%)
Decrease from baseline in CrCl	17 (59%)
Decrease from baseline in platelet count	25 (86%)

One patient does not have any post-baseline assessment, thus percentages are calculated based on 29 individuals.

CrCl: creatinine clearance.

Source: CAAA000A1/pk/pk_1/pgm/pkpd/Task02-PK-Toxicity.R

Output: CAAA000A1/pk/pk_1/pgm/pkpd/Task02-PK-Toxicity.Rout (Lines 589-592)